FINAL REPORT
On Grant NAG3-550

TITLE:     "Development    and    Computer    Implementation    of
           Design/Analysis  Techniques  for  Multilayered  Composite
           Structures"

FINAL REPORT

PRINCIPAL INVESTIGATOR - Paul X. Bellini

PERIOD OF GRANT:   9-1-84 to 10-1-90

NAME AND ADDRESS OF GRANTEE INSTITUTION
           Cleveland State University
           1983 East 24th Street
           Cleveland, Ohio 44115

GRANT NUMBER:   NAG3-550

DATE:   June 19, 1995

# PROBABILISTIC FIBER COMPOSITE MICROMECHANICS

THOMAS A. STOCK

Bachelor of Science in Civil Engineering

Northwestern University

June, 1983

This thesis has been approved

for the Department of Civil Engineering

and the College of Graduate Studies by

_Paul X Bellini 3/26/87_
Prof. Paul X. Bellini, Thesis Committee Chairman

_____

_CCChamis /3-24-87_____
Dr. C C. Chamis, Adjunct Associate Professor

_____

_Joh H Hemann 3/24/87_____
Dr. John H. Hemann, Department Chairman

_____

ii

# ACKNOWLEDGEMENTS

I wish to express my gratitude to Dr. Christos Chamis, from the Structures Division at Lewis, for his insight, enthusiasm, patience, and wit, all of which contributed to my learning, of which this thesis is a small part. His example is an inspiration to me, in school, work, and life. Dr. Bellini, my advisor, deserves thanks for patiently reading the many drafts, and supplying perspective and criticism to aid in clarifying my ideas. He has been a teacher and a friend.

Finally, I wish to thank my parents, whose love, compassion, and understanding leave me with a debt I can never repay.

ABSTRACT


Probabilistic composite micromechanics methods are developed that simulate expected uncertainties in unidirectional fiber composite properties. These methods are in the form of computational procedures using Monte Carlo simulation. The variables in which uncertainties are accounted for include constituent and void volume ratios, constituent elastic properties and strengths, and fiber misalignment. A graphite/epoxy unidirectional composite (ply) is studied to demonstrate fiber composite material property variations induced by random changes expected at the material micro level. Regression results are presented to show the relative correlation between predictor and response variables in the study. These computational procedures make possible a formal description of anticipated random processes at the intraply level, and the related effects of these on composite properties.

# TABLE OF CONTENTS

# LIST OF TABLES

# LIST OF FIGURES

xiii

# CHAPTER I

## INTRODUCTION

### A. Background

The diverse requirements of recent engineering applications have
motivated designers to explore specialized structural and material
systems. Ceramic materials, for example, have several attractive
structural properties, such as their high stiffness/weight ratios, and
low variation of stiffness and strength over wide ranges of
environmental conditions. A significant disadvantage inherent to
brittle structural materials is their vulnerability to failure due to
cracks propagating from flaws. The increased probability of a flaw
occurring in a material as the volume increases leads to bulk strengths
which are a fraction of the theoretical strength of the material. The
size effect on material strength (Ref. 1) can be explained by the
"weakest link" concept. Griffith ( Ref. 2) reasoned that very small
solids, for example wires or fibers, might be expected to be stronger
than large ones, due to the additional restriction on the size of the
flaws. In the limit, a single line of molecules must possess the
theoretical molecular tensile strength of a material. A consequence of

1

the size effect on strength was the development of fiber composite materials which consist of thin, strong fibers bound together by a ductile matrix. The advantages of fine, strong fibers can explain the current trend toward increased use of fiber composite materials in demanding aerospace applications.

Properties of a composite laminate depend on the properties of the constituent materials, their distribution, and orientation. Laminates are composed of layers of unidirectionally reinforced plies (laminae). The lamina is typically considered the basic unit of material in a composite structural analysis, which requires knowledge of the material properties of each individual lamina and its geometric orientation. The branch of composite mechanics that predicts ply material properties based on the properties, concentration, and orientation of its constituents is known as composite micromechanics, and frequently incorporates the traditional Mechanics of Materials assumptions. The desired laminate is created by stacking of plies in specific directions. The integration of ply properties to yield laminate properties is called laminate theory. Laminate variables such as ply orientation and stacking sequence can be tailored to yield a laminate with the desired material properties. Thus, the laminated composite is a suitable material for component design.

Analysis of fiber composite structures is currently performed using a variety of computer codes. From the original codes based on classical micromechanics and laminate theory, recent codes (Ref. 3,4) have been developed which incorporate the current state of the art. Complete

mechanical, thermal, and hygral properties are calculated, and can be used to compute response. Advanced failure criteria are used to calculate composite strengths. Environmental effects are also quantified. The usefulness of these codes has been demonstrated by comparison with experimental and finite element results (Ref. 5,6).

The analytical capability of many codes is limited by the deterministic nature of the computations. Specifically, fixed values for constituent material properties, fabrication process variables (i.e. constituent volume ratios) and internal geometry must be used as input. However, random variations in these parameters are not only expected, but easily observed experimentally. (See Fig. 1)

The analysis of composite structures requires reliable predictive models for material properties and strengths. However, the prediction efforts have been complicated by inherent scatter in experimental data. Since uncertainties in the constituent properties, fabrication variables, and internal geometry would lead to uncertainties in the measured composite properties, the question arises:

> How much of the "statistical" scatter of experimentally observed composite properties can be explained by reasonable statistical distribution of input parameters in composite micromechanics and laminate theory predictive models?

The increasing use of probabilistic methods in structural mechanics has been shown to provide a more realistic depiction of structural response due to load variations. (Ref. 7) The recognition that material parameters are characterized by a spectra of values ( that is, are

statistical in nature ) rather than by a unique set of values, points to probabilistic methods as a logical analysis approach.
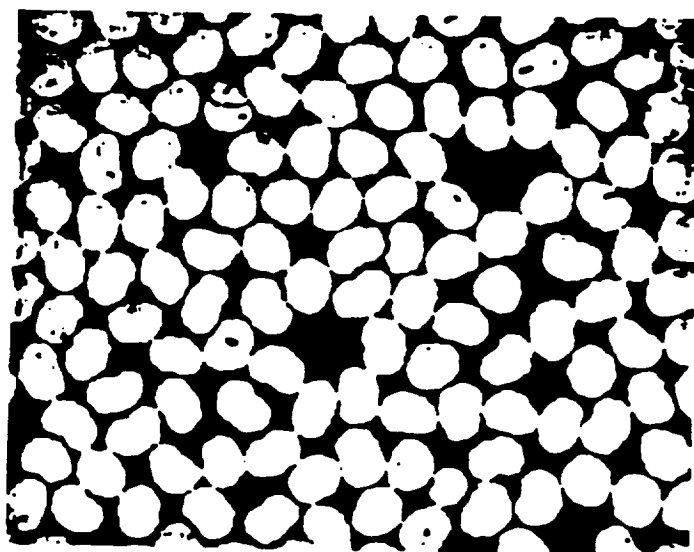
Fig. 1- Photomicrograph of Graphite/Epoxy cross section
showing variation in fiber content.   (Ref. 19)

## B. Purpose

The aim of this thesis is to develop a computational capability to simulate the probabilistic variations in the mechanical behavior of unidirectional fiber composites. The Monte Carlo method is used to simulate a variety of random processes, to quantify fiber composite material variations induced by random changes in composite fiber alignment, constituent properties, and fabrication process variables. This random process description is an attempt to more accurately predict the behavior of manufactured materials, which inherently include these random variations. The characterization of fiber reinforced composites through simulation of local nonuniformities provides an economical alternative to experimentation to measure material properties.

## C. Formulation of the Model

The model commonly used in characterizing fiber composites is based on the calculation of properties of the basic unit of an orthotropic ply. The layup geometry is then used in laminate equations to calculate composite properites (See Figs. 2a, 2b). In this work, however, the basic unit is taken as the sub-ply, which consists of only one fiber-matrix level in the material. Micromechanics theory is used to calculate the properties of the assumed orthotropic sub-ply, each with randomly distributed fabrication variables and material properties. Distributed fiber directions, due to possible misalignment within the ply, are then used in the laminate equations to calculate ply properties. This substructuring of the composite ply represents a novel attempt at characterization of fiber composite material properties based on probabilistically distributed constituent properties, individual fiber misalignment, and fabrication process variables (See Figs. 3a,3b).

This formulation is particularly well suited to the probabilistic description of fiber composite material properties. Since the micromechanics and laminate equations can be used to calculate ply properties at any number of points in a ply, a tractable finite element structural analysis based only on simple distributional assumptions for physical parameter variations can be performed. This model supplies a rational procedure for composite material property assessment, because it treats the material as the result of a series of random processes which occur at the intraply level.

(a) orthotropic ply          (b) laminate
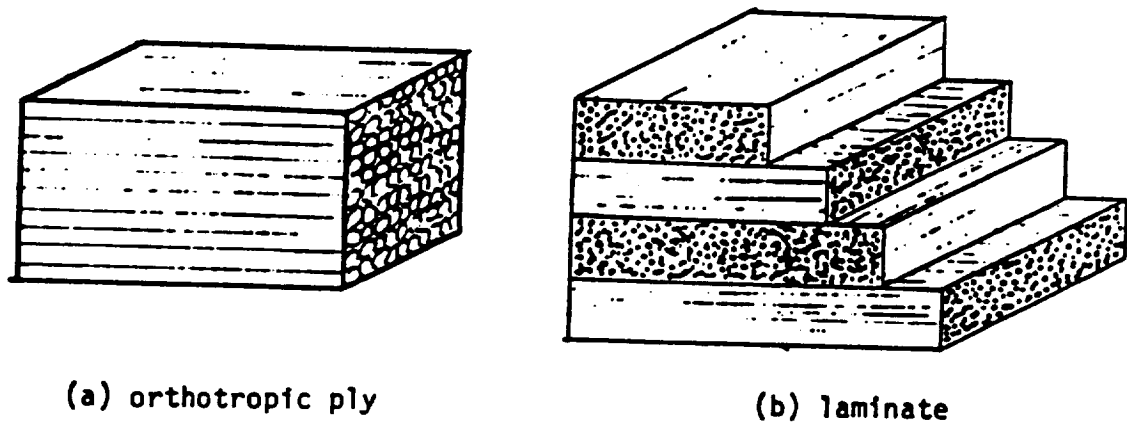
Fig. 2- Conventional Model



(a) subply          (b) ply
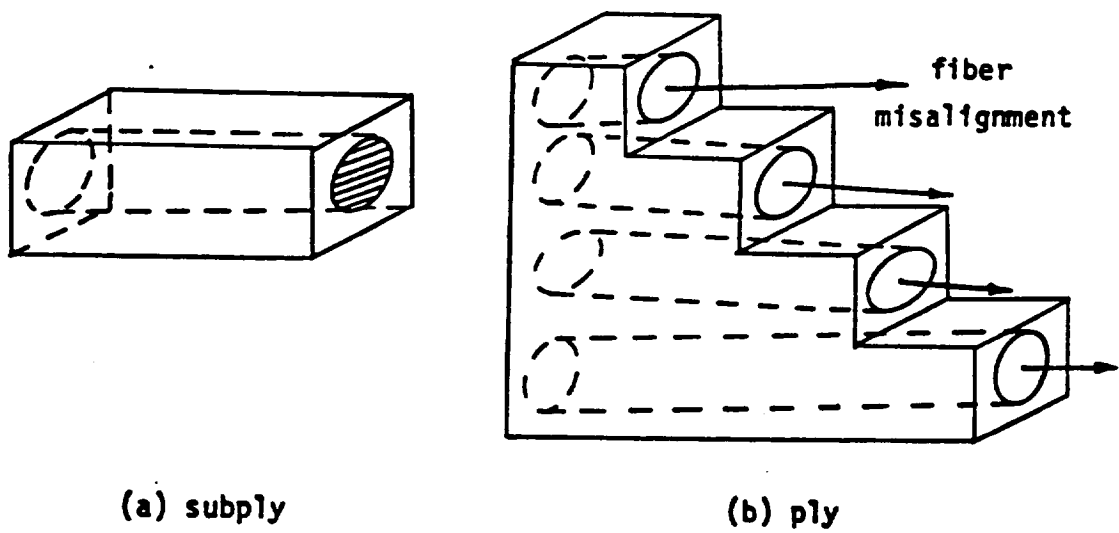
Fig. 3- Substructure Model

D. Method of Investigation

1. Brief Description of ICAN

The Integrated Composite Analyzer (ICAN) is a computer program for comprehensive linear analysis of multilevel fiber composite structures. The program contains the essential features required to effectively design structural components made from fiber composites. It now represents the culmination of research conducted since the early 1970's, at the National Aeronautics and Space Administration (NASA) Lewis Research Center (LeRC), to develop and code reliable composite mechanics theories. This user friendly, publicly available code incorporates theories for

1. conventional laminate analysis
2. intraply and interply hybrid composites
3. hygral, thermal, mechanical properties and response
4. ply stress-strain influence coefficients
5. microstresses and microstress influence coefficients
6. stress concentration factors around a circular hole
7. predictions of delamination locations around a circular hole
8. Poisson's ratio mismatch details near a straight free edge
9. free edge interlaminar stresses
10. laminate failure stresses
11. normal and transverse shear stresses
12. explicit specification of matrix-rich interply layers
13. finite element material cards for NASTRAN, MARC

A detailed description of ICAN can be found in Reference (3). The ICAN code and documentation are available through COSMIC, the Computer Software Management and Information Center, Suite 112, Barrow Hall, Athens GA, 30602.

## 2. Summary of Variables

The variables studied in this work can be separated into two categories. The independent variables to be simulated using random sampling consist of the following (see Fig. 4a for fiber coordinate system):

Geometry:
    fiber orientation angle         (THETA)
Fabrication variables:
    fiber volume ratio          (FVR)
    void volume ratio           (VVR)
Fiber properties
    longitudinal elastic modulus   (EFP1)
    transverse elastic modulus    (EFP2)
    shear modulus, 1-2 plane     (GFP12)
    shear modulus, 2-3 plane     (GFP23)
    fiber tensile strength       (SFPT)
    fiber compressive strength    (SFPC)

Matrix properties
    elastic modulus            (EMP)
    matrix tensile strength      (SMPT)
    matrix compressive strength   (SMPC)
    matrix shear strength       (SMPS)

The dependent variables to be calculated using ICAN consist of the following ply properties, measured about the material axes (see Fig. 4b):

    normal modulus in 1-1 direction   (EC11)
    normal modulus in 2-2 direction   (EC22)
    shear modulus in 1-2 plane     (EC12)
    Poisson's ratio for strains in 2 direction induced
        by stresses in 1 direction    (NUC12)
    Poisson's ratio for strains in 1 direction induced
        by stresses in 2 direction    (NUC21)
    Coefficients of thermal expansion
        in 1-1 direction         (CTE11)
        in 2-2 direction         (CTE22)
        coupling coefficient      (CTE12)

(a) fiber  (b) material
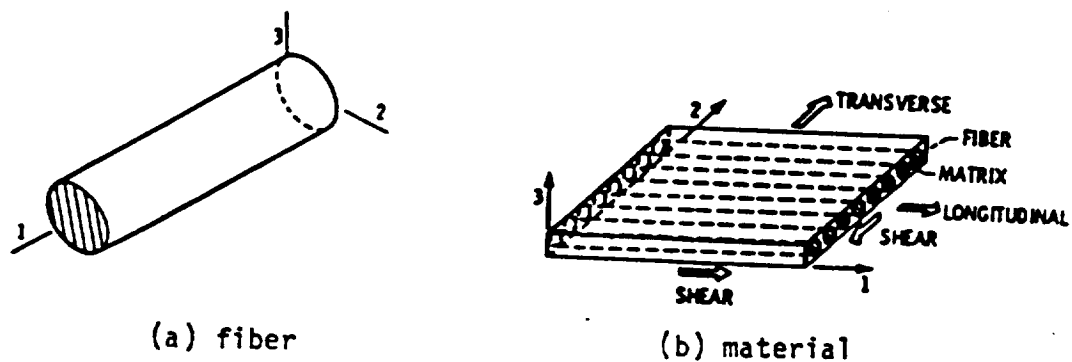
Fig. 4- Coordinate Systems
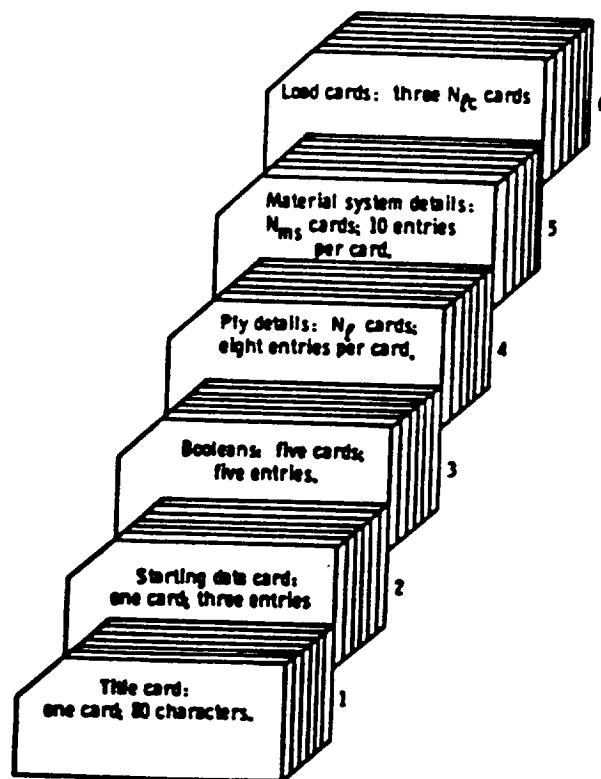


Fig. 5- Order of ICAN input data cards

Ply strengths in material directions
    longitudinal tensile              (SCXXT)
    longitudinal compressive    (SCXXC)
    transverse tensile            (SCYYT)
    transverse compressive      (SCYYC)
    in-plane shear               (SCXYS)

The descriptions above should be consulted periodically for the definitions of variables that henceforth will be referred to symbolically.

### 3.Monte Carlo Methods

Complicated stochastic processes can be simulated by a variety of numerical methods generally referred to as Monte Carlo methods (Ref. 8). The term refers to that branch of experimental mathematics concerned with experiments on random numbers. Since the advent of high speed computers, they have found extensive use in most fields of science and engineering, in analyzing many physical processes of a statistical nature, or where direct experimentation is not feasible. In general, they can be economically used to achieve a level of precision between 90 and 95 percent.

A Monte Carlo experiment refers to the procedure of randomly assigning a value to an independent random variable in a chosen model, and observing the dependent variable at the conclusion of the process being modeled. A Monte Carlo procedure is composed of n such independent experiments. When n is sufficiently large, the observations will yield, by virtue of the laws of large numbers, a statistically meaningful description of the physical problem.

The form of Monte Carlo used in this study is as follows:

1.  Define the system model by assuming

  a.  model regression function
  b.  method of error incorporation
  c.  probability distributions of all errors (for all independent variables)
  d.  any equations used to model the phenomena of interest

2.  Use the computer and random sampling techniques to select values of the independent variables.

3.  Calculate dependent (output) variables using the prescribed

equations.

4.  Estimate regression parameters for the assumed model.

5.  Replicate the experiment, each time with a new set of input values.

6   Use appropriate statistical methods to calculate properties of the distribution of parameter estimates.

## E. Brief Summary of Results

A ply made from the AS-Graphite /IMHS epoxy composite system is studied. The monte carlo scheme is used to generate a number of response results, which are analyzed in graphical and numerical form, to supply a random process description of composite ply elastic constants, thermal expansion coefficients, and strengths. Histogram and distribution plots of results for assumed narrow and wide variations in input properties are compared with a deterministic base case for an aligned ply. The figures demonstrate the range of values that response variables assume for the example data under consideration.

Confidence intervals are calculated for response variables in subsequent samples, which are normalized with respect to an appropriate independent variable, to yield plots of normalized response as a function of fiber volume ratio, for various values of distribution parameters for the related independent variable. These plots demonstrate the sensitivity of ply properties to randomly selected uncertainties in constituent and fabrication variables.

Several multiple linear regression models were calculated for response variables. The relative correlation of predictor (independent) variables with response is studied for all output properties considered. Varying levels of significance were achieved in the regression equations, due to the differences in complexity of response variables. Elastic constants can be described adequately with simple regressor functions, and generally explain between 80 and 99 percent of the observed response variations about a mean. The regression models

studied for strength, although achieving better reliability with higher order regressor functions, demonstrate such low significance as to be practically useless for predictive purposes. This is not an unexpected result, because of the complex nature of strength behavior in composite materials.

# CHAPTER II

## METHODS OF CALCULATION

A. Overall plan

    1. Input structure for ICAN

The input data for a typical execution of the available ICAN

program consists of (see Fig 5)

    1. header card
    2. control cards
    3. ply data cards
    4. material system cards
    5. load cards

For repeated use of the ICAN program, input data files must be

created and used one at a time. Each successive run of the master

program (of which ICAN is made a subroutine) writes the input file from

user-supplied parameters and calls ICAN. The ply data cards contain

randomly generated fiber orientation angle values. The material system

cards contain randomly generated values for fiber and void volume

ratios.

## 2. Constituent Property Variations

Each successive execution of ICAN uses a distinct set of material
properties for fiber and matrix. The random number generation is
performed with user-supplied parameters which are stored in a separate
file. The options of using either generated properties or using the
values contained in the resident data bank are available. Any subset of
the parameters described may be generated or held constant with proper
specification of the Booleans which control the input to the ICAN
program. (see Figs. 6,7)

```
FIBER STRENGTH VARIES; CONSTANT FIBER VOLUME RATIO OF 0.30;TAPE 003131
  STDATA       15        1      15       T
    T     50        T      F      T      T
    F          000.0   10.0  0.300  0.200   3.00      5
    F
    F
    T
    PLY                        70.00   70.00      .0               .000
  MATCRDAS-1IMHS                     AS-1IMHS     0.0       .57     .03
   PLOAD    10.        0.0     0.0      0.0
   PLOAD    0.0        0.0     0.0
   PLOAD    0.0        0.0
  OPTION       0
```

Fig. 6- Command Input

```
EFP1         T     0.3100E 08      0.3000E 07
EFP2         T     0.2000E 07      0.2000E 06
GFP12        T     0.2000E 07      0.2000E 06
GFP23        F     0.1000E 07      0.1000E 06
SFPT         T     0.4000E 06      0.1000E 02
SFPC         T     0.4000E 06      0.1000E 02
EMP          T     0.5000E 06      0.5000E 05
SMPT         T     0.1500E 05      0.1000E 02
SMPC         T     0.3500E 05      0.1000E 02
SMPS         F     0.1300E 05      0.1000E 02
```

Fig. 7- Constituent Variation Input.  Example for AS-1 Graphite
       fiber and IMHS Epoxy matrix, with wide variations of
       stiffnesses and strengths.

### 3. Repeated runs

The user must specify the number of ICAN runs desired in a given sample. In this study, fifty (50) runs were used throughout, to take advantage of the simplification in statistics by using suitably large samples. From elementary statistics, it is known that any process that is the result of the combined interaction of several probabilities can be assumed to approximate a normal distribution. For phenomena that are assumed to approximate a normal distribution, the simplest forms for calculating statistics apply to suitably large samples (usually greater than thirty). The sample size of fifty was chosen to supply a practicably large amount of data, within the restrictions imposed on computation time.

The data generated by repeated execution of the ICAN routines is stored in a sequential access dataset, where the 50 output files are separated by end of file markers. This arrangement allows a single Fortran unit to be used for output throughout. A simple flowchart of the data generation routines is shown in Fig. 8(a).

### 4. Data collection

The ICAN output files are searched to locate the specific material properties and strengths of interest in this study. The flowchart of data collection routines is shown in Fig. 8(b). After obtaining the sample of ICAN output, the investigator may choose to scrutinize parameters or calculate statistics aside from those chosen in this study. This is likely, in light of the large quantity of data available and the need for limiting the scope of this particular study to

representative properties. The user would have to supply additional code or adapt existing code to suit his purposes in this case. The coded modifications to ICAN used in this study are included in Appendix A.
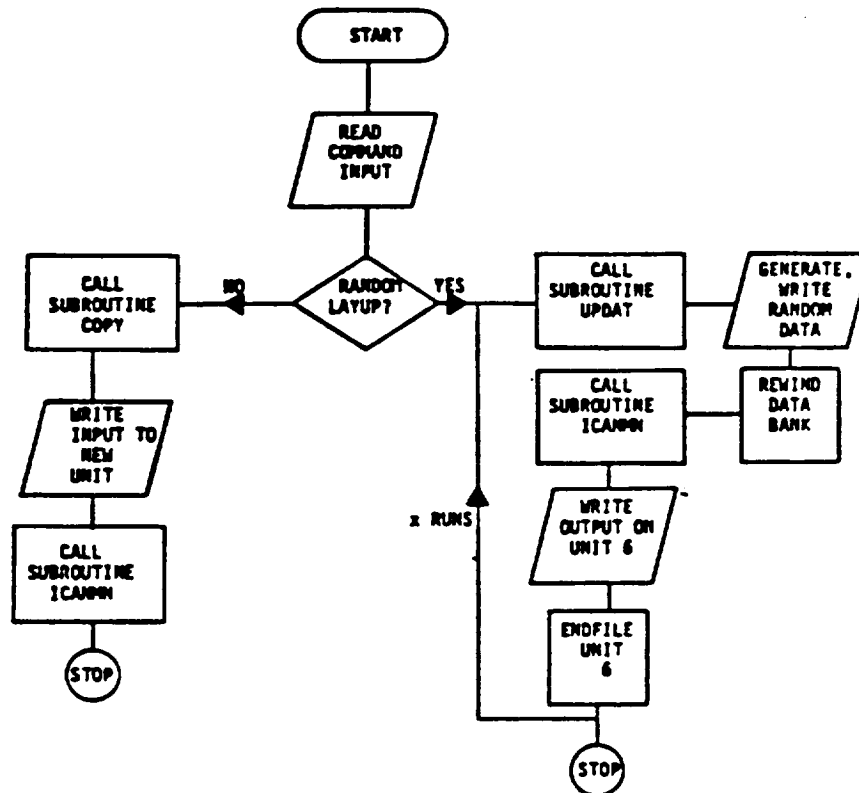
(a) data generation program
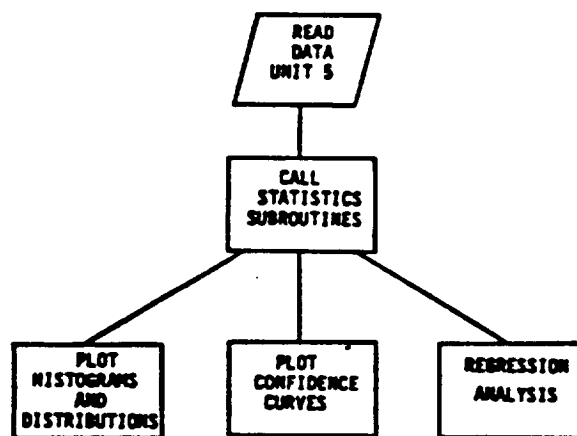


(b) analysis procedures

Fig. 8- Flow chart of Probabilistic Integrated
Composites Analyzer

## B. Generation of Pseudo Random Numbers

An integral part of any monte carlo simulation is the use of random numbers having a specified distribution which is assumed to characterize the process under study. Indeed, many statistics textbooks carry tables of random numbers as appendices. Simulations using large samples require many repeated calculations, each with different "random" numbers. Since filling of a computer memory with a large table of random numbers is wasteful, algorithms have been developed (Ref. 9) to generate streams of random numbers whenever needed in the process of calculations. The numbers used are usually obtained using some form of a recursion relation, hence the sequence is termed pseudo-random.

### 1. Uniform Distribution

The starting point for many random number schemes is the uniform random number generator, which simulates a sample from the uniform distribution. A continuous random variable has a uniform distribution over an interval a to b ( b > a ) if it is equally likely to take on any value in this interval. The probability density function is thus constant over ( a,b ) and has the form

$$f(x) = \frac{1}{b - a} \quad a \leq x \leq b$$
$$= 0 \quad \text{elsewhere}$$

The probability distribution function is, on integrating

$$F(x) = 0 \quad \quad x < a$$
$$= \frac{x - a}{b - a} \quad a \leq x \leq b$$

$$= 1 \qquad\qquad x > b$$

The uniform distribution is shown in density and distribution form in Figs. 9a and 9b.

Lehmer (Ref. 10) proposed the congruential method of generating pseudo random numbers conforming to the uniform distribution. The recurrence relation takes the form:

$$x_i = (ax_{i-1} + b ) \quad \text{modulo } m$$

where the notation signifies that $x_i$ is the remainder when $(ax_{i-1} + b)$ is divided by m. The multiplier a, increment b, and modulus m are integers. The starting value $x_0$ must be assumed, and is known as the "seed" of the generator. Generators for which b = 0 are known as multiplicative. They are called mixed when b is nonzero. Because selection of the multiplier a and modulus m strongly influence the generator, most generators in use are of the multiplicative form. A discussion of the choice of parameters, maximum period, and degree of correlation of this generator is available (Ref. 11).

For a given uniform random number u on the interval (0,1) a random number x having a desired distribution $F(x)$ is often obtained by solving the equation $u = F(x)$ for x (Ref. 12). Since the process requires the determination of the inverse distribution function $F^{-1}(x)$, its use depends on the ease of deriving the expression or some approximation. The following sections describe the distributions used, and methods for generating random numbers on those distributions.

## 2. Normal (Gaussian) Distribution

The most common distribution is the familiar normal distribution, with the "bell shaped" density function, given by

$$f(x;\mu,\sigma^2) = \frac{1}{\sqrt{2\pi\sigma^2}} \exp\left[ -\frac{(x-\mu)^2}{2\sigma^2} \right]$$

$$-\infty < x < \infty, \quad \mu < \infty, \quad \text{and} \quad \sigma > 0$$

with mean $\mu$ and standard deviation $\sigma$. The distribution function is written

$$F(x) = \frac{1}{\sqrt{2\pi\sigma^2}} \int_{-\infty}^{x} \exp\left[ -\frac{(u-\mu)^2}{2\sigma^2} \right] du$$

which cannot be expressed in closed form analytically but can be numerically evaluated at any value of x.

The Box-Muller or "Polar" method (Ref. 13) is most commonly used for generating random deviates from a mean to approximate the normal distribution. If $x_1$ and $x_2$ are independent uniform random variables, then

$$y_1 = \sigma(-2 \ln x_1)^{0.5} \cos 2\pi x_2 + \mu$$
$$y_2 = \sigma(-2 \ln x_1)^{0.5} \sin 2\pi x_2 + \mu$$

are independent random variables with the standard normal distribution having mean $\mu$ and standard deviation $\sigma$.

## 3. Gamma Distribution

The gamma distribution is a two-parameter distribution which is flexible in fitting a variety of random processes. It is a one sided distribution in that physical quantities that are limited to values in the positive range are frequently modeled by it. Its density function is given by

$$f(x) = \frac{\lambda^k}{\Gamma(k)} e^{-\lambda x} x^{k-1}$$

where $x, \lambda, k > 0$, and $k$ is an integer.

The parameters $\lambda$ and $k$ may be interpreted as scale and shape parameters, respectively. $\Gamma(k)$ is the well known gamma function,

$$\Gamma(k) = \int_0^\infty u^{k-1} e^{-u} du,$$

which is widely tabulated. The gamma distribution function is given by

$$F(x) = \frac{\lambda^k}{\Gamma(k)} \int_0^x u^{k-1} e^{-\lambda u} du$$

$$= \frac{\Gamma(k, \lambda x)}{\Gamma(k)} \qquad x \geq 0$$

$$= 0 \qquad \text{elsewhere}$$

where $\Gamma(k, u)$ is the incomplete gamma function

$$\Gamma(k, u) = \int_0^u x^{k-1} e^{-x} dx$$

which is also widely tabulated. For integer values of $k$,

$$\Gamma(k) = (k-1)!$$

and the gamma distribution is known as the Erlangian distribution after A. K. Erlang, who introduced it in the theory of queues and Markov processes.

Gamma variates are generated using the sequence

$$u_1, u_2, u_3, \cdots \cdots u_k$$

satisfying the uniform distribution on the interval $(0,1)$.

The recursion relation is

$$y_i = - \frac{1}{\lambda} \ln u_i,$$

$$x = \sum_{i=1}^{k} y_i = - \frac{1}{\lambda} \ln \prod_{i=1}^{k} u_i$$

where $x$ is a gamma variate having parameters $\lambda$ and $k$ (Ref. 14).

## 4. Weibull Distribution

The Weibull distribution (Ref. 15) is most popular when modeling problems of reliability, material strength, and fatigue. The Weibull density function is given by

$$f(x;\alpha,\beta) = \alpha\beta x^{\beta-1} \exp(-\alpha x^\beta)$$

$$0 \leq x < \infty, \quad \alpha > 0, \quad \beta > 1$$

where $\alpha$ and $\beta$ are the shape and scale parameters, respectively. The cumulative distribution function

$$y = F(x) = 1 - \exp[-(x/\beta)^\alpha]$$

leads immediately to the inverse relationship

$$F^{-1}(y) = x = -\beta[\ln(1-y)]^{1/\alpha}$$

as the desired Weibull random generator when $y$ is a uniform random variable.

Figures 9-12 show the above distributions in analytical form.

(a) density       (b) distribution
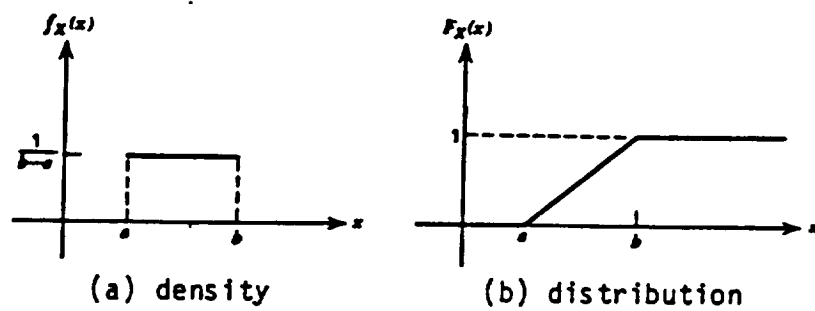
Fig. 9- Uniform Distribution:  general form.



(a) density
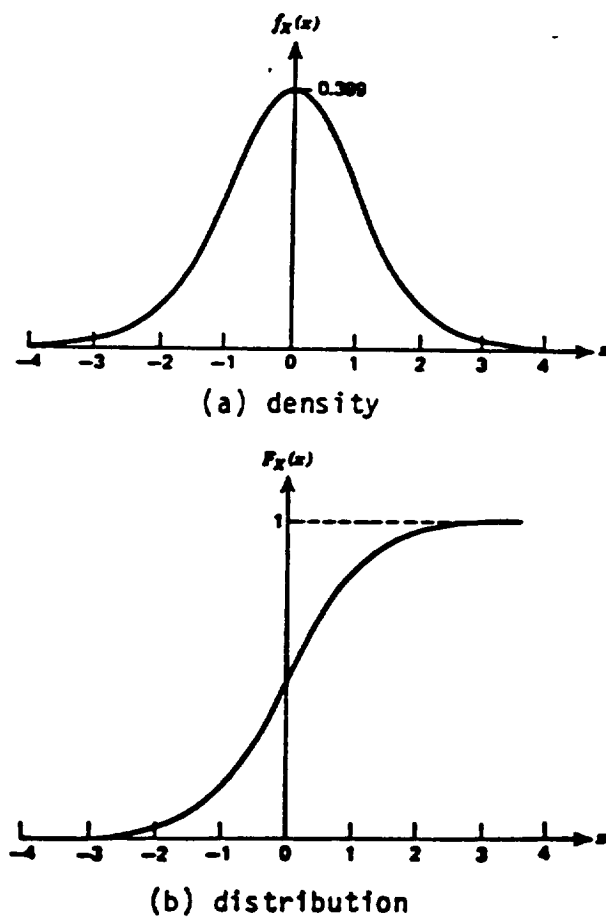


(b) distribution

Fig. 10- Normal Distribution
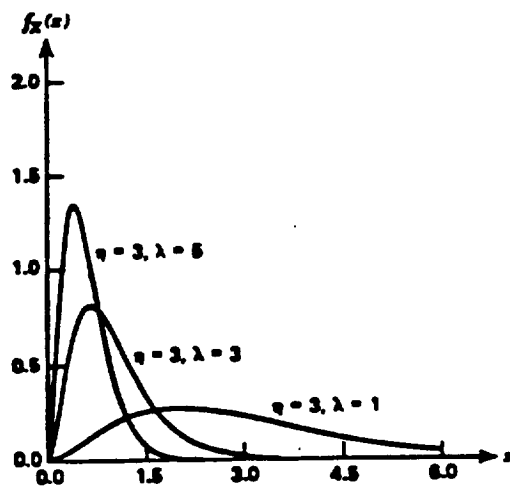
Fig. 11- Gamma Distribution density functions.
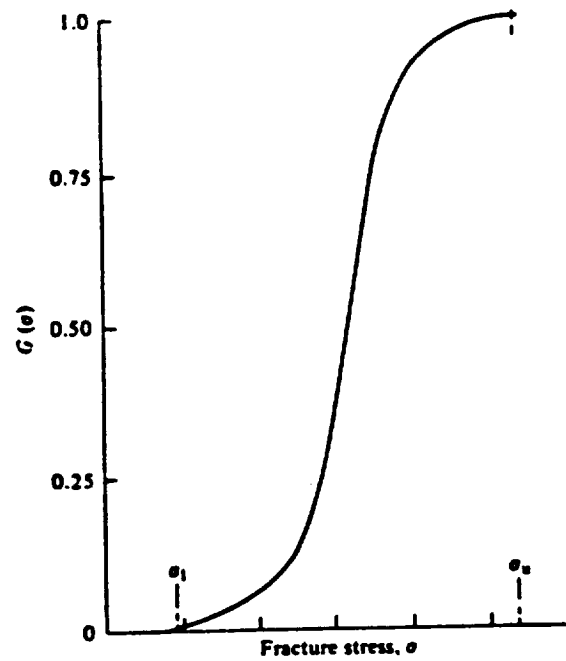


Fig. 12- Weibull Distribution function.

## C. Distribution Assumptions

The variables chosen for variation are those for which reasonable assumptions can be made to describe their distribution. The fiber geometric configuration with respect to ply axes is assumed to follow a normal distribution with mean of zero (degrees) and some small standard deviation, to be specified. The fiber volume ratio is assumed to be normally distributed about some mean between 0.3 and 0.7. The void volume ratio, which is ideally small, is assumed to follow a gamma distribution skewed toward zero. (Note that in the gamma distribution used, a value of zero has a probability of zero. This model is chosen because the state of most present manufacturing technology precludes the fabrication of a fiber composite completely free of void.)

The properties of individual fibers and matrix are varied. The normal and shear moduli are assumed to follow the normal distribution, and the strengths are assumed to be Weibull distributed.

Figs. 13-27 show the results of random number generation in each distribution studied. The density (or histogram) and cumulative distribution plots are shown. Several weibull and gamma distribution simulations are shown, to demonstrate the effects of assumed parameter variations on the distribution sampling.

## HISTOGRAM FOR
## NORMAL GENERATOR



Mean = 0.0

Standard
Deviation = 1.0
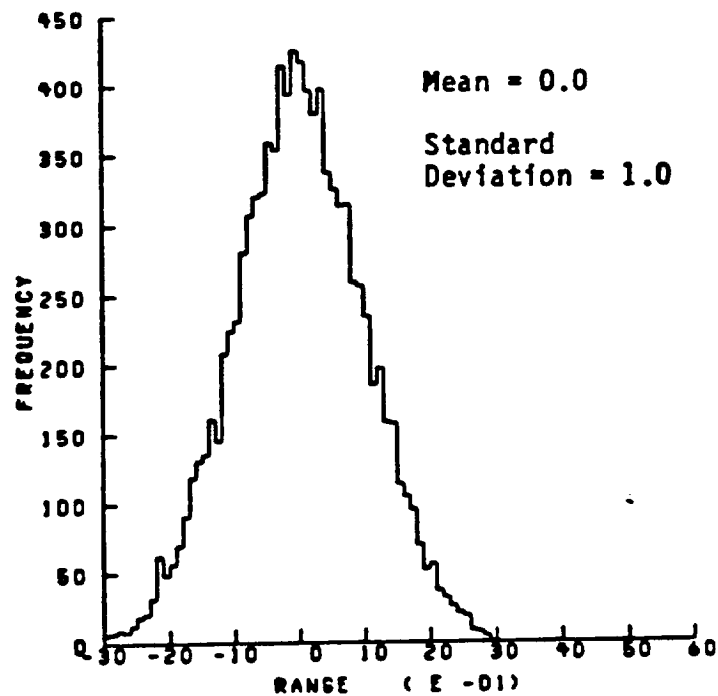
(a) histogram

## DISTRIBUTION OF
## NORMAL GENERATOR



Mean = 0.0

Standard
Deviation = 1.0
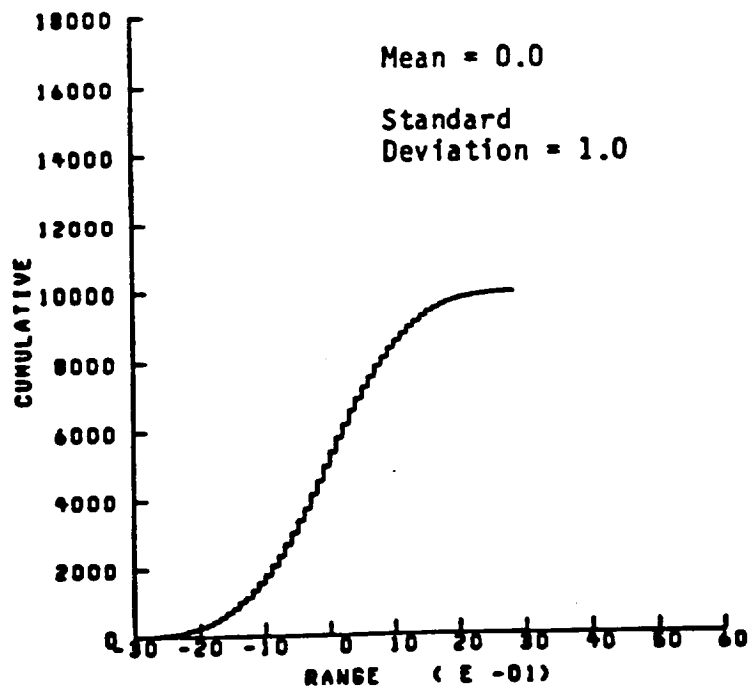
(b) cumulative distribution

Fig. 13- Normal Distribution Simulation with mean of
0.0 and standard deviation of 1.0.

**HISTOGRAM FOR
GAMMA GENERATOR**
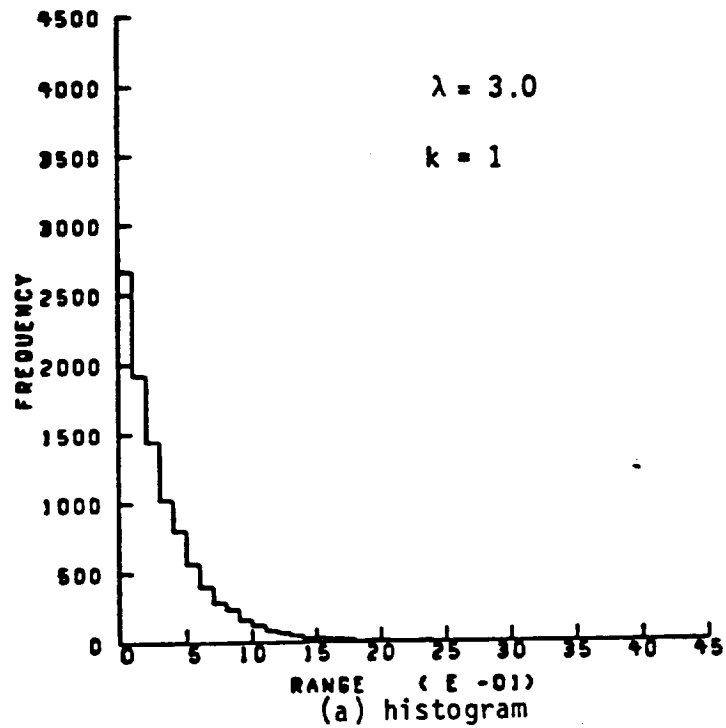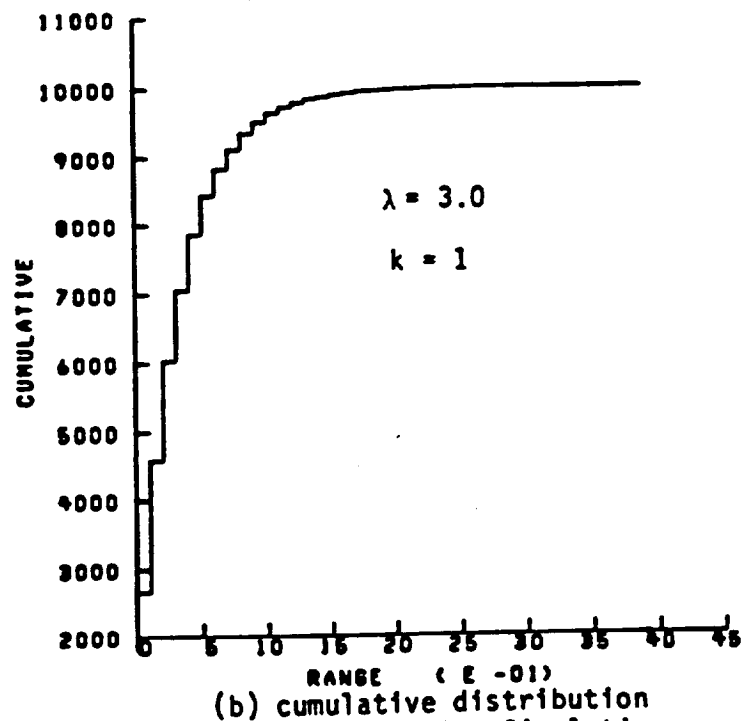
$\lambda = 3.0$

$k = 1$

(a) histogram

**DISTRIBUTION OF
GAMMA GENERATOR**

$\lambda = 3.0$

$k = 1$

(b) cumulative distribution

Fig. 14- Gamma Distribution Simulation

HISTOGRAM FOR
GAMMA GENERATOR



$\lambda = 5.0$

$k = 3$

(a) histogram

DISTRIBUTION OF
GAMMA GENERATOR



$\lambda = 5.0$

$k = 3$

(b) cumulative distribution

Fig. 15- Gamma Distribution Simulation

HISTOGRAM FOR
GAMMA GENERATOR

$\lambda = 3.0$

$k = 3$

(a) histogram

DISTRIBUTION OF
GAMMA GENERATOR

$\lambda = 3.0$

$k = 3$

(b) cumulative distribution

Fig. 16- Gamma Distribution Simulation

**HISTOGRAM FOR**
**GAMMA GENERATOR**

$\lambda = 3.0$

$k = 5$

FREQUENCY

RANGE ( E -01)

(a) histogram

**DISTRIBUTION OF**
**GAMMA GENERATOR**

$\lambda = 3.0$

$k = 5$

CUMULATIVE

RANGE ( E -01)
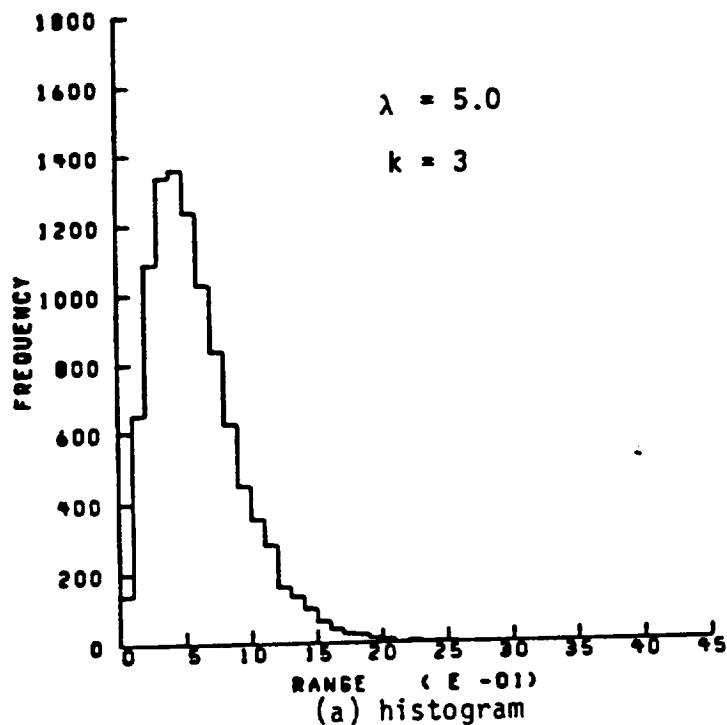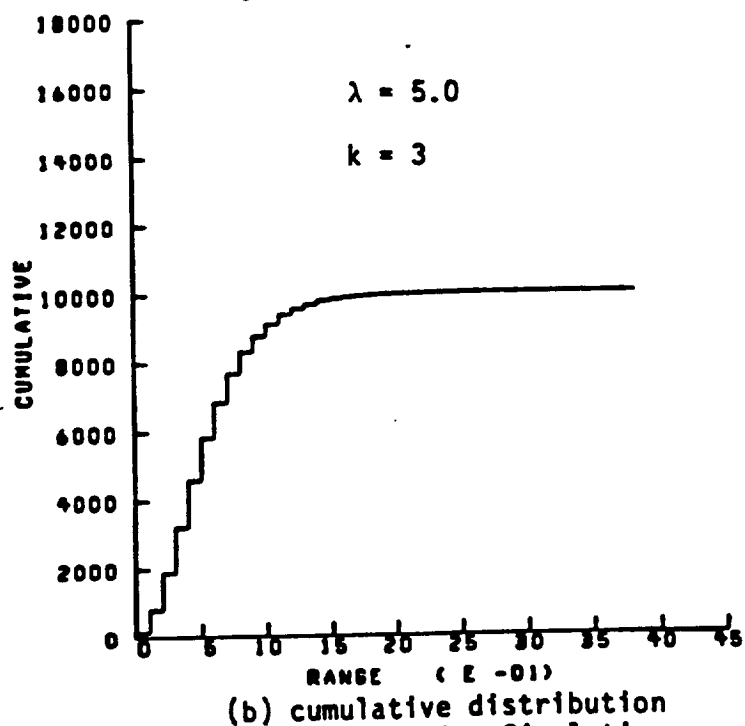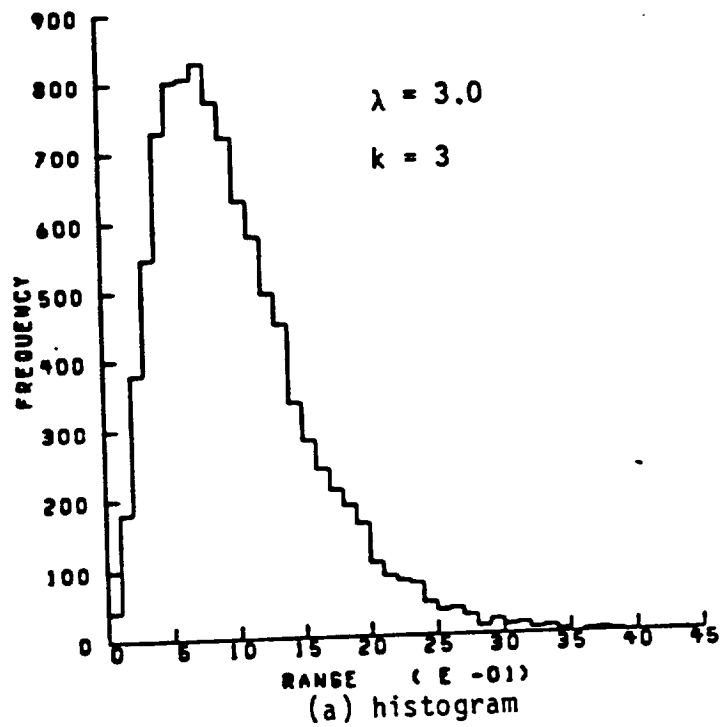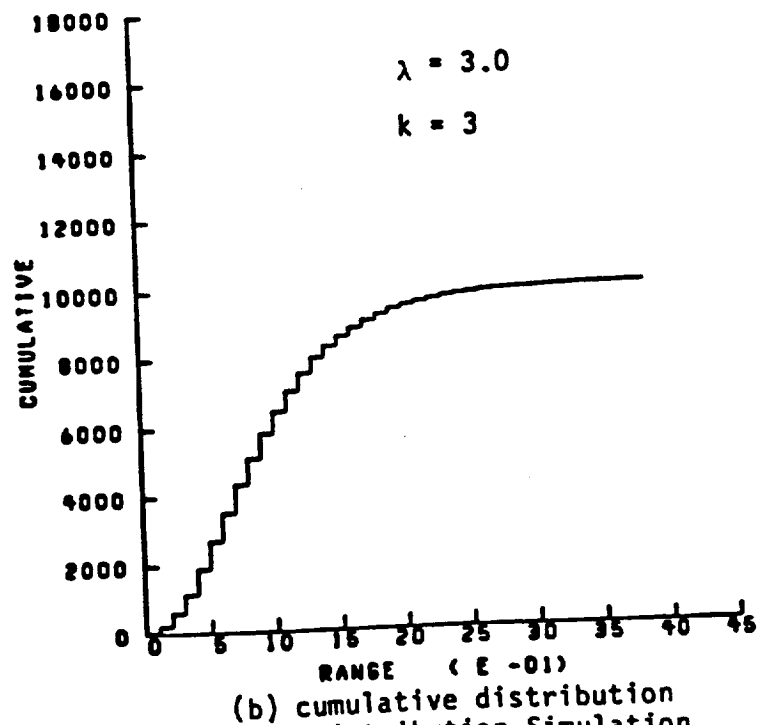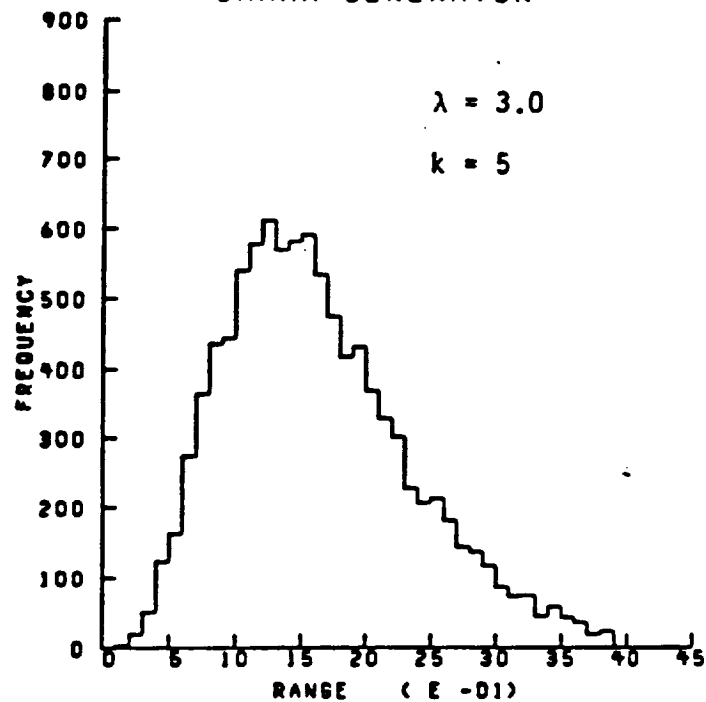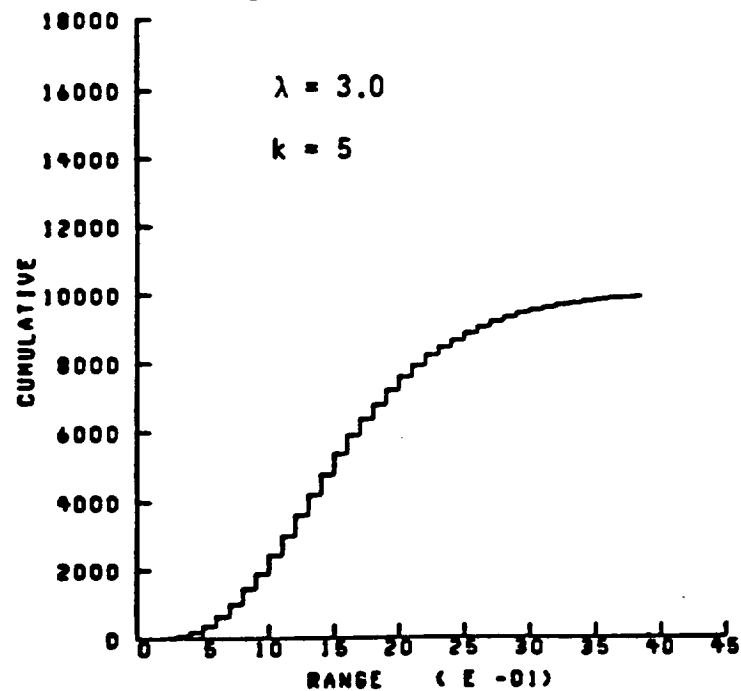
(b) cumulative distribution

Fig. 17- Gamma Distribution Simulation

# HISTOGRAM FOR
# HEIBULL GENERATOR

β = 13 ksi.

α = 10



RANGE ( E 00) (ksi)

(a) histogram

# DISTRIBUTION OF
# HEIBULL GENERATOR

β = 13 ksi.

α = 10



RANGE ( E 00) (ksi)
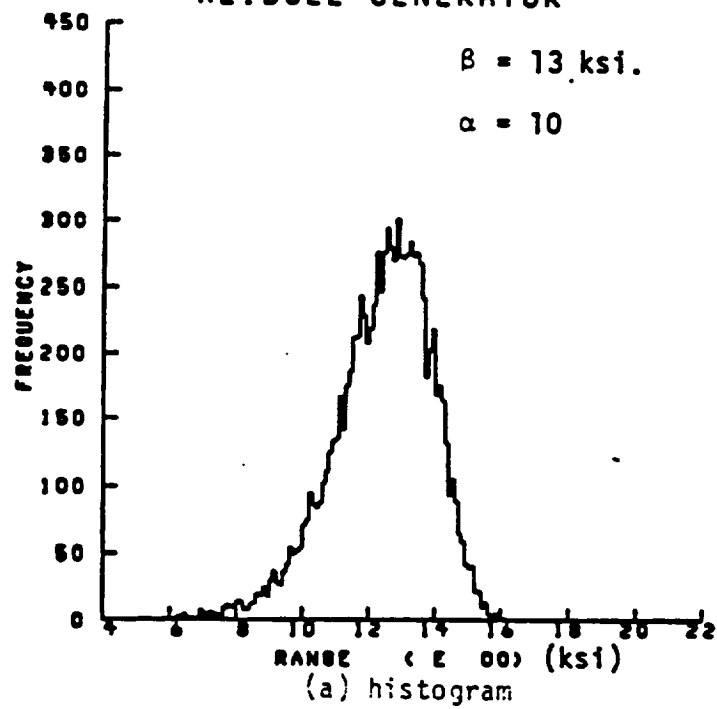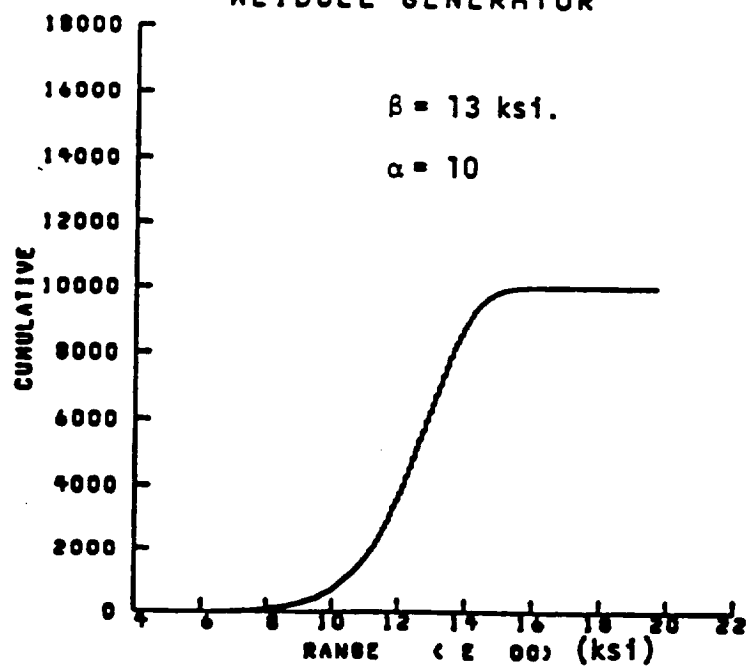
(b) cumulative distribution
Fig. 18- Weibull Distribution Simulation
Matrix Shear Strength

HISTOGRAM FOR
HEIBULL GENERATOR

β = 13 ksi.

α = 20

(a) histogram

DISTRIBUTION OF
HEIBULL GENERATOR

β = 13 ksi.

α = 20
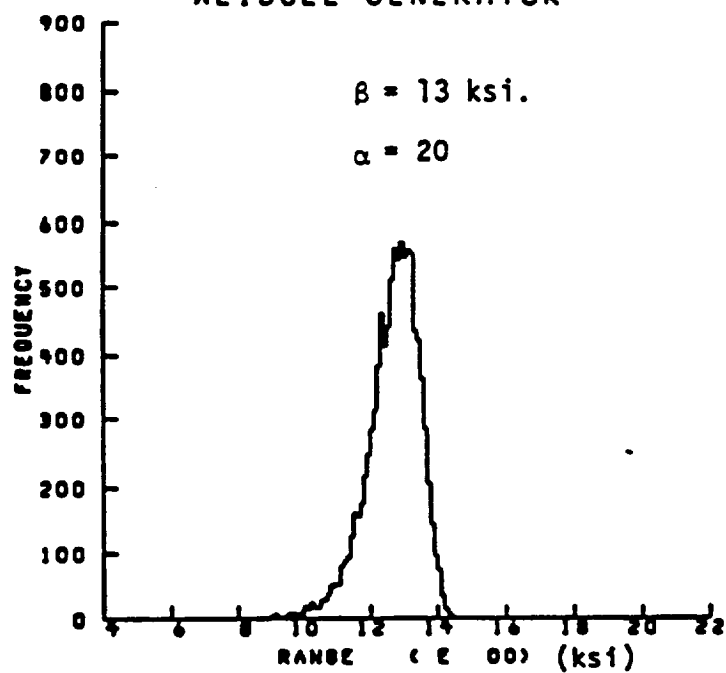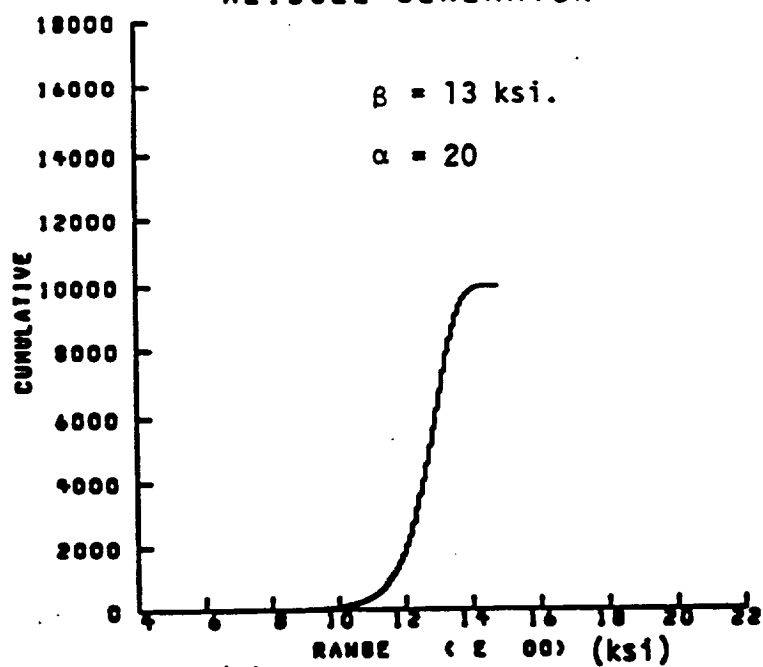
(b) cumulative distribution

Fig. 19- Weibull Distribution Simulation
Matrix Shear Strength

## HISTOGRAM FOR
## WEIBULL GENERATOR



(a) histogram

## DISTRIBUTION OF
## WEIBULL GENERATOR



(b) cumulative distribution

Fig. 20- Weibull Distribution Simulation
Matrix Tensile Strength

# HISTOGRAM FOR
## WEIBULL GENERATOR

β = 15 ksi.

α = 10

FREQUENCY

RANGE ( E 00) (ksi)

(a) histogram

# .DISTRIBUTION OF
## WEIBULL GENERATOR

β -=15 ksi.

α =10

CUMULATIVE

RANGE ( E 00) (ksi)
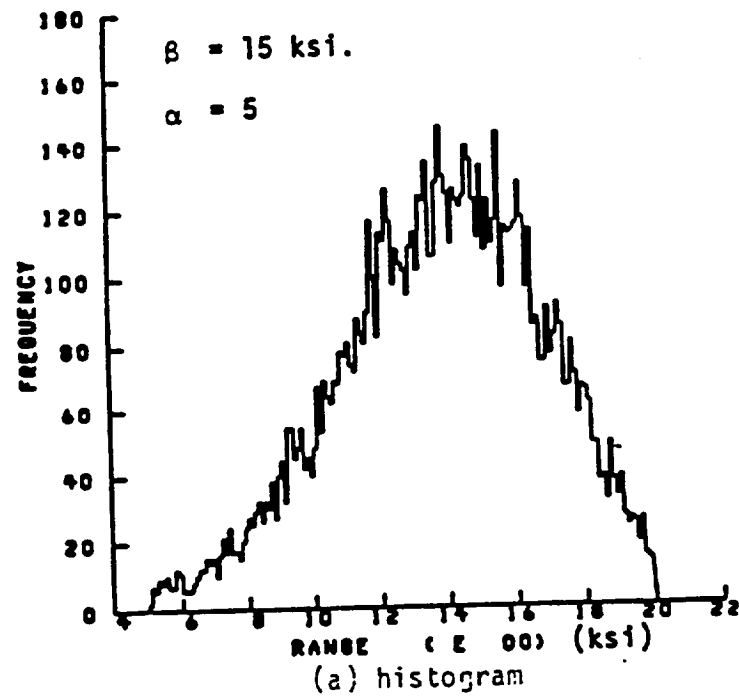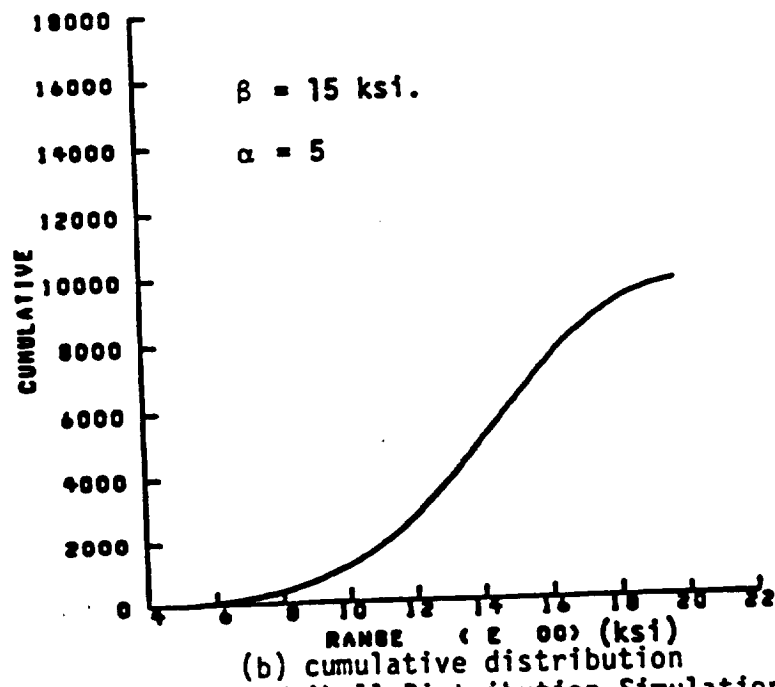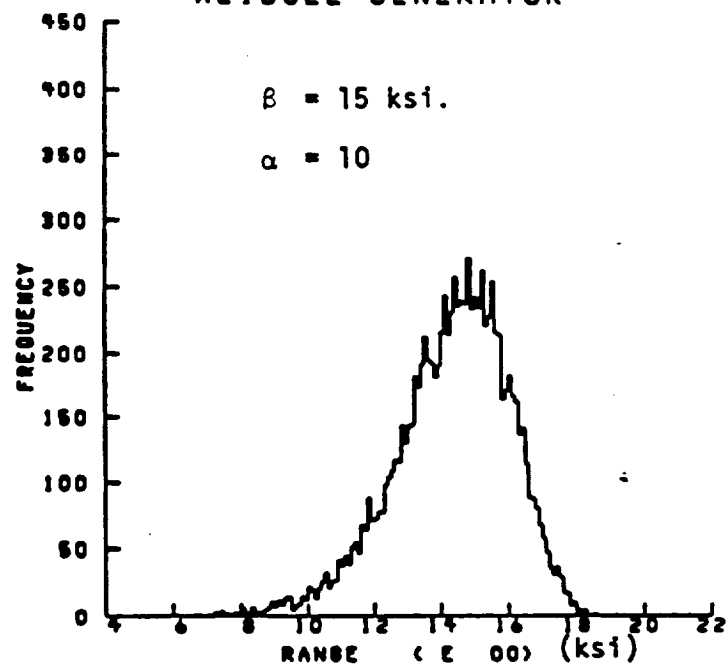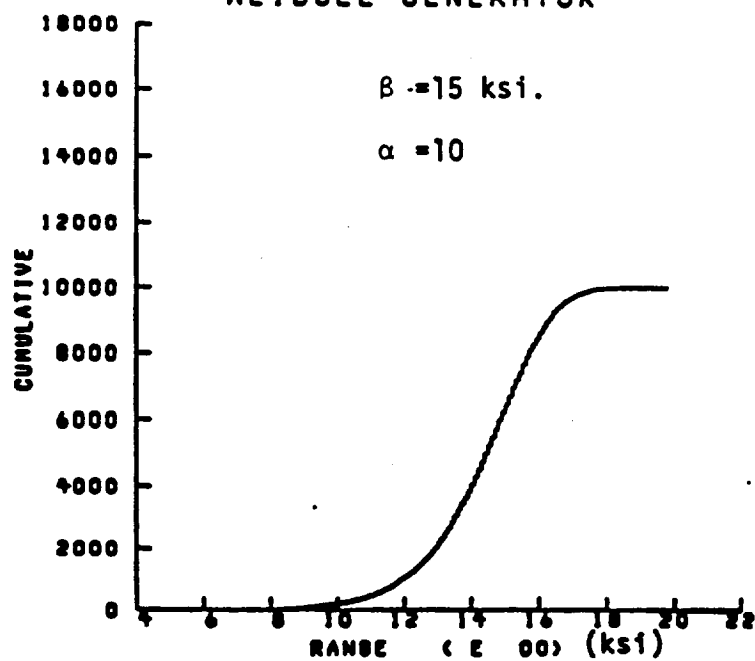
(b) cumulative distribution

Fig. 21- Weibull Distribution Simulation
Matrix Tensile Strength

HISTOGRAM FOR
HEIBULL GENERATOR

β = 15 ksi.

α = 15

FREQUENCY

RANGE ( E 00) (ksi)

(a) histogram

DISTRIBUTION OF
HEIBULL GENERATOR

β = 15 ksi.

α = 15

CUMULATIVE

RANGE ( E 00) (ksi)
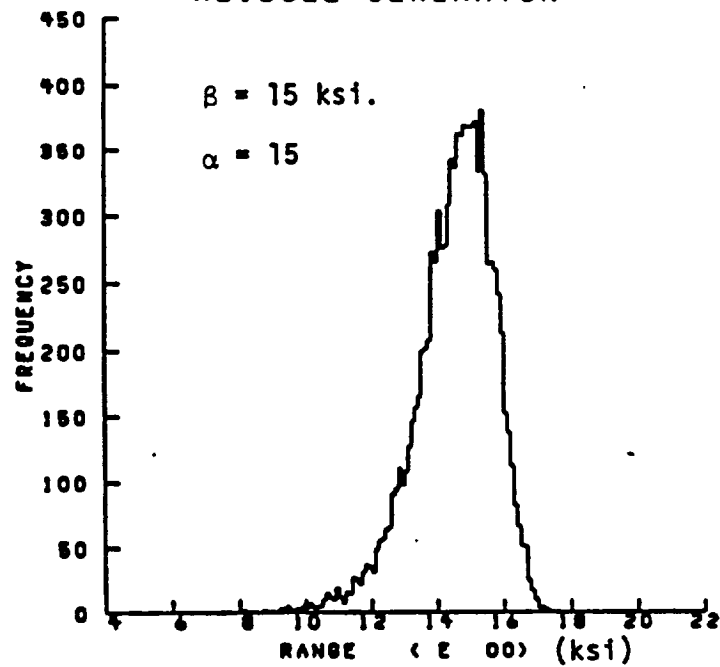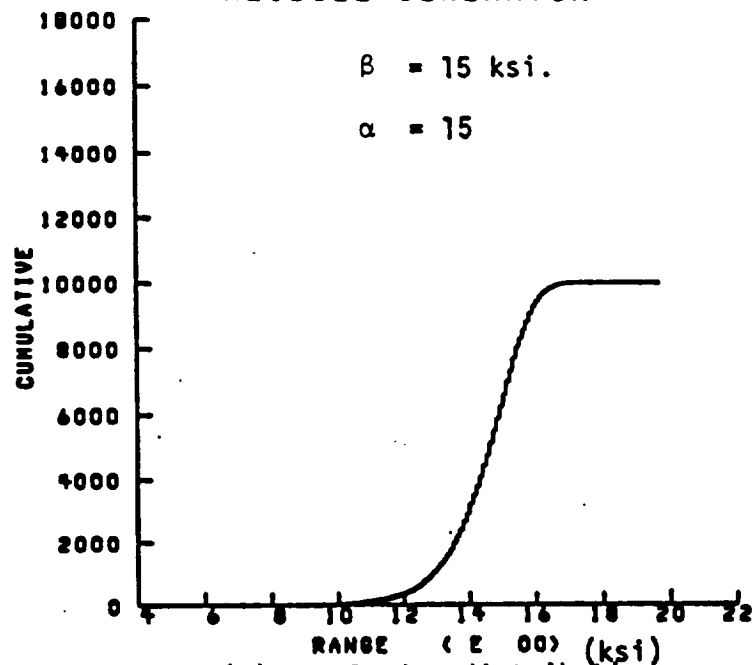
(b) cumulative distribution

Fig. 22- Weibull Distribution Simulation
Matrix Tensile Strength

HISTOGRAM FOR
WEIBULL GENERATOR

$\beta = 35$ ksi.

$\alpha = 10$

FREQUENCY

RANGE ( E 00) (ksi)

(a) histogram

DISTRIBUTION OF
WEIBULL GENERATOR

$\beta = 35$ ksi.

$\alpha = 10$

CUMULATIVE

RANGE ( E 00) (ksi)
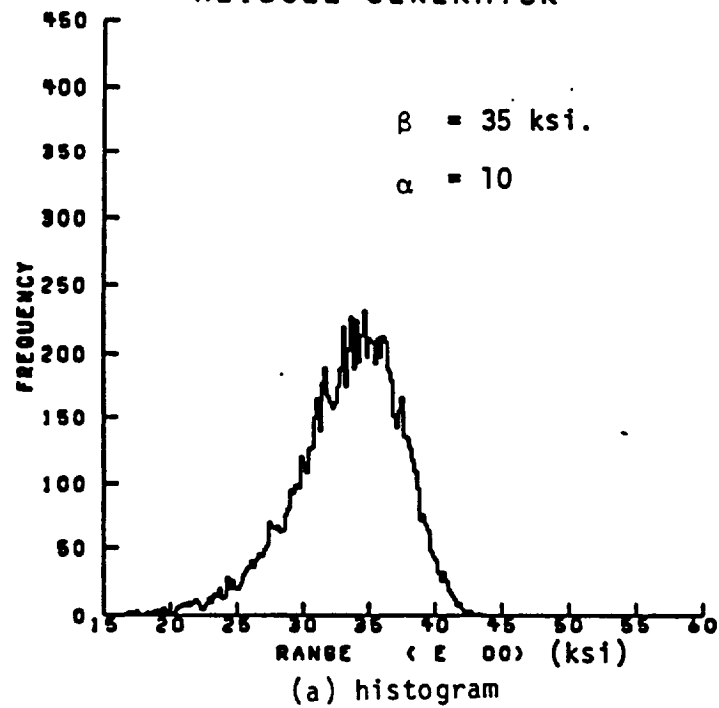
(b) cumulative distribution
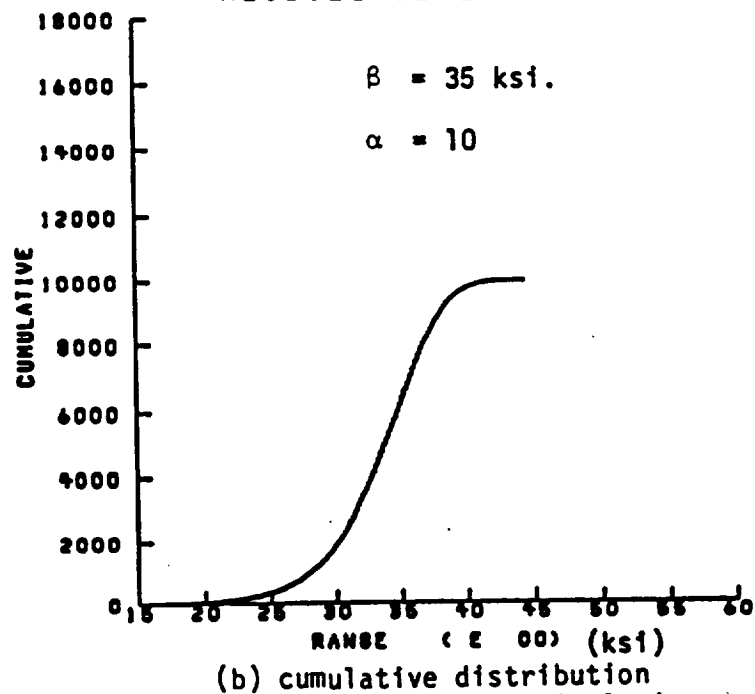
Fig. 23- Weibull Distribution Simulation
Matrix Compressive Strength

HISTOGRAM FOR
WEIBULL GENERATOR
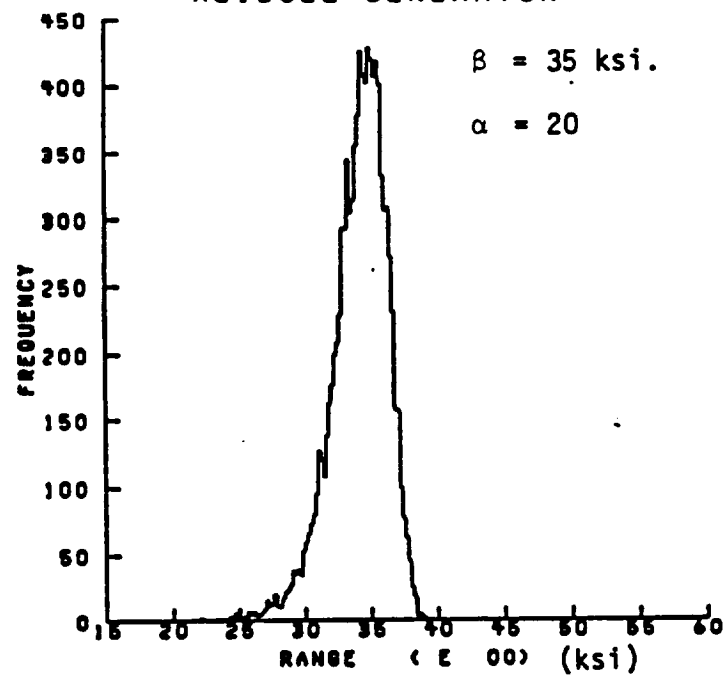


(a) histogram

DISTRIBUTION OF
WEIBULL GENERATOR
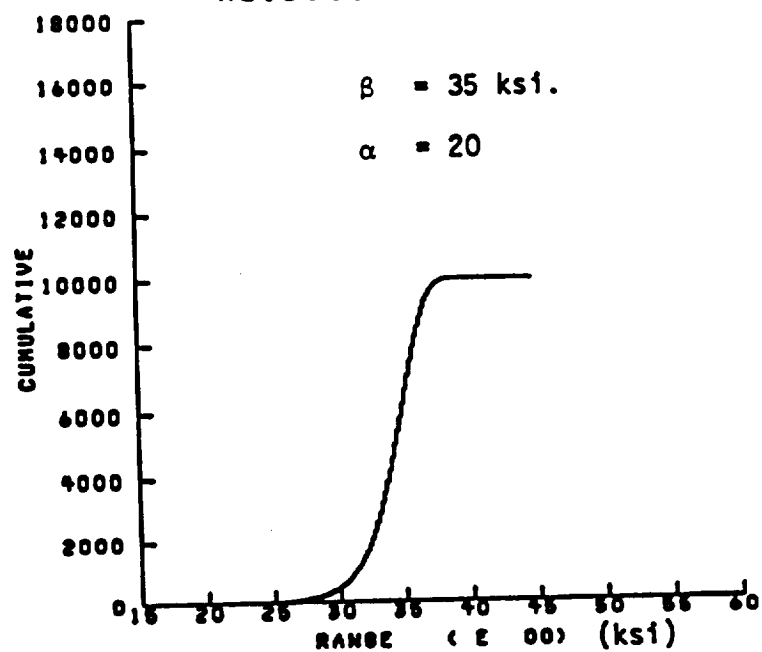


(b) cumulative distribution

Fig. 24- Weibull Distribution Simulation
Matrix Compressive Strength

# HISTOGRAM FOR
# WEIBULL GENERATOR

β = 400 ksi.

α = 10

FREQUENCY

RANGE    ( E  01) (ksi)

(a) histogram

# DISTRIBUTION OF
# WEIBULL GENERATOR

β = 400 ksi.

α = 10

CUMULATIVE

RANGE    ( E  01) (ksi)

(b) cumulative distribution

Fig. 25- Weibull Distribution Simulation
Fiber Tensile and Compressive Strength

HISTOGRAM FOR
WEIBULL GENERATOR



β = 400 ksi.

α = 15

(a) histogram

DISTRIBUTION OF
WEIBULL GENERATOR



β = 400 ksi.

α = 15
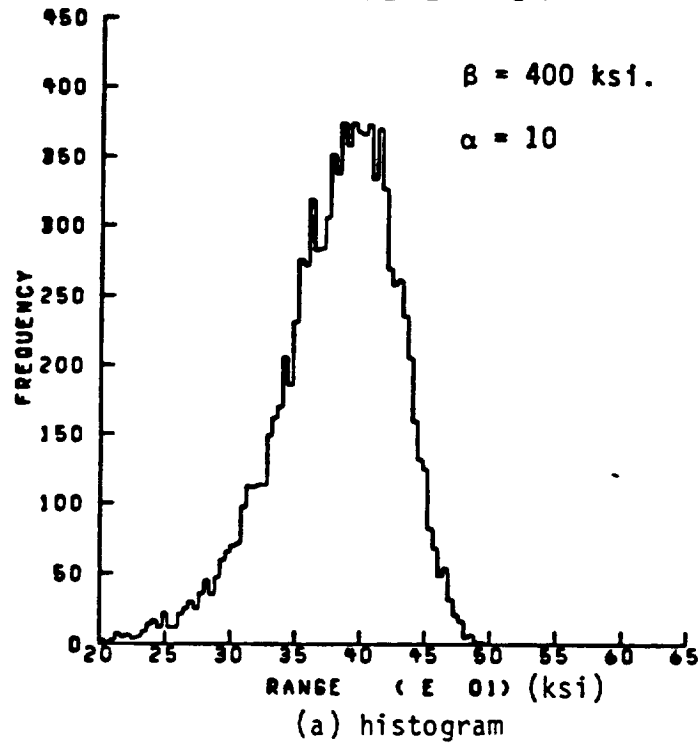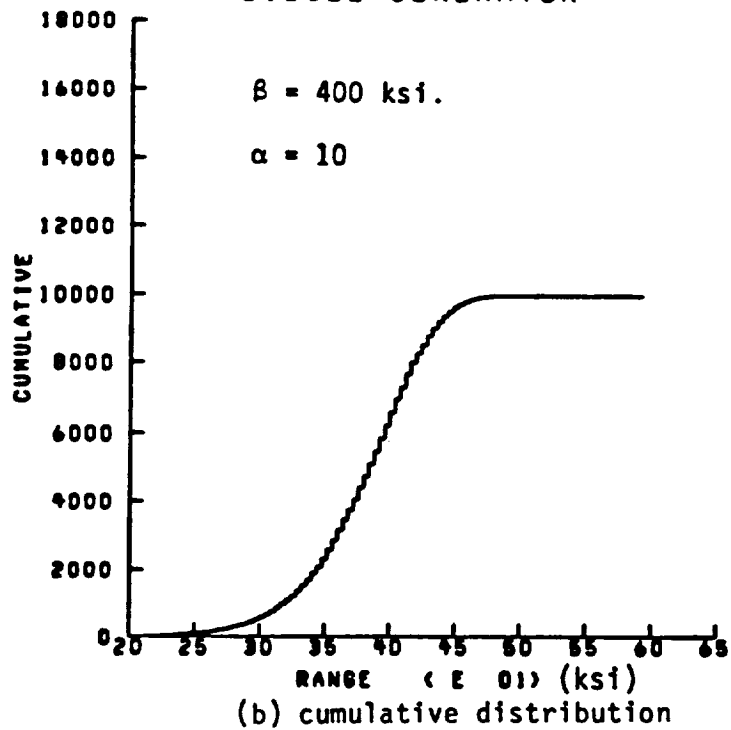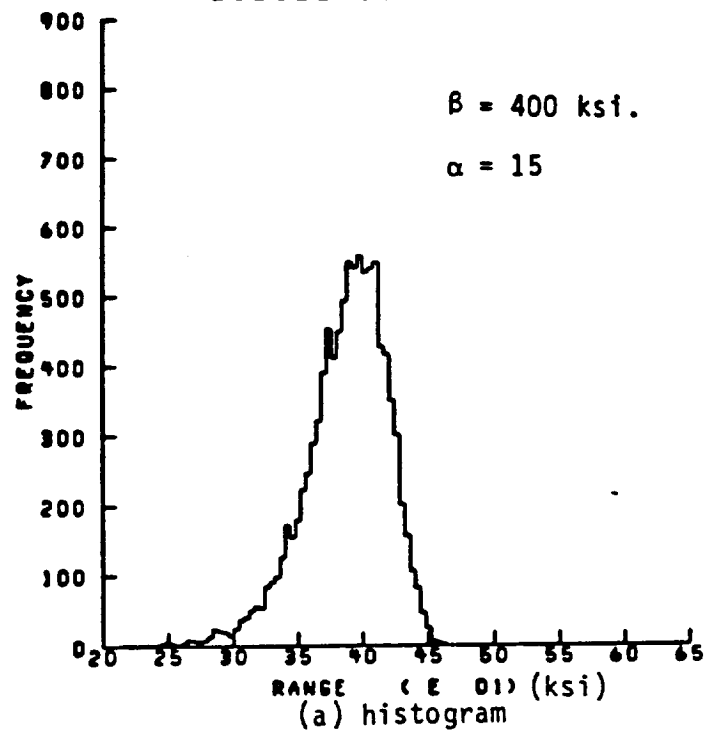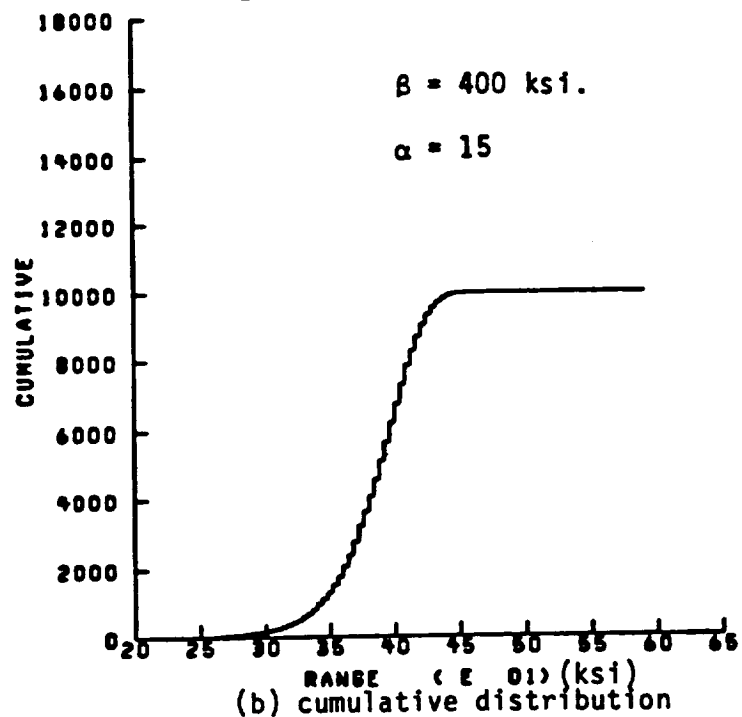
(b) cumulative distribution
Fig. 26- Weibull Distribution Simulation
Fiber Tensile and Compressive Strength

HISTOGRAM FOR
WEIBULL GENERATOR



$\beta$ = 400 ksi.

$\alpha$ = 20

(a) histogram

DISTRIBUTION OF
WEIBULL GENERATOR



$\beta$ = 400 ksi.

$\alpha$ = 20
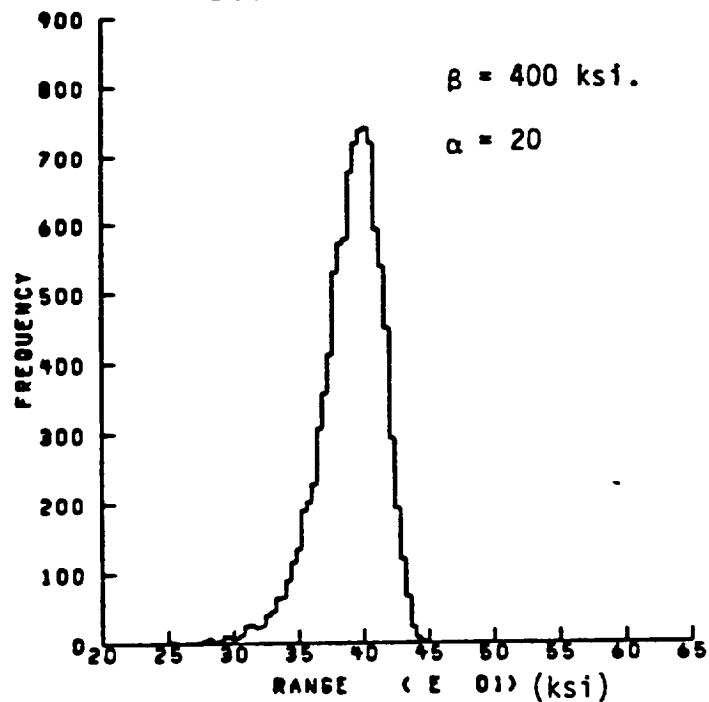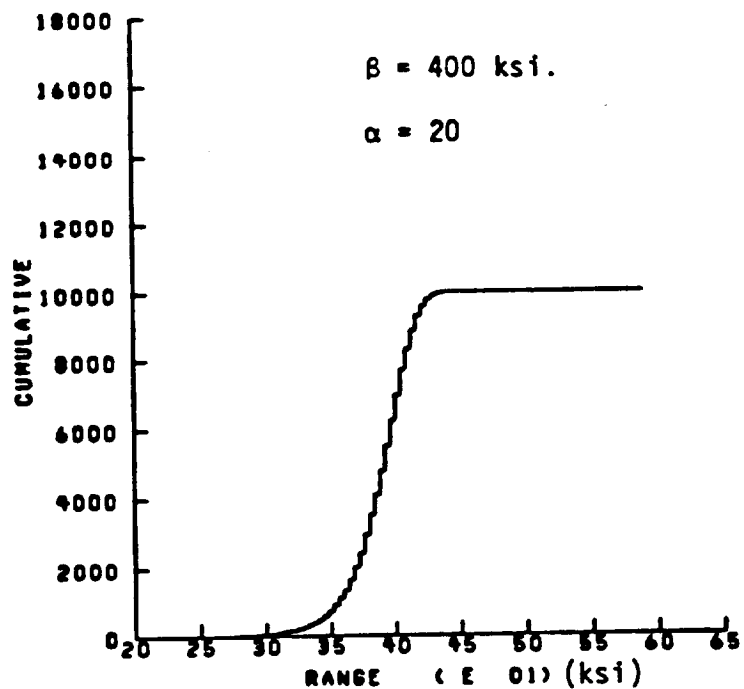
(b) cumulative distribution

Fig. 27- Weibull Distribution Simulation
Fiber Tensile and Compressive Strength

## D. Use of ICAN

This section describes the essential theories and assumptions incorporated in the ICAN program. The symbolic notation conventions, formulations, and definitions are included in Appendix B.

### 1. Composite Micromechanics

The branch of composite mechanics which relates ply properties to constituent properties is known as composite micromechanics. The inputs consist not only of constituent material properties (fiber and matrix), but geometric configuration and fabrication process. Output includes ply hygral, thermal, and mechanical properties. The assumptions for equation development are: (Ref. 16)

1. The Mechanics of Materials are used to derive the equations, allowing each property to be individually identified.
2. The ply resists in-plane loads according to the schematic shown in Fig. 4(b).
3. The ply and its constituents behave in a linear elastic manner to fracture (see Fig. 28).
4. The ply is transversely isotropic in the 2-3 plane.
5. The matrix is isotropic.
6. Complete bond exists at the fiber-matrix interface.

The direction conventions and terminology used in the equations are:

1. Properties measured along fiber direction are called longitudinal.
2. Properties measured transverse to fiber direction are called transverse.
3. In-plane shear is also known as intralaminar shear.
4. All ply properties are defined with respect to ply material axes (1,2,3) for description and analysis.

## 2. Laminate Theory

Classical laminate theory supplies a convenient procedure to predict the response of a laminate to external load. The theory uses anisotropic elasticity to obtain the stress-strain relationship for the basic lamina. The stress-strain relations of individual laminae are transformed to coincide with a global set of reference axes. The stress-stain law of the laminate in terms of the properties and distribution of individual laminae are calculated using a summation. Resultant forces and moments are defined by integrating the stresses through the thickness of the laminate. The plate constitutive equation is inverted, giving midplane strains and plate curvatures in terms of applied forces and moments. These strains and curvatures are substituted into the lamina stress-strain equation to obtain lamina stresses in the global system. The stresses obtained are then transformed into the principal material system of the lamina in question and compared with ultimate stresses obtained using failure criteria.

3. Strength Theories

The strength theories in ICAN make use of several assumptions. First, it is assumed that there are five characteristic values of strength of a unidirectional composite:

1. longitudinal tensile strength

2. longitudinal compressive strength (3 separate criteria)

    a. rule of mixtures

    b. fiber microbuckling

    c. delamination

3. transverse tensile strength

4. transverse compressive strength

5. in-plane or intralaminar shear strength

The fracture modes usually associated with these strengths are shown schematically in Fig. 29.

Once ply strengths are calculated (in the ply coordinate systems), geometric transformations are used to calculate composite failure loads. The process used is briefly described below.

1. Calculate loads (in composite system) required to induce load equal to ply strengths (in ply systems) for each mode.

2. Calculate minimum of failure loads for each ply.

3. Calculate minimum of failure loads of all plies, and use this load as the failure strength of the composite for a particular failure mode.
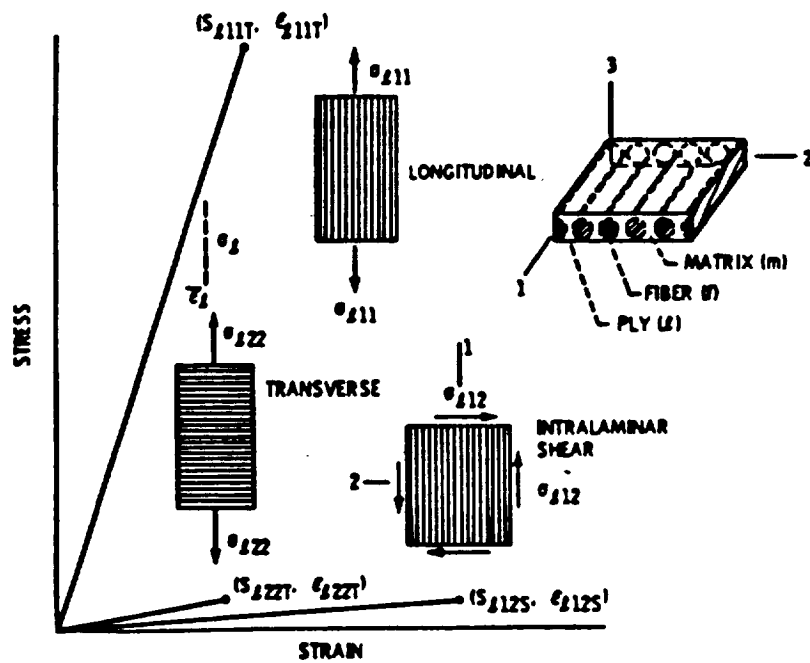
Fig. 28- Typical Stress-Strain behavior of unidirectional fiber composites.
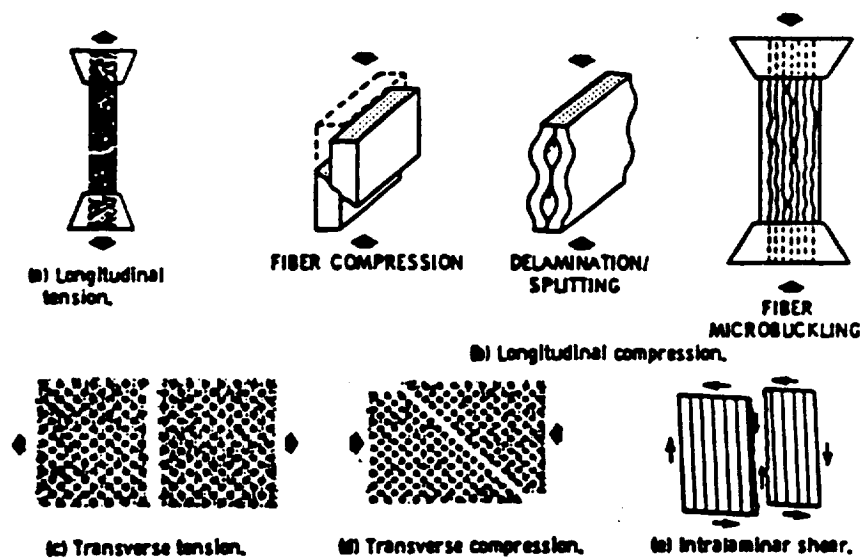


Fig. 29- In-plane fracture modes of unidirectional (ply) fiber composites.

## E. Review of Applicable Statistical Concepts

Composite properties are calculated for large samples using a specific set of distributions of input properties. In this context, small sampling theory does not apply, because the samples used are sufficiently large.

### 1. Sample Means

Calculation of the mean sample values proceeds by defining

$$\text{mean} = \bar{x} = \frac{\sum_{i=1}^{n} x_i}{n}$$

where   n = sample size

$x_i$ = sample data values

The population mean is unknown, so the sample mean is assumed to be the best estimator of the population mean.

### 2. Sample Standard Deviation

An estimate of the population standard deviation is calculated using the statistically efficient estimator

$$\sigma = \left[ \frac{n}{n-1} \sum_{i=1}^{n} (x_i - \bar{x})^2 \right]^{1/2} \quad , \quad n \geq 30$$

### 3. Confidence Interval Estimates

An important problem in the area of statistical inference is the estimation of population parameters (such as mean, variance, etc.) from sample statistics. Parameters $\bar{x}$ and $\sigma$ are the mean and standard

deviation of the sampling distribution of a statistic S. The sampling distribution of S is assumed as approximately normal (which is true for many statistical distributions if $n \geq 30$). Confidence interval estimates are constructed for the statistic S. Thus, intervals are identified for which it can be asserted with a reasonable degree of certainty that they contain the parameter considered. Obviously, the degree of certainty (or confidence level) will vary with the size of the interval chosen. Values of confidence coefficients, $z_c$ , are associated with confidence levels. For example, an actual sample statistic S is expected to be found lying in the interval $(\bar{x} - z_c\sigma)$ to $(\bar{x} + z_c\sigma)$ (where $\sigma$ is the unknown population standard deviation) some percent of the time. Let the $z_c$ value in this example be 1. Assuming a normal sampling distribution, (with $z_c = 1$) the normal distribution area function specifies that S falls between $(\bar{x} - \sigma)$ and $(\bar{x} + \sigma)$ about 68.27% of the time. Similarly, the confidence of $\bar{x}$ lying in the interval $(S - \sigma)$ to $(S + \sigma)$ is about 68.27%. The endpoints of the intervals are known as confidence limits. Various confidence coefficients $z_c$, corresponding to frequently used confidence levels, have been tabulated.

In this work, the confidence interval for means is given in terms of the sample statistics by

$$\bar{x} \pm z_c \frac{\sigma}{\sqrt{n}}$$

where $z_c$ is the confidence coefficient, which takes on values of 1.645, 1.960, and 2.580 for the 90, 95, and 99% confidence levels,

respectively.

## 4. Regression

The term "regression" as used in the area of statistics refers to the process of formulating a mathematical model to explain randomly observed phenomena. Some functional form for the way each variable enters the model must be assumed. Comparison of the degree of fit of different assumed models ideally leads to a better model. The basic regression strategy used here consists of:

1. Assume a multiple linear regression model. The normal equations for such a model are:

$$\{Y\} = [X]\{\beta\} + \{\epsilon\}$$

where

$\{Y\}$ = vector of dependent variable values

$[X]$ = matrix of functions of independent variable

$\{\beta\}$ = regression "true" values

$\{\epsilon\}$ = errors

The normal equations can be solved as follows:

$$[X]^T\{Y\} = [X]^T[X]\{\beta\} + [X]^T\{\epsilon\}$$
$$\{b\} = [X^TX]^{-1}[X]^T\{Y\}$$

where

$\{b\}$ = parameter estimates

2. Use a standard statistical package (Ref. 17) to estimate regression parameters.

3. Calculate properties of regression parameter distributions to

assess model precision.

In the event that $[X^TX]$ is singular, implying that some of the

normal equations are linearly dependent, $[X^TX]^{-1}$ does not exist. The

model should be expressed in terms of fewer parameters, or should

include assumed restrictions on the parameters.

The square of the multiple correlation coefficient, $R^2$, is usually

calculated for each regression model, and supplies a convenient measure

of the degree of fit between data values $\{Y\}$ and values $\{\hat{Y}\}$

predicted by the regression equation. It is defined by

$$R^2 = \frac{\text{Sum of Squares due to regression model}}{\text{Total Sum of squares about mean } Y}$$

$$= \frac{\sum (\hat{Y}_i - \bar{Y})^2}{\sum (Y_i - \bar{Y})^2}$$

Frequently, it is necessary to determine if inclusion of particular

terms in a regression model is worthwhile. To this end, the extra

portion of the regression sum of squares which arises due to the terms

under consideration is calculated. The mean square (defined as the sum

of squares divided by the corresponding degrees of freedom) derived from

this extra sum of squares can be compared with $s^2$, the estimate of $\sigma^2$,

to see if it appears significantly large. If it does, the terms under

consideration should be included. The statistic is frequently compared to the appropriate percentage point of the F- distribution, which is tabulated.

Supopose the extra sum of squares due to a parameter, given that a number of other parameters are already in the model, is calculated. Symbolically,

$$SS(b_i \mid b_0, b_1, \ldots, b_{i-1}, b_{i+1}, \ldots, b_k) \qquad i = 1, 2, \ldots, k$$

represents a one degree of freedom ( 1 df ) sum of squares which measures the portion of the regression sum of squares due to the coefficient $b_i$. This is a measure of the value of adding a $\beta_i$ term to the model which previously did not include $\beta_i$. The corresponding mean square, equal to the SS (since it has one df) can be compared by an F- test to $s^2$. This is known as a partial F- test for the single parameter $\beta_i$, which is a special case of the F- test described earlier.

The stepwise regression procedure (Ref. 18) is a structured way to insert variables in order of correlation until the regression equation is satisfactory. The partial correlation coefficient measures the relative importance of terms not yet in the model, to choose the next candidate for entry. The analagous statistic, F- to enter (or F- to remove) is usually evaluated for each predictor at every stage as though it were the last term to enter the model, to determine if terms retained at a previous step have become superfluous, because of some linear dependence with terms now in the model. The largest F- statistic calculated at each step is compared with the appropriate percentage point of the F- distribution, and the predictor variable is entered (or

removed) based on the significance of this F- test. Testing of the least useful predictor is performed at every step. The $R^2$ statistic is calculated, to provide a measure of the value of the regression at each step. This stepwise linear regression scheme is used in this work because of its computational economy, and because it allows the analyst to assess the relative influence (or correlation) between individual predictor variables of a selected model and response for a particular data sample. Other schemes are available (Ref. 18), such as backward elimination. The stepwise procedure is recommended for its direct nature in testing the model with only significant predictor terms.

# CHAPTER III

## RESULTS

### A. Property Histograms and Distributions

In this work, fiber and matrix properties are allowed to assume a range of values to assess the sensitivity of the composite ply properties to constituent perturbations. Graphite fiber and epoxy matrix are used as the constituents. Initially, two separate samples of output data are generated and studied to demonstrate the effects of input parameter changes on composite material properties. These two cases are compared with a deterministic base case with no random input property generation. The data for all three cases is given in Table I.

The results of cases 2 and 3 are shown in histogram and cumulative distribution form in Figs. 30 - 42. The results of the deterministic case 1 are summarized in Table II, and can be easily compared with the histograms and distributions.

57

## TABLE I- INPUT DATA FOR SAMPLING

| INPUT | CASE 1 | CASE 2 | CASE3 |
|---|---|---|---|
| THETA(degrees) | 0.0 | – | – |
| $\mu$ | – | 0.0 | 0.0 |
| $\sigma$ | – | 5.0 | 10.0 |
| FVR | 0.50 | – | – |
| $\mu$ | – | 0.5 | 0.5 |
| $\sigma$ | – | 0.1 | 0.2 |
| VVR | 0.01 | – | – |
| $\lambda$ | – | 3.0 | 3.0 |
| k | – | 3 | 5 |
| EFP1(ksi) | 31000 | – | – |
| $\mu$ | – | 31000 | 31000 |
| $\sigma$ | – | 1500 | 3000 |
| EFP2(ksi) | 2000 | – | – |
| $\mu$ | – | 2000 | 2000 |
| $\sigma$ | – | 100 | 200 |
| GFP12(ksi) | 2000 | – | – |
| $\mu$ | – | 2000 | 2000 |
| $\sigma$ | – | 100 | 200 |
| GFP23(ksi) | 1000 | – | – |
| $\mu$ | – | 1000 | 1000 |
| $\sigma$ | – | 50 | 100 |
| SFPT(ksi) | 400 | – | – |
| $\beta$ | – | 400 | 400 |
| $\alpha$ | – | 20 | 10 |
| SFPC(ksi) | 400 | – | – |
| $\beta$ | – | 400 | 400 |
| $\alpha$ | – | 20 | 10 |
| EMP(ksi) | 500 | – | – |
| $\mu$ | – | 500 | 500 |
| $\sigma$ | – | 25 | 50 |
| SMPT(ksi) | 15 | – | – |
| $\beta$ | – | 15 | 15 |
| $\alpha$ | – | 20 | 10 |
| SMPC(ksi) | 35 | – | – |
| $\beta$ | – | 35 | 35 |
| $\alpha$ | – | 20 | 10 |
| SMPS(ksi) | 13 | – | – |
| $\beta$ | – | 13 | 13 |
| $\alpha$ | – | 20 | 10 |

## TABLE II- CASE 1 RESULTS

| PROPERTY | VALUE |
|---|---|
| EC11 | 15750 ksi |
| EC22 | 1065 ksi |
| EC12 | 516 ksi |
| NUC12 | 0.275 |
| NUC21 | 0.018 |
| CTE11 | $0.775 \times 10^{-8}$ |
| CTE22 | $0.181 \times 10^{-4}$ |
| CTE12 | 0.000 |
| SCXXT | 203 ksi |
| SCXXC | 165 ksi |
| SCYYT | 11.74 ksi |
| SCYYC | 27.41 ksi |
| SCXYS | 10.01 ksi |

HISTOGRAM FOR EC11

LONGITUDINAL MODULUS
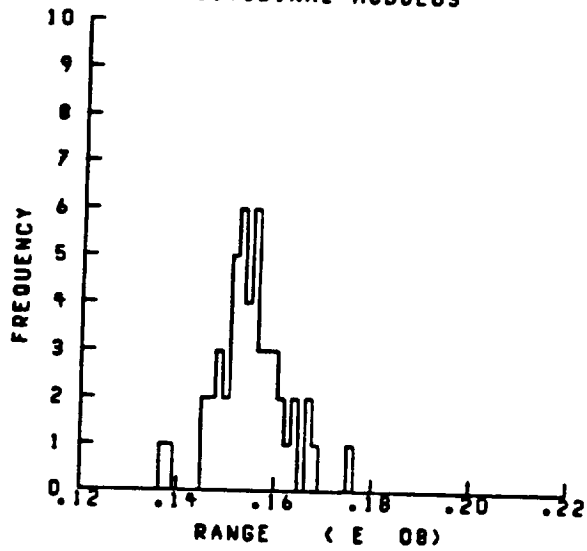
(a) case 2 histogram

HISTOGRAM FOR EC11

LONGITUDINAL MODULUS
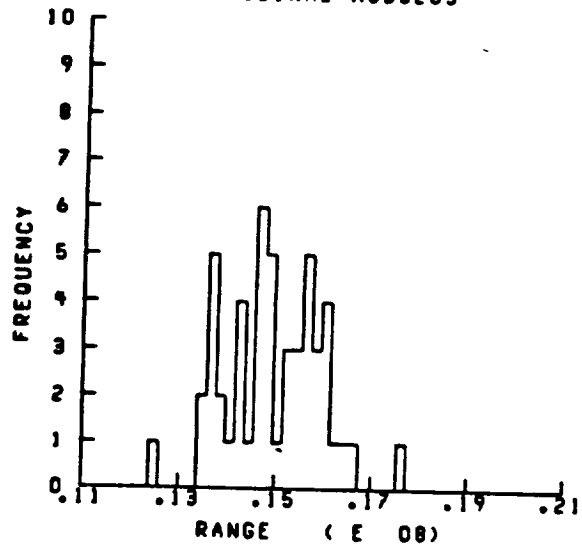
(b) case 3 histogram

DISTRIBUTION OF EC11

LONGITUDINAL MODULUS
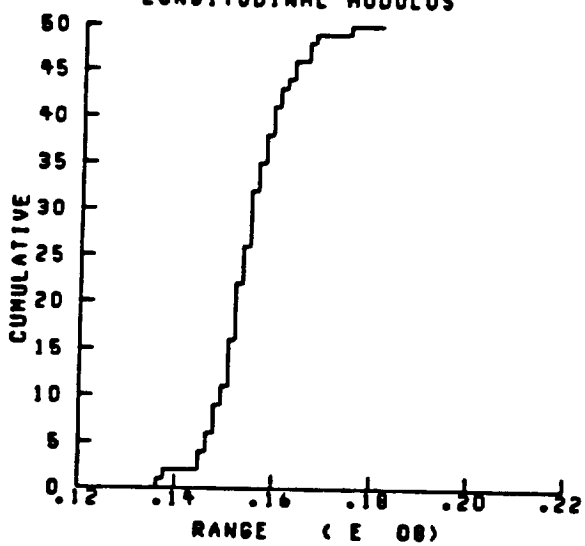
(c) case 2 distribution

DISTRIBUTION OF EC11

LONGITUDINAL MODULUS
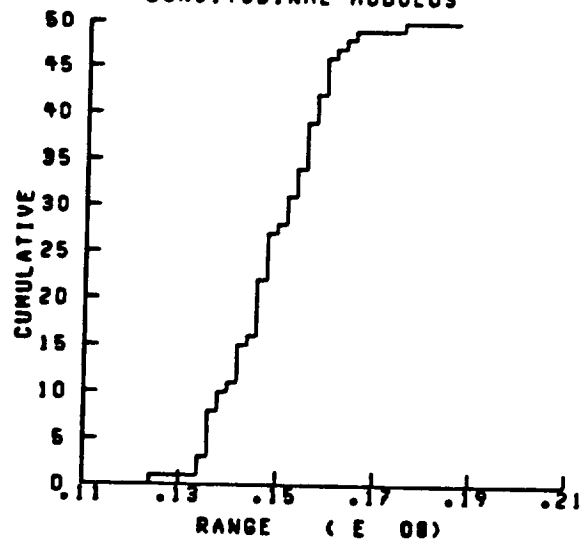
(d) case 3 distribution

Fig. 30- Sampling results for Longitudinal Elastic Modulus

HISTOGRAM FOR EC22

TRANSVERSE MODULUS



(a) case 2 histogram

HISTOGRAM FOR EC22

TRANSVERSE MODULUS



(b) case 3 histogram

DISTRIBUTION OF EC22

TRANSVERSE MODULUS



(c) case 2 distribution

DISTRIBUTION OF EC22

TRANSVERSE MODULUS



(d) case 3 distribution
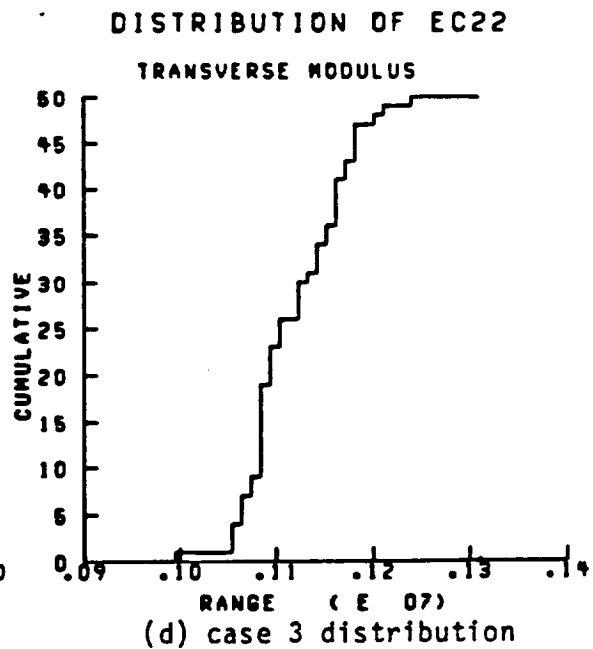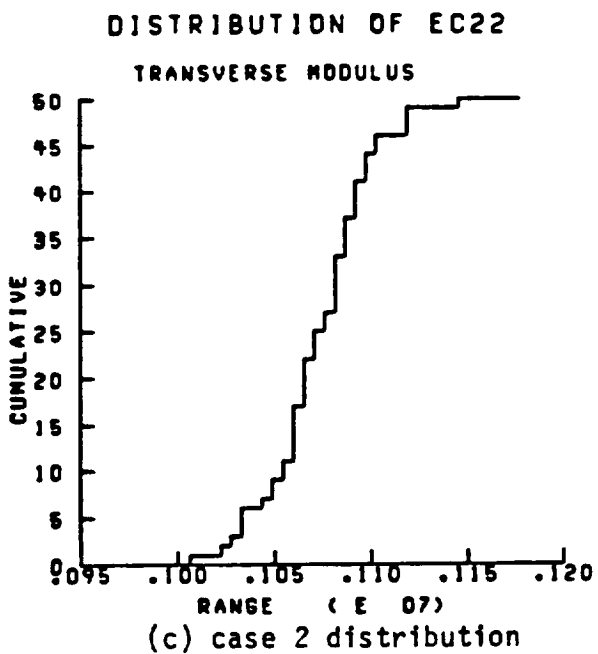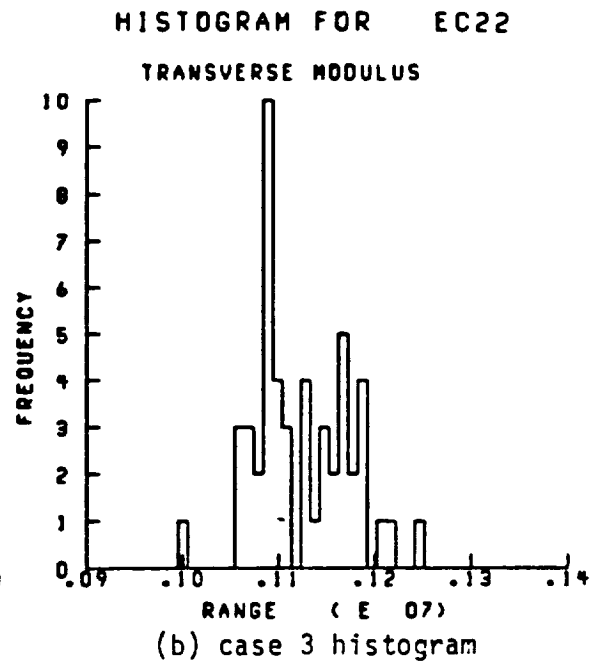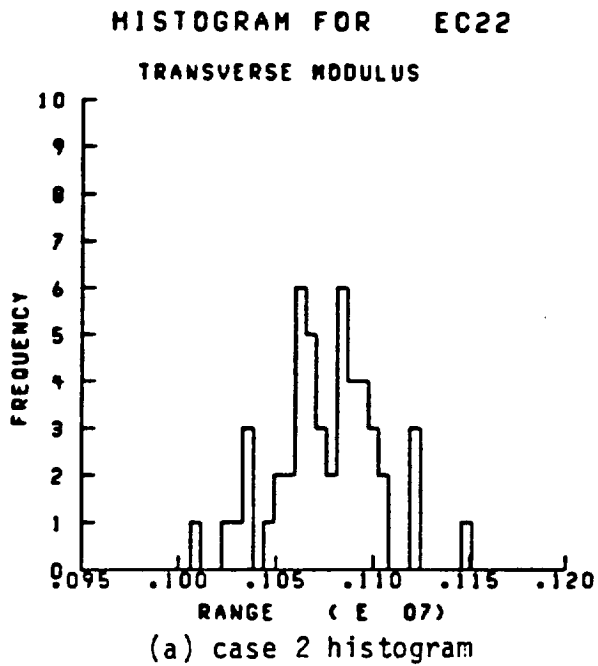
Fig. 31- Sampling results for Transverse Elastic Modulus

HISTOGRAM FOR    EC12
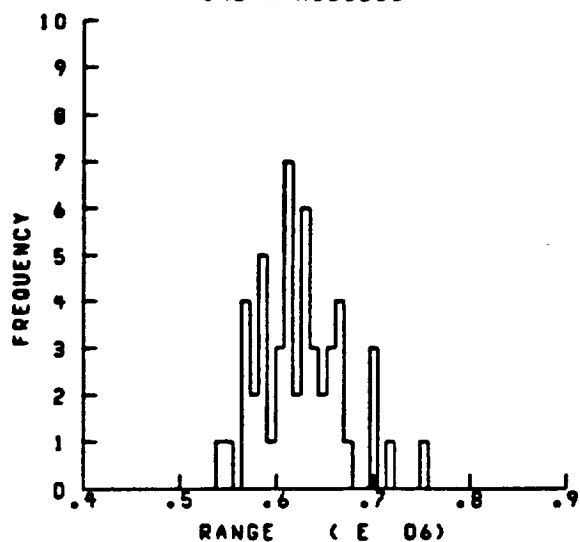
SHEAR MODULUS

HISTOGRAM FOR    EC12

SHEAR MODULUS

(a) case 2 histogram

(b) case 3 histogram
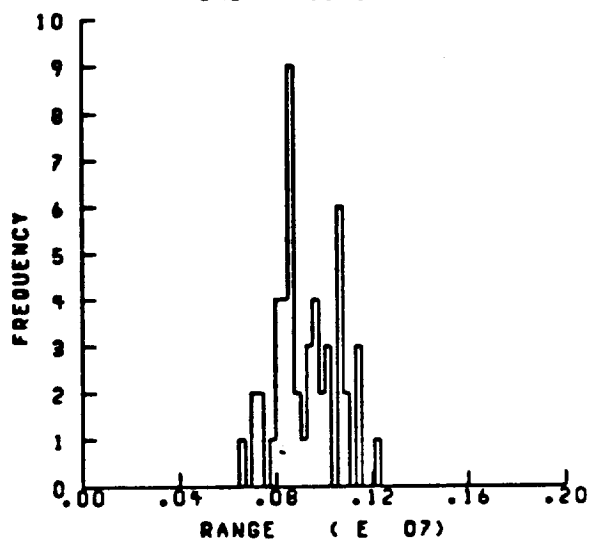
DISTRIBUTION OF EC12
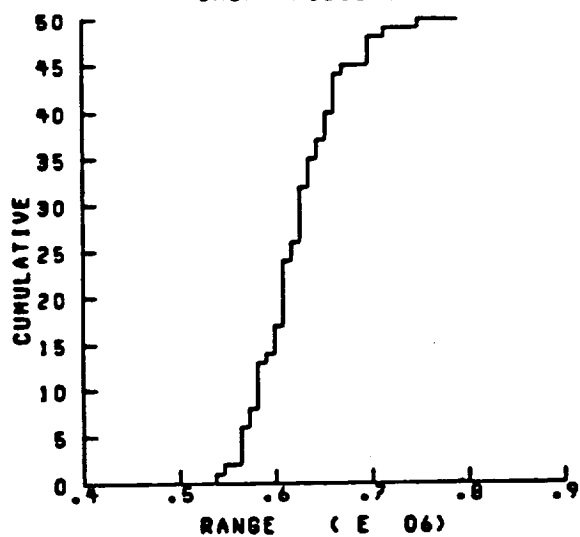
SHEAR MODULUS

DISTRIBUTION OF EC12

SHEAR MODULUS

(c) case 2 distribution
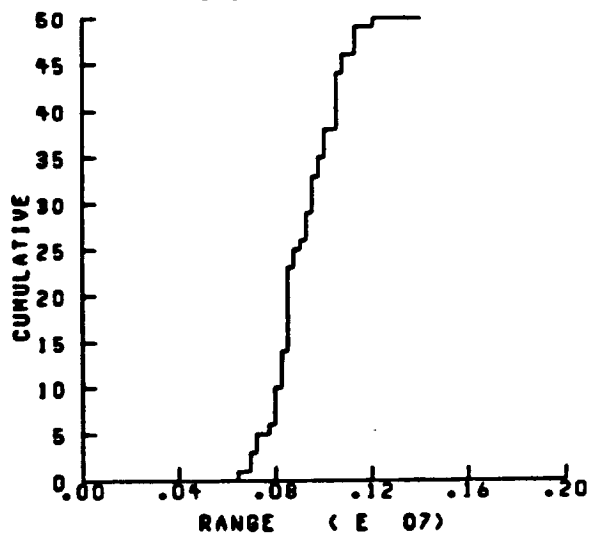
(d) case 3 distribution

Fig. 32- Sampling results for In-plane Shear Modulus
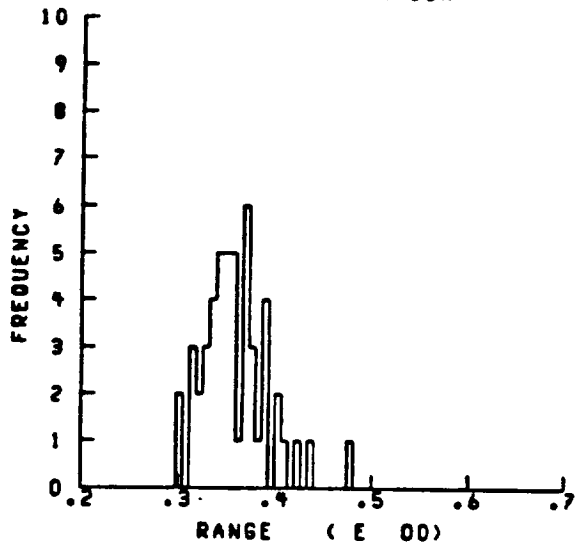
HISTOGRAM FOR NUC12
POISSON RATIO- MAJOR
(a) case 2 histogram

HISTOGRAM FOR NUC12
POISSON RATIO- MAJOR
(b) case 3 histogram
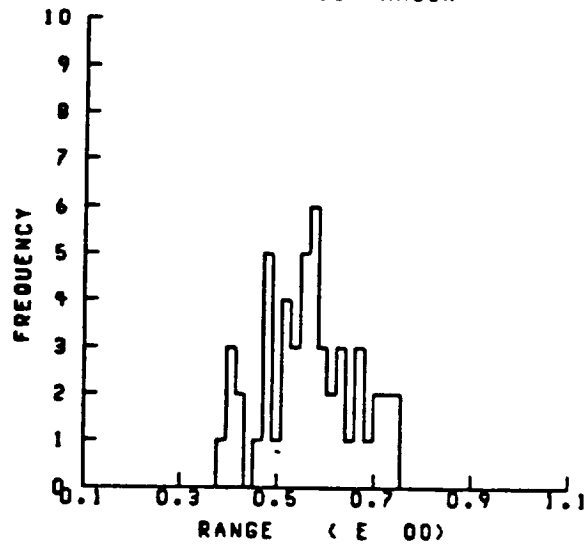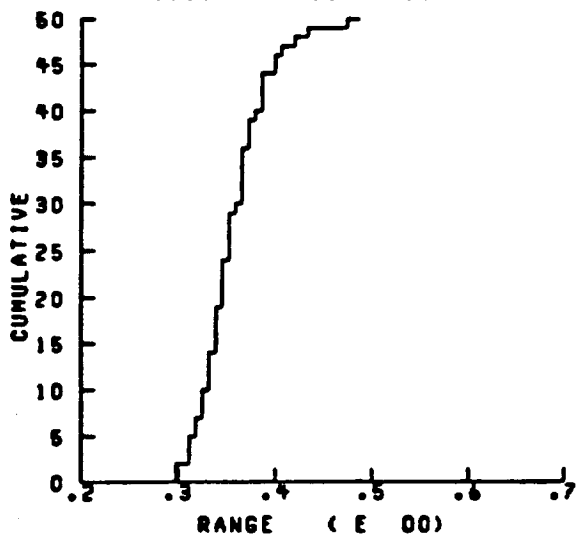
DISTRIBUTION OF NUC12
POISSON RATIO- MAJOR
(c) case 2 distribution
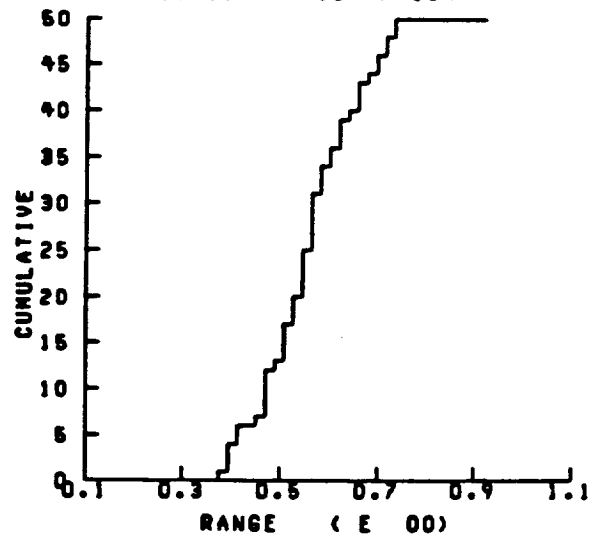
DISTRIBUTION OF NUC12
POISSON RATIO- MAJOR
(d) case 3 distribution

Fig. 33- Sampling results for Poisson Ratio (major)
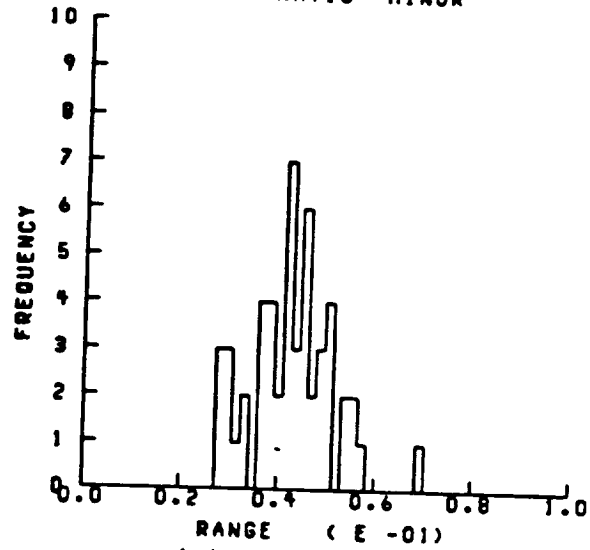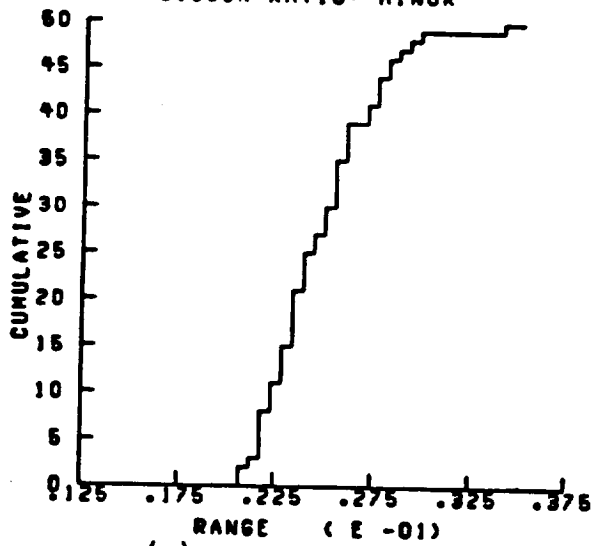
(a) case 2 histogram

(b) case 3 histogram

(c) case 2 distribution
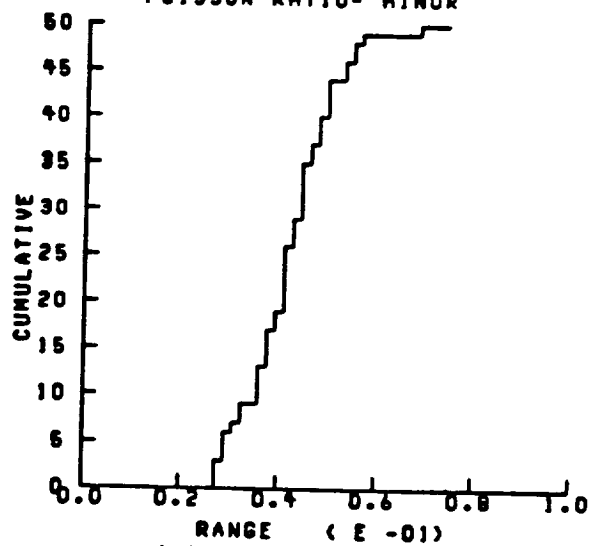
(d) case 3 distribution

Fig. 34- Sampling results for Poisson Ratio (minor)

**HISTOGRAM FOR CTE11**

LONG. THERMAL EXPANSION

(a) case 2 histogram

**HISTOGRAM FOR CTE11**

LONG. THERMAL EXPANSION

(b) case 3 histogram

**DISTRIBUTION OF CTE11**

LONG. THERMAL EXPANSION

(c) case 2 distribution

**DISTRIBUTION OF CTE11**

LONG. THERMAL EXPANSION

(d) case 3 distribution

Fig. 35- Sampling results for Longitudinal Thermal Expansion
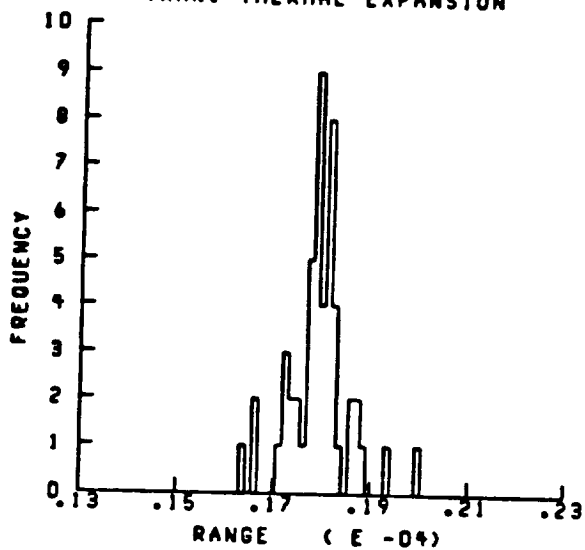
HISTOGRAM FOR CTE22
TRAN. THERMAL EXPANSION

(a) case 2 histogram

HISTOGRAM FOR CTE22
TRAN. THERMAL EXPANSION
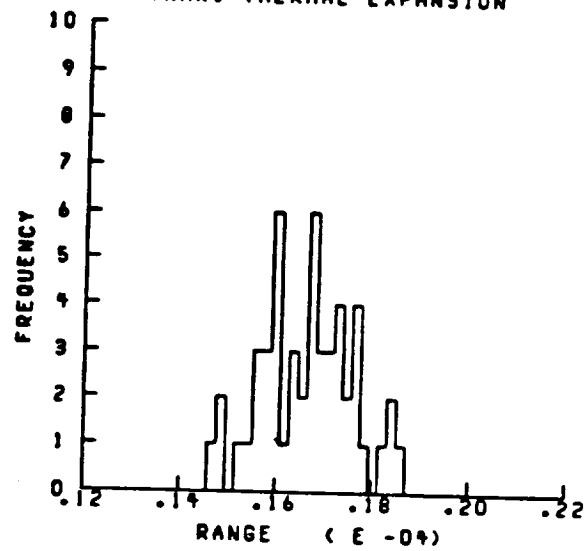
(b) case 3 histogram

DISTRIBUTION OF CTE22
TRAN. THERMAL EXPANSION
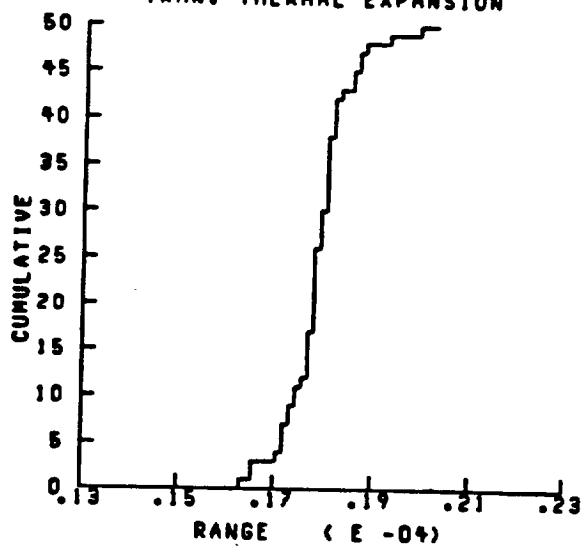
(c) case 2 distribution

DISTRIBUTION OF CTE22
TRAN. THERMAL EXPANSION
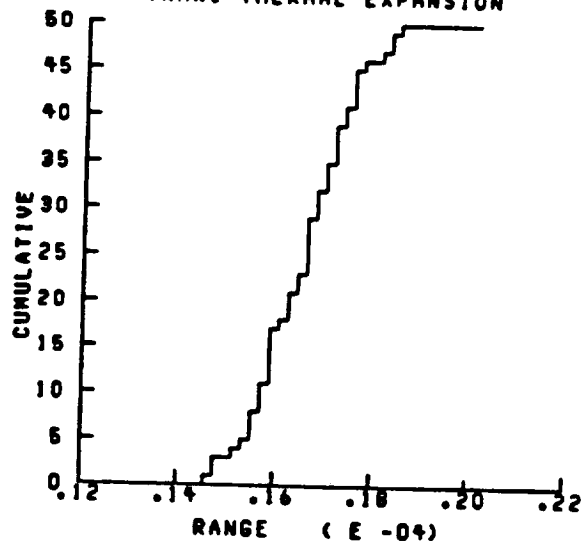
(d) case 3 distribution

Fig. 36- Sampling results for Transverse Thermal Expansion
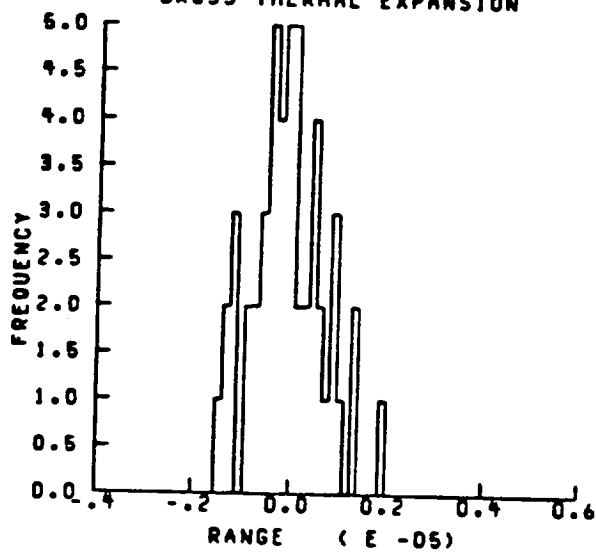
HISTOGRAM FOR    CTE12

CROSS THERMAL EXPANSION

HISTOGRAM FOR    CTE12

CROSS THERMAL EXPANSION
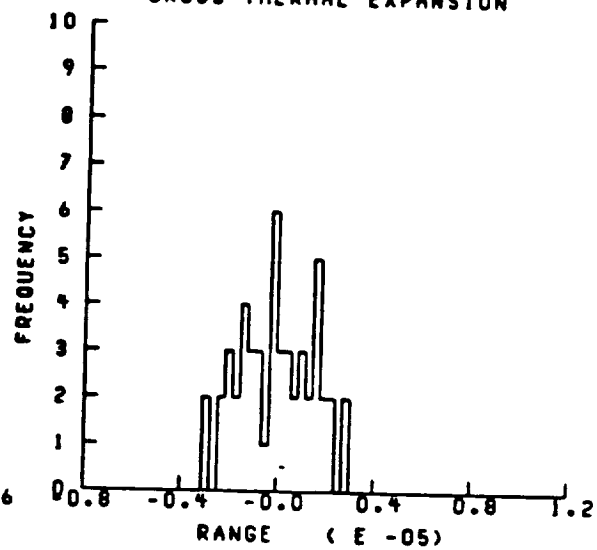
(a) case 2 histogram

(b) case 3 histogram

DISTRIBUTION OF CTE12

CROSS THERMAL EXPANSION
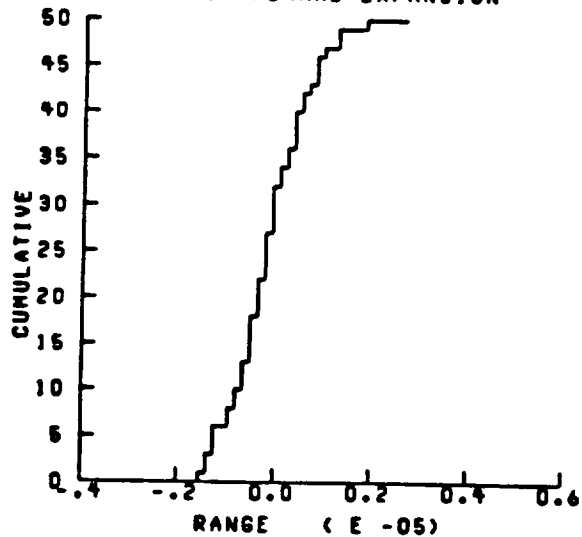
DISTRIBUTION OF CTE12

CROSS THERMAL EXPANSION

(c) case 2 distribution
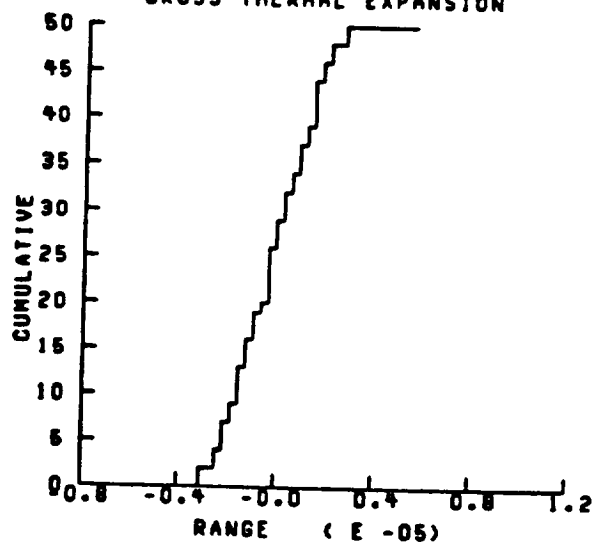
(d) case 3 distribution

Fig. 37- Sampling results for Thermal Expansion Coupling

HISTOGRAM FOR SCXXT

LONG. TENSILE STRENGTH

HISTOGRAM FOR SCXXT

LONG. TENSILE STRENGTH

(a) case 2 histogram

(b) case 3 histogram

DISTRIBUTION OF SCXXT

LONG. TENSILE STRENGTH

DISTRIBUTION OF SCXXT

LONG. TENSILE STRENGTH

(c) case 2 distribution

(d) case 3 distribution

Fig. 38- Sampling results for Longitudinal Tensile Strength

HISTOGRAM FOR    SCXXC

LONG. COMPRESS STRENGTH

(a) case 2 histogram

HISTOGRAM FOR    SCXXC

LONG. COMPRESS STRENGTH

(b) case 3 histogram

DISTRIBUTION OF SCXXC

LONG. COMPRESS STRENGTH

(c) case 2 distribution

DISTRIBUTION OF SCXXC

LONG. COMPRESS STRENGTH

(d) case 3 distribution
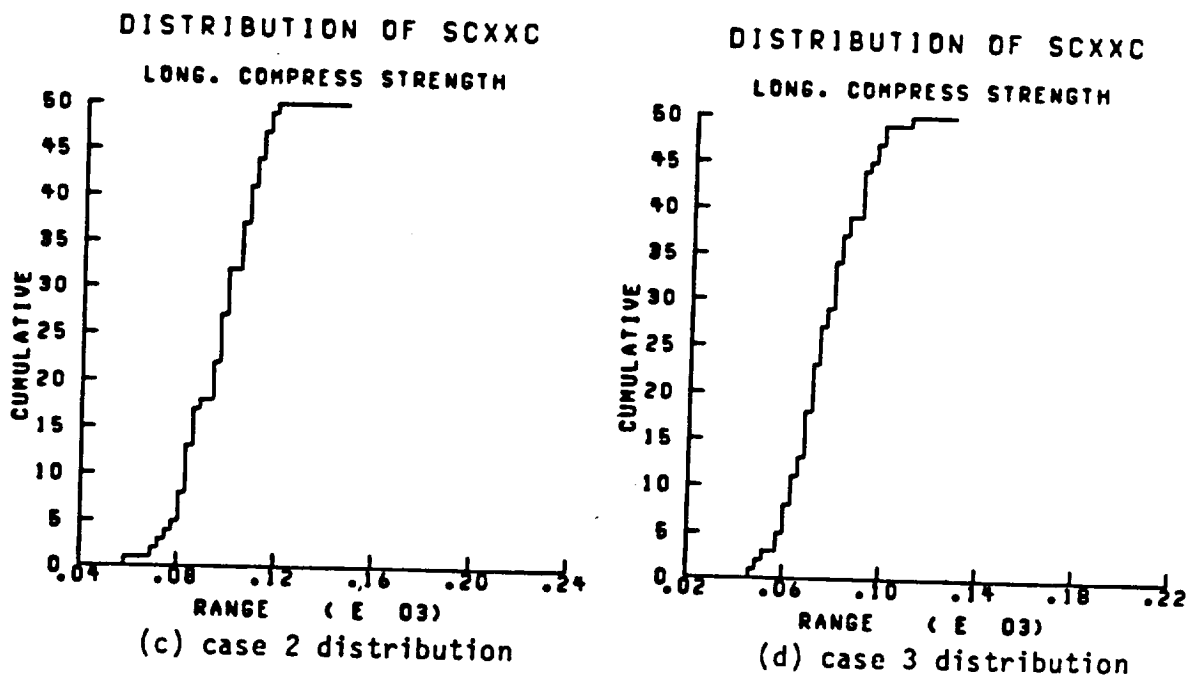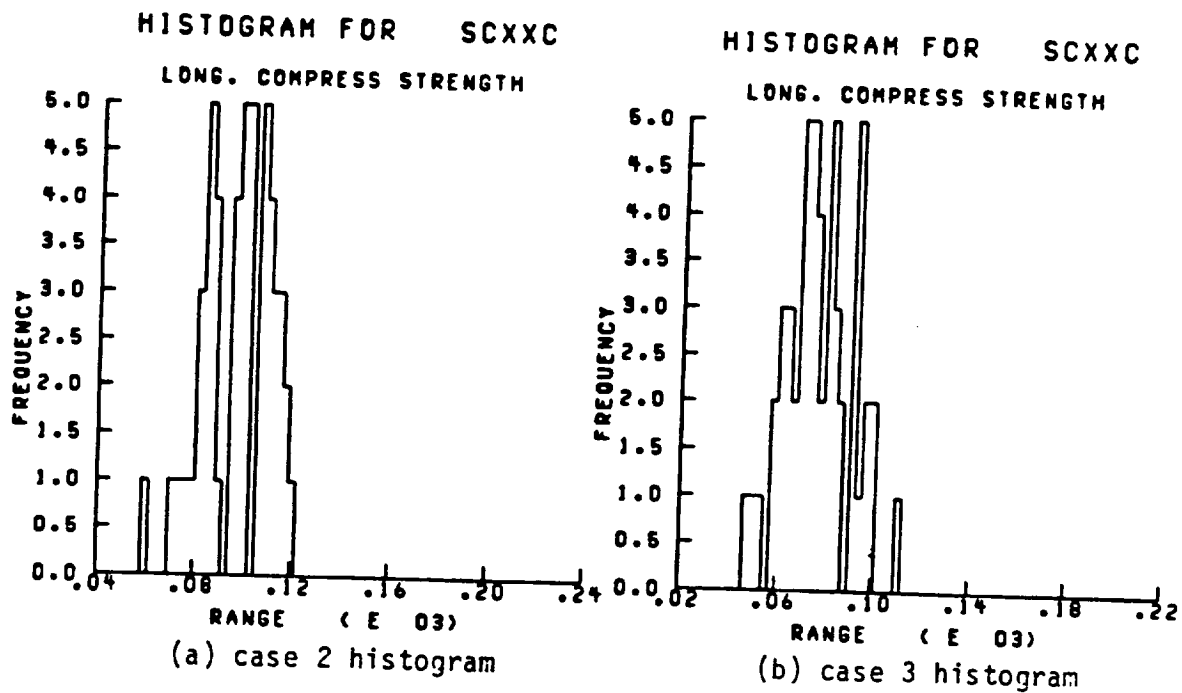
Fig. 39- Sampling results for Longitudinal Compressive Strength

HISTOGRAM FOR SCYYT

TRAN. TENSILE STRENGTH

(a) case 2 histogram

HISTOGRAM FOR SCYYT

TRAN. TENSILE STRENGTH

(b) case 3 histogram

DISTRIBUTION OF SCYYT

TRAN. TENSILE STRENGTH

(c) case 2 distribution

DISTRIBUTION OF SCYYT

TRAN. TENSILE STRENGTH

(d) case 3 distribution
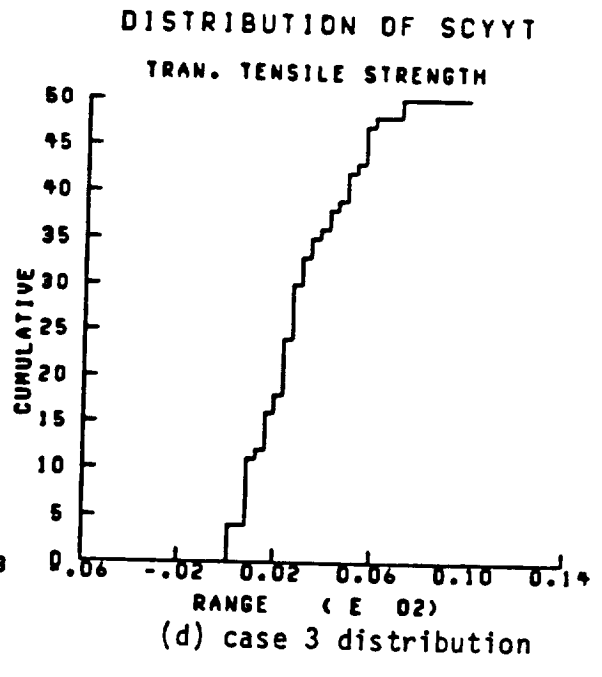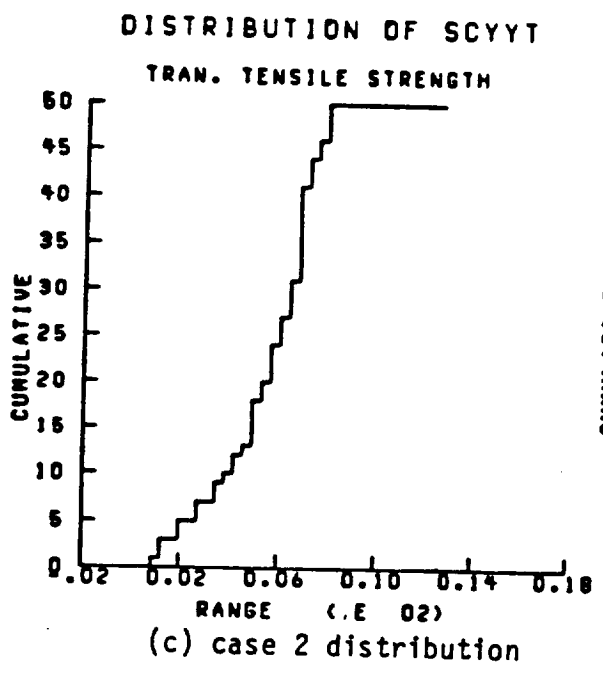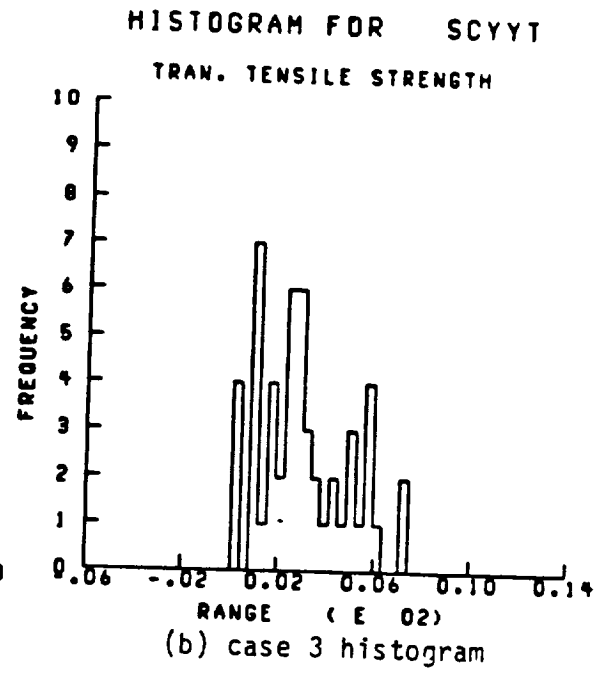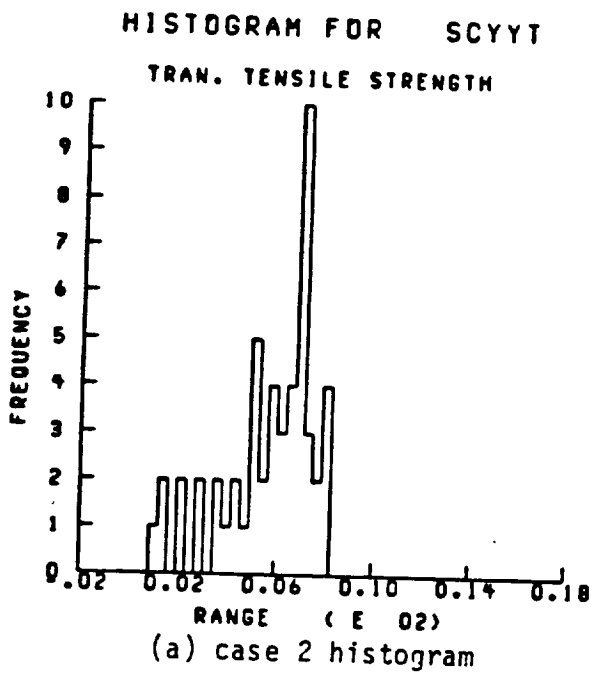
Fig. 40- Sampling results for Transverse Tensile Strength
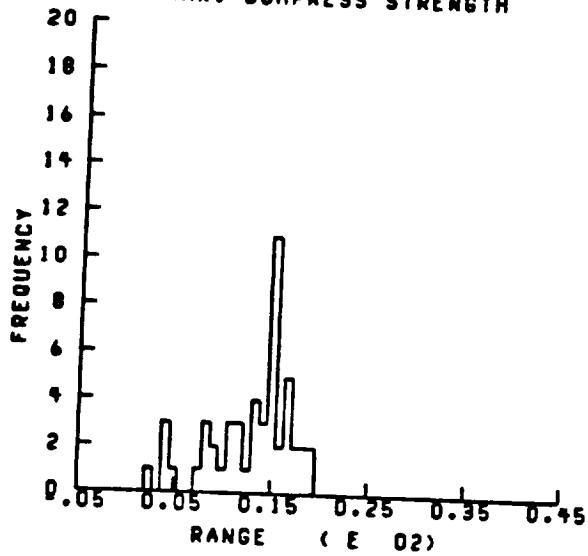
HISTOGRAM FOR SCYYC

TRAN. COMPRESS STRENGTH

(a) case 2 histogram

HISTOGRAM FOR SCYYC

TRAN. COMPRESS STRENGTH
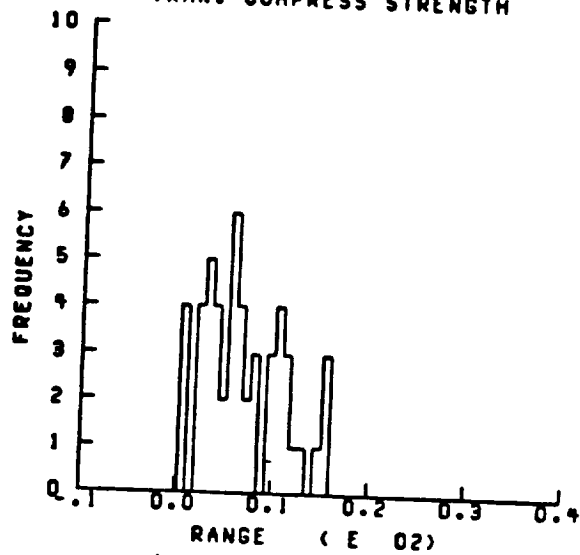
(b) case 3 histogram

DISTRIBUTION OF SCYYC

TRAN. COMPRESS STRENGTH
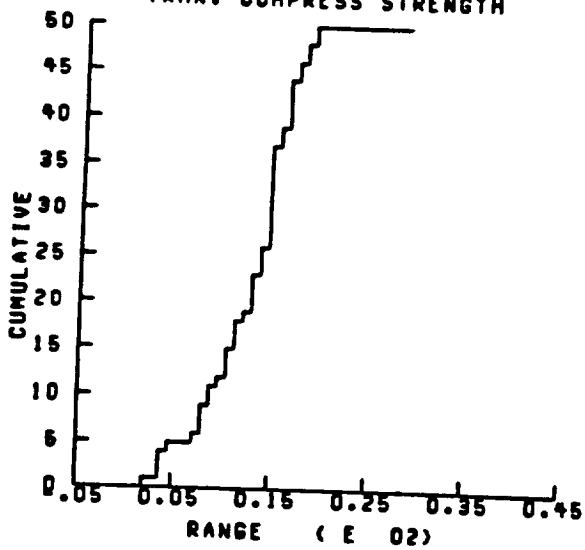
(c) case 2 distribution

DISTRIBUTION OF SCYYC

TRAN. COMPRESS STRENGTH
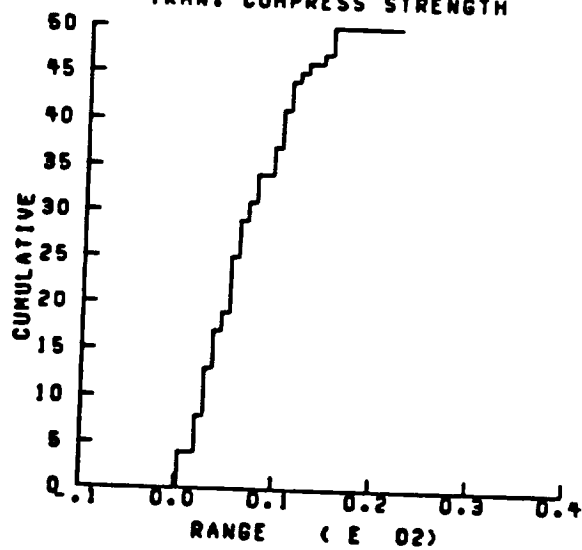
(d) case 3 distribution

Fig. 41- Sampling results for Transverse Compressive Strength

HISTOGRAM FOR SCXYS
IN-PLANE SHEAR STRENGTH
(a) case 2 histogram

HISTOGRAM FOR SCXYS
IN-PLANE SHEAR STRENGTH
(b) case 3 histogram

DISTRIBUTION OF SCXYS
IN-PLANE SHEAR STRENGTH
(c) case 2 distribution

DISTRIBUTION OF SCXYS
IN-PLANE SHEAR STRENGTH
(d) case 3 distribution
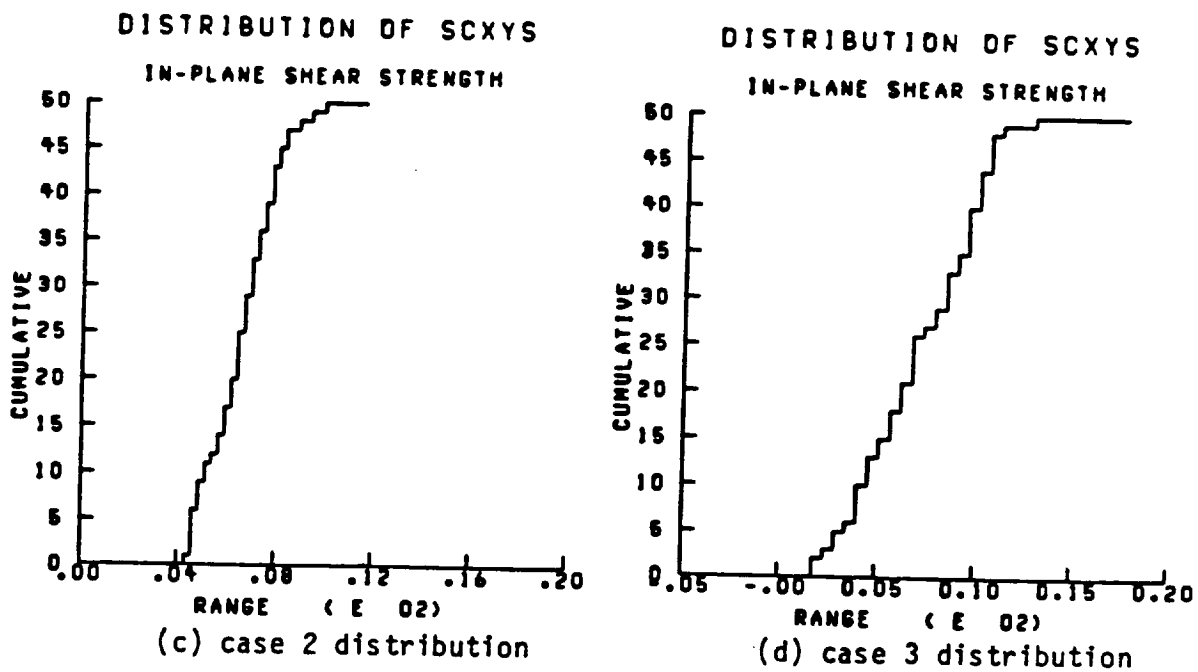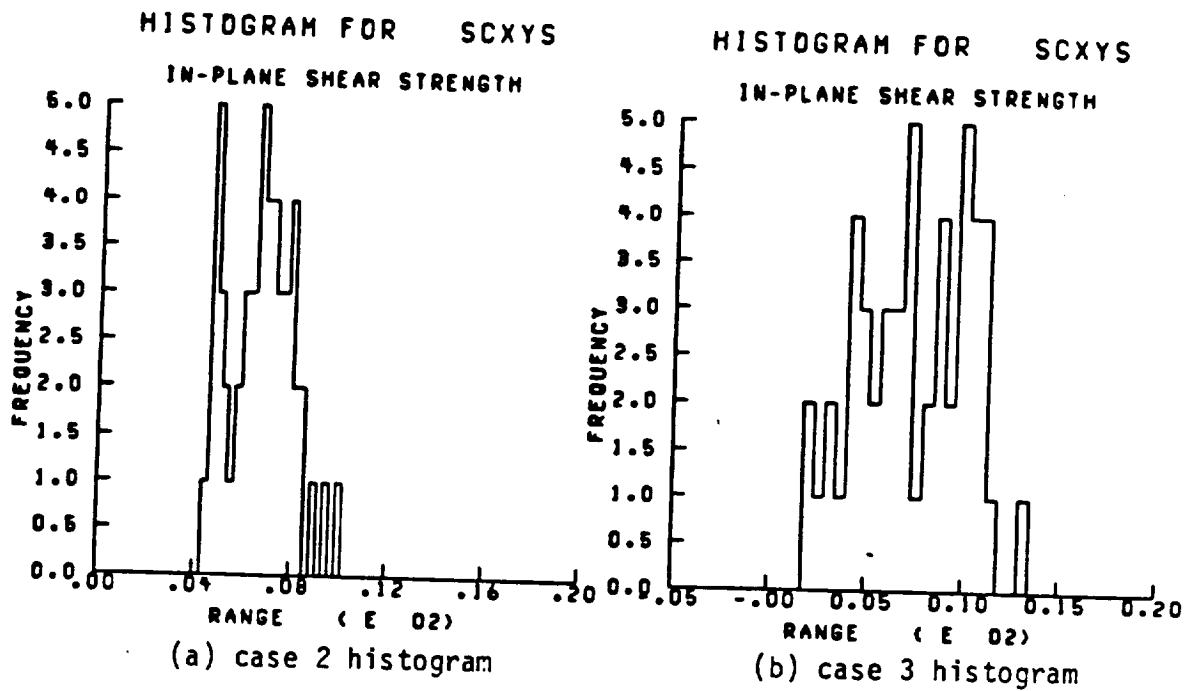
Fig. 42- Sampling results for In-plane Shear Strength

## B. Fiber Strength Effect

To show the effect of fiber strength changes on the longitudinal strengths of the composite, several shape parameters of the weibull distribution for fiber strength are assumed. The monte carlo procedure is then conducted at several fiber volume ratio values. All properties are varied, except fiber volume ratio. The distribution parameters of all properties except fiber strengths are held constant. The curves generated are shown in Figs. 43 and 44. In the figures the solid lines and symbols show the means of the 95% confidence interval estimates for the sample size of 50 chosen at each point. The points on both sides of each curve locate the upper and lower bounds of the confidence intervals. The convention described is intended to provide a convenient indication of the dispersion of the sample values at each point.

# LONG. TENSILE STRENGTH
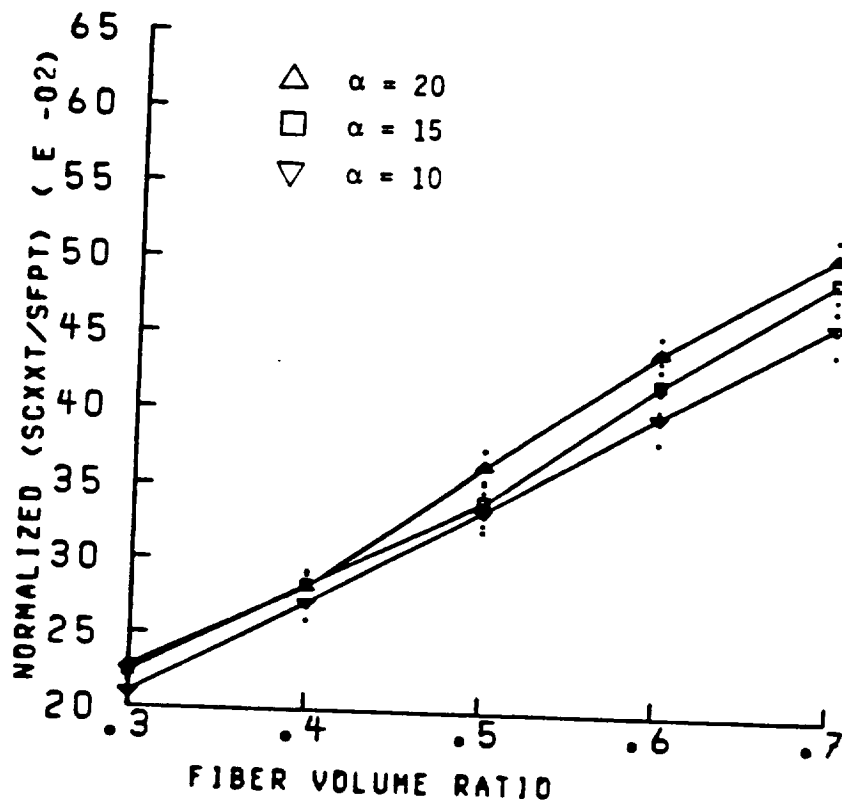


Fig. 43- Longitudinal Tensile Strength; for various shape parameters of fiber strength.

# LONG. COMPRESS. STRENGTH
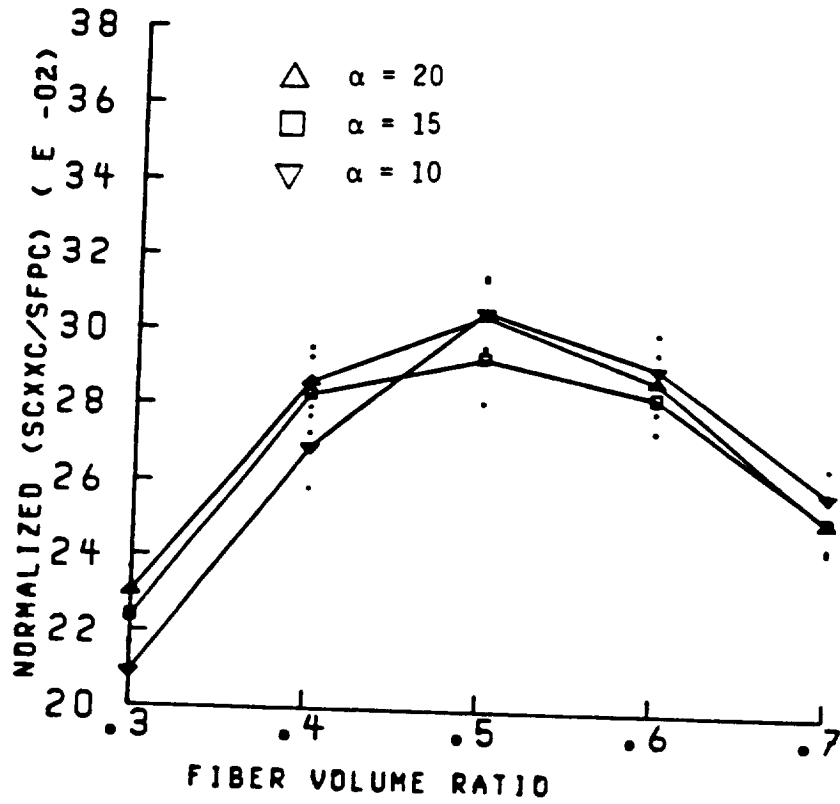


Fig. 44- Longitudinal Compressive Strength; for various shape parameters of fiber strength.

## C. Matrix Strength Effect

The effects of changes in matrix strength on composite strengths are studied by suitable variation of the shape parameters governing the matrix strength distributions. Analagous to the plots given for fiber strength effects, the matrix effects are shown in Figs. 45 - 47.

# TRANS. TENSILE STRENGTH
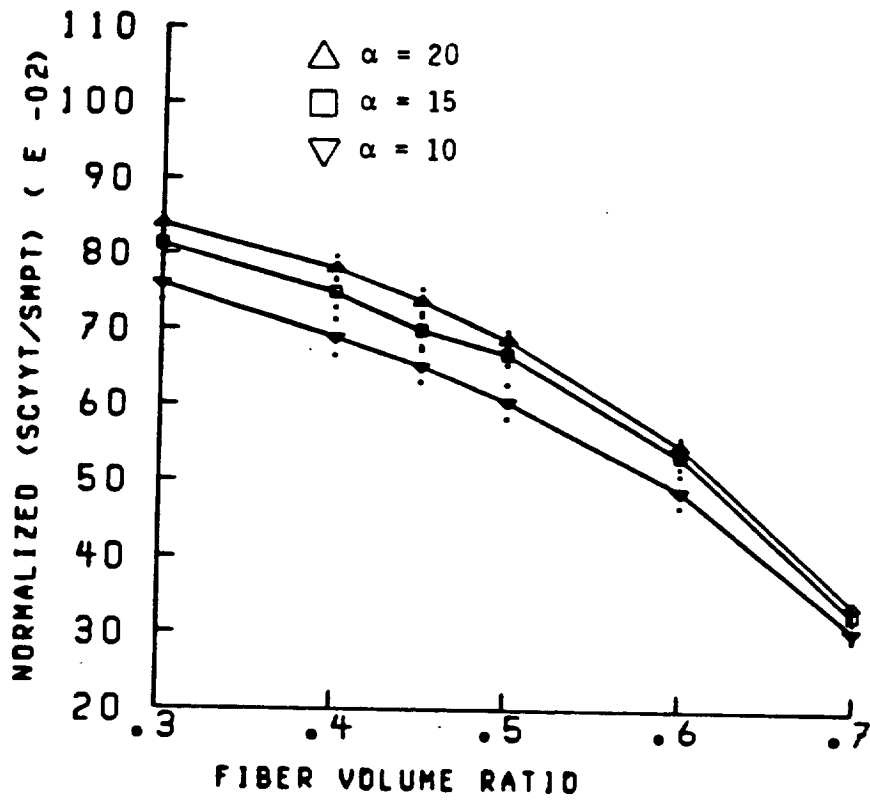


Fig. 45- Transverse Tensile Strength; for various shape parameters of matrix strengths.

# TRANS. COMPR. STRENGTH
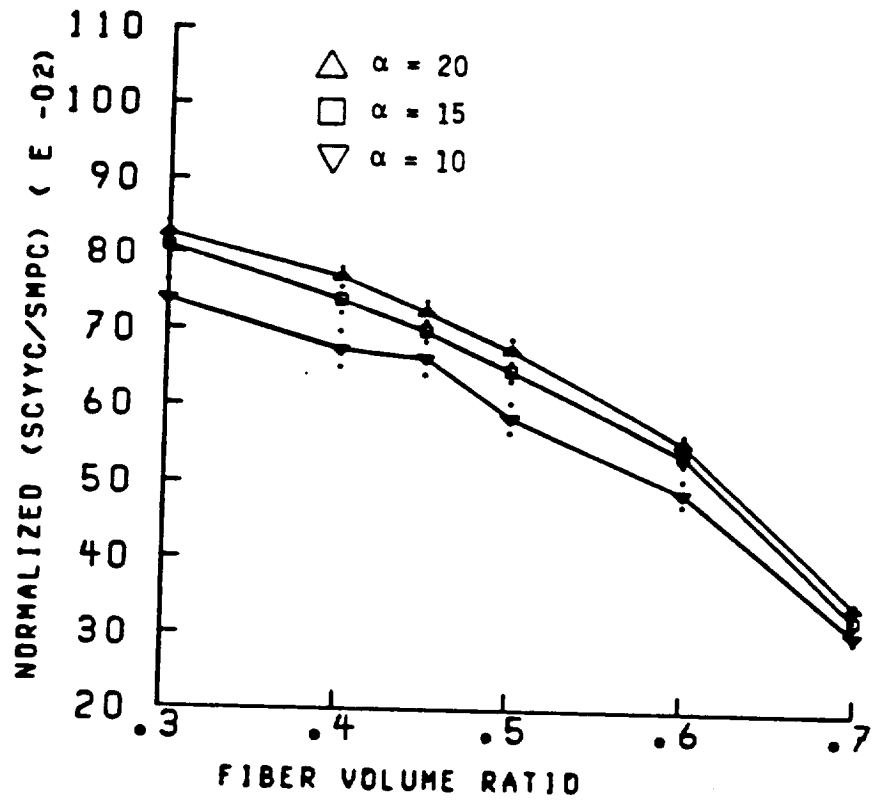


Fig. 46- Transverse Compressive Strength; for various shape parameters of matrix strengths.

# IN-PLANE SHEAR STRENGTH
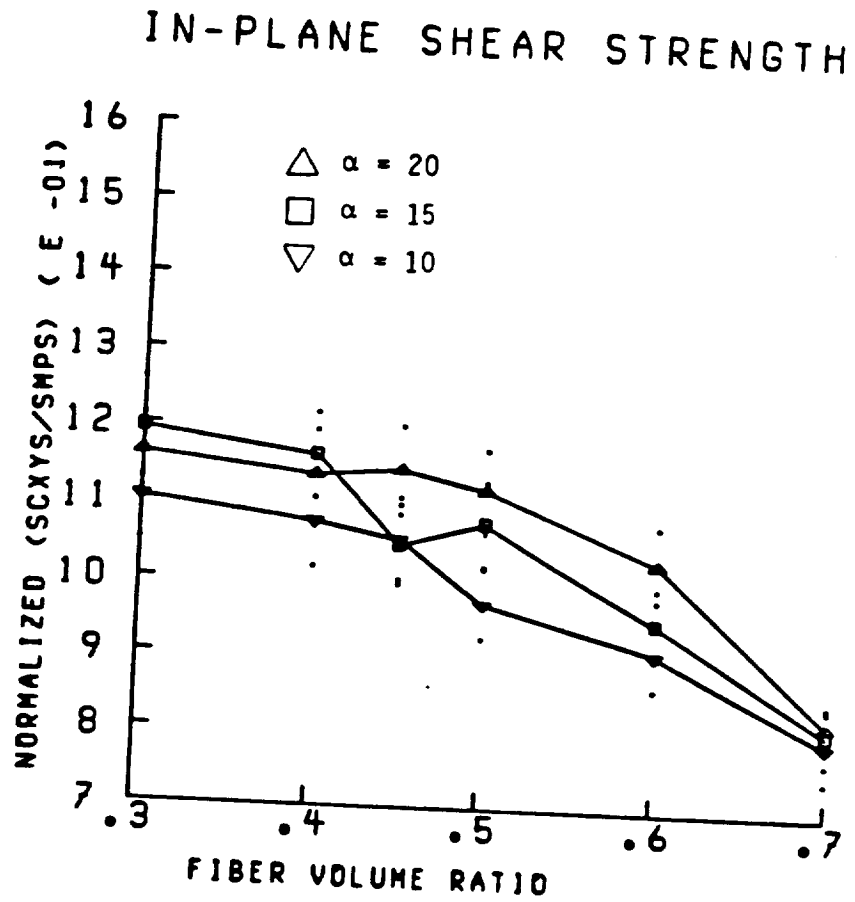


Fig. 47- In-plane Shear Strength; for various shape parameters of matrix strengths.

## D. Fiber Orientation Effect

Assumed values of the fiber orientation angle distribution parameter are consecutively used in the monte carlo procedure to assess the effects on several composite properties. These plots are shown in Figs. 48 - 57.

## E. Fiber Stiffness Effect

Assumed values of the fiber modulus distribution parameter are used in the simulation to similarly assess the effects on the related composite properties. The plots thus generated are shown in Figs. 58-67.

# LONG. ELASTIC MODULUS
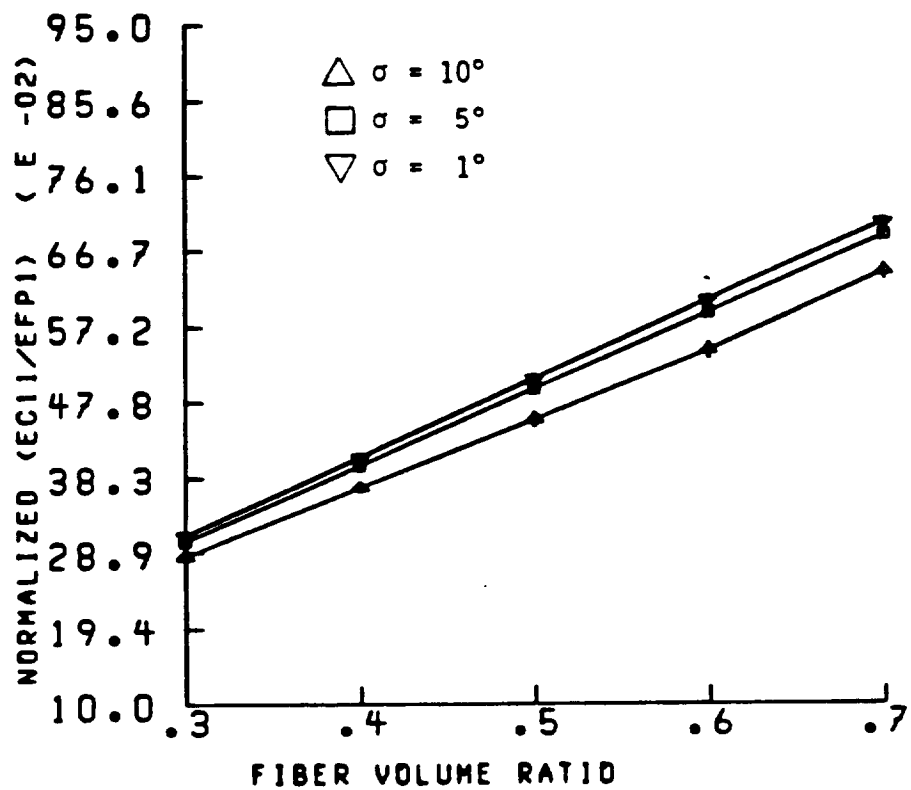


Fig. 48- Longitudinal Elastic Modulus; for various shape parameters of fiber orientation.

C-2

# TRANS. ELASTIC MODULUS
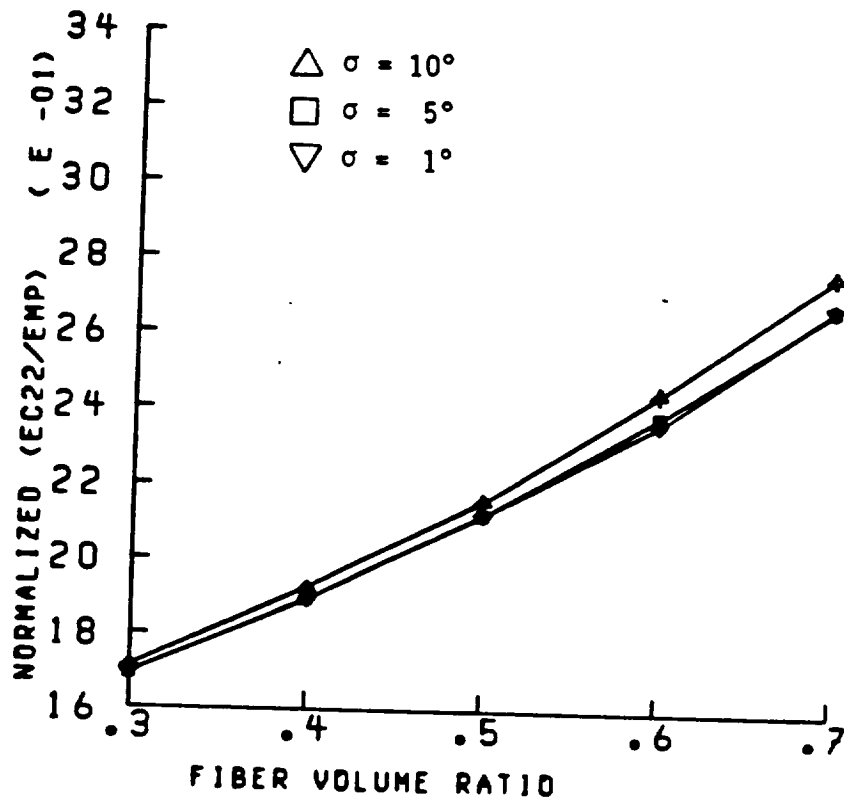


Fig. 49- Transverse Elastic Modulus; for various
shape parameters of fiber orientation.

# IN PLANE SHEAR MODULUS
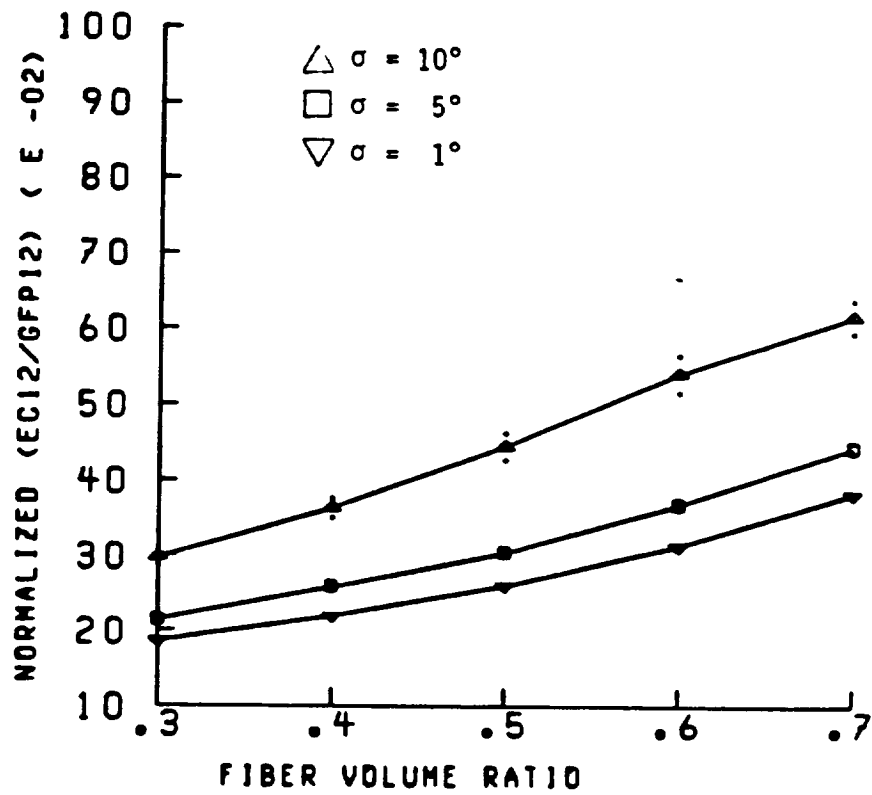


Fig. 50- In-plane Shear Modulus; for various
shape parameters of fiber orientation.

# LONG. TENSILE STRENGTH
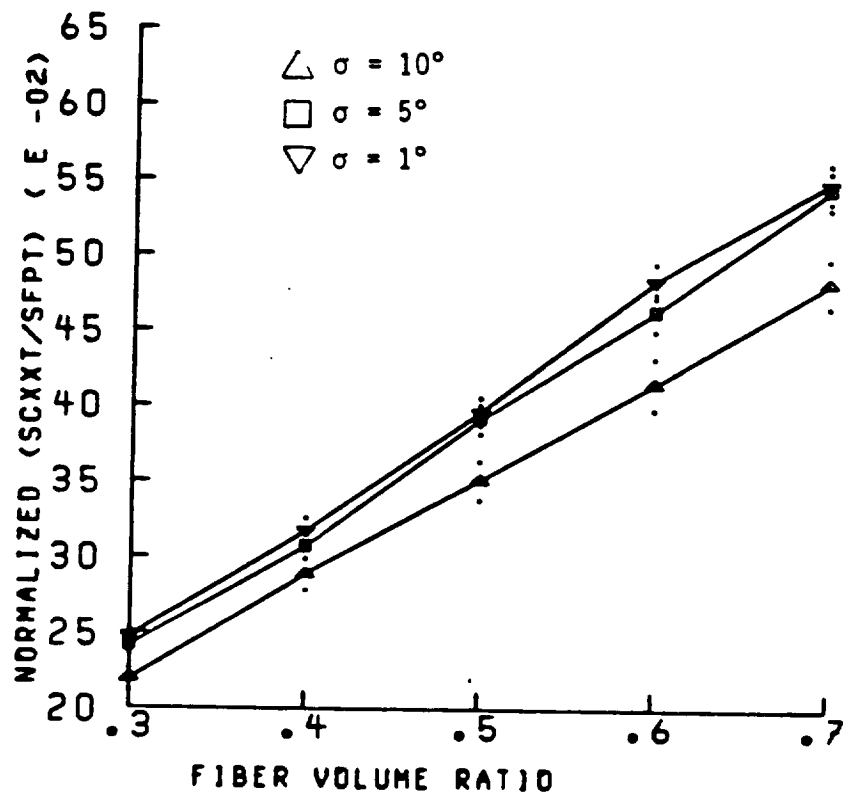


Fig. 51- Longitudinal Tensile Strength; for various
shape parameters of fiber orientation.

# LONG. COMP. STRENGTH
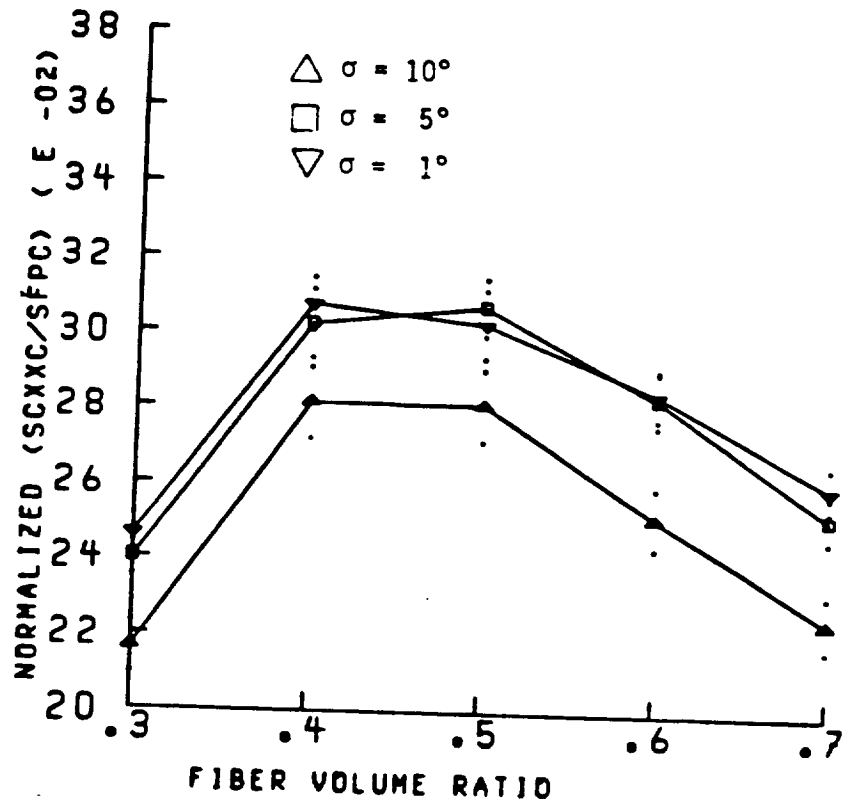


Fig. 52- Longitudinal Compressive Strength; for various
shape parameters of fiber orientation.

# TRANS. TENSILE STRENGTH
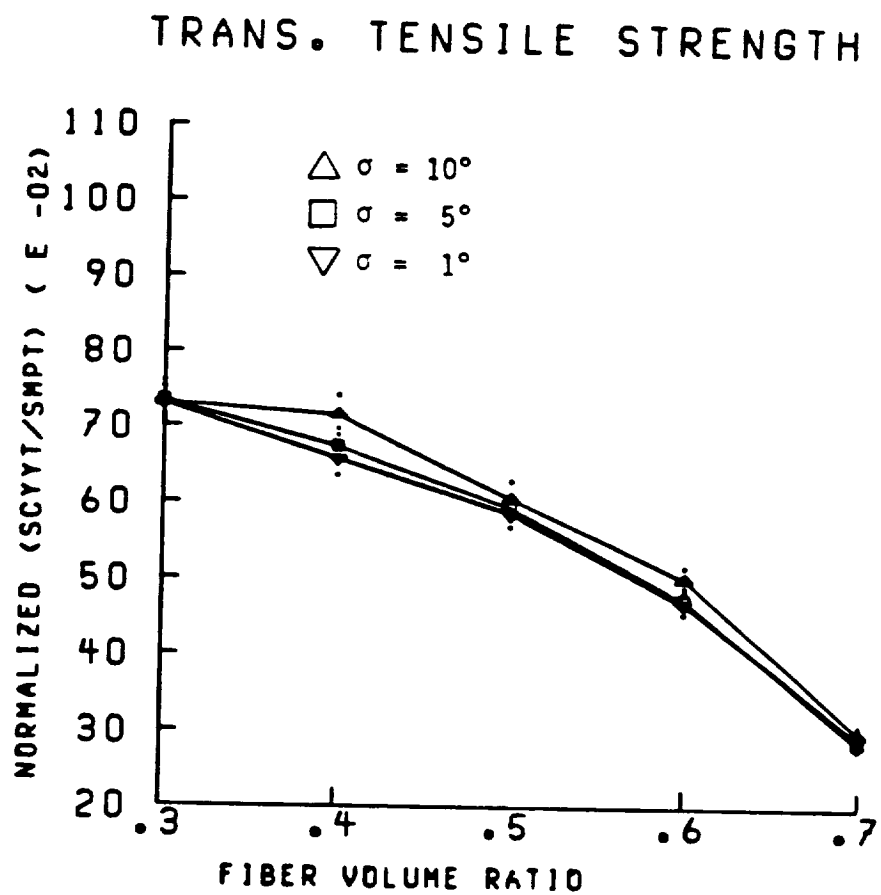


Fig. 53- Transverse Tensile Strength; for various shape parameters of fiber orientation.

# TRANS. COMP. STRENGTH
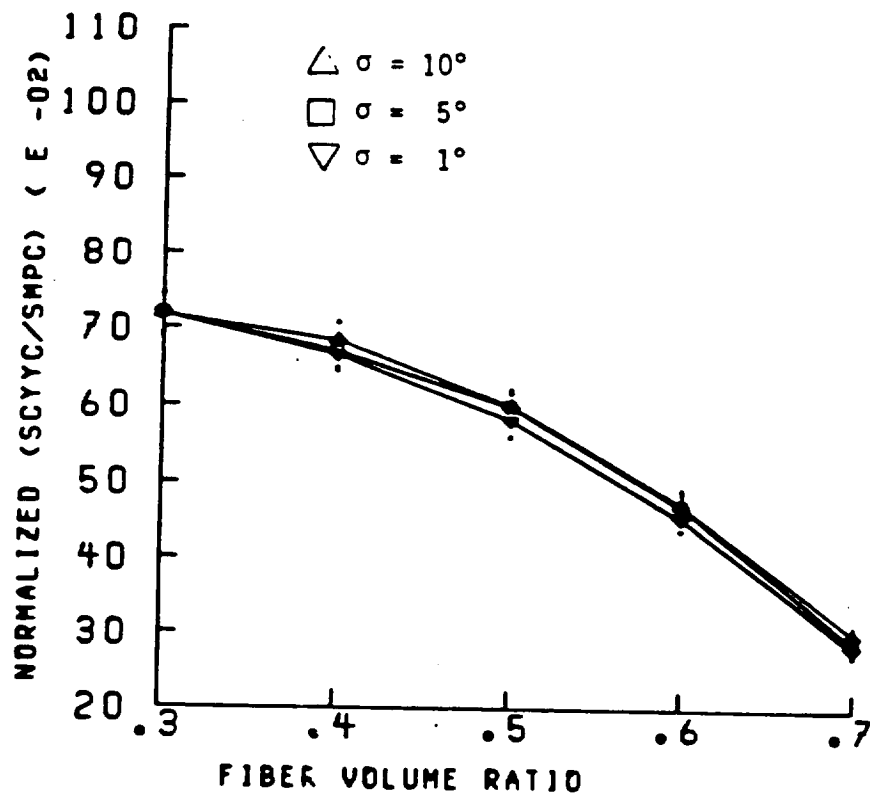


Fig. 54- Transverse Compressive Strength; for various
shape parameters of fiber orientation.

# IN PLANE SHEAR STRENGTH
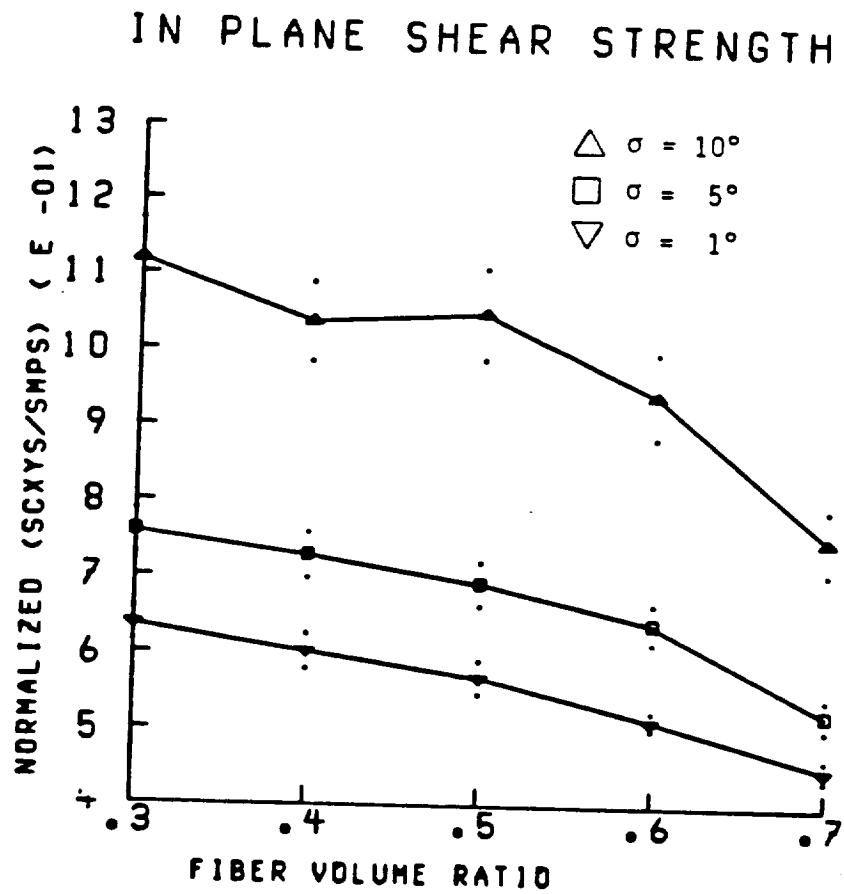


Fig. 55- In-plane Shear Strength; for various
shape parameters of fiber orientation.

# POISSON'S RATIO (MAJOR)
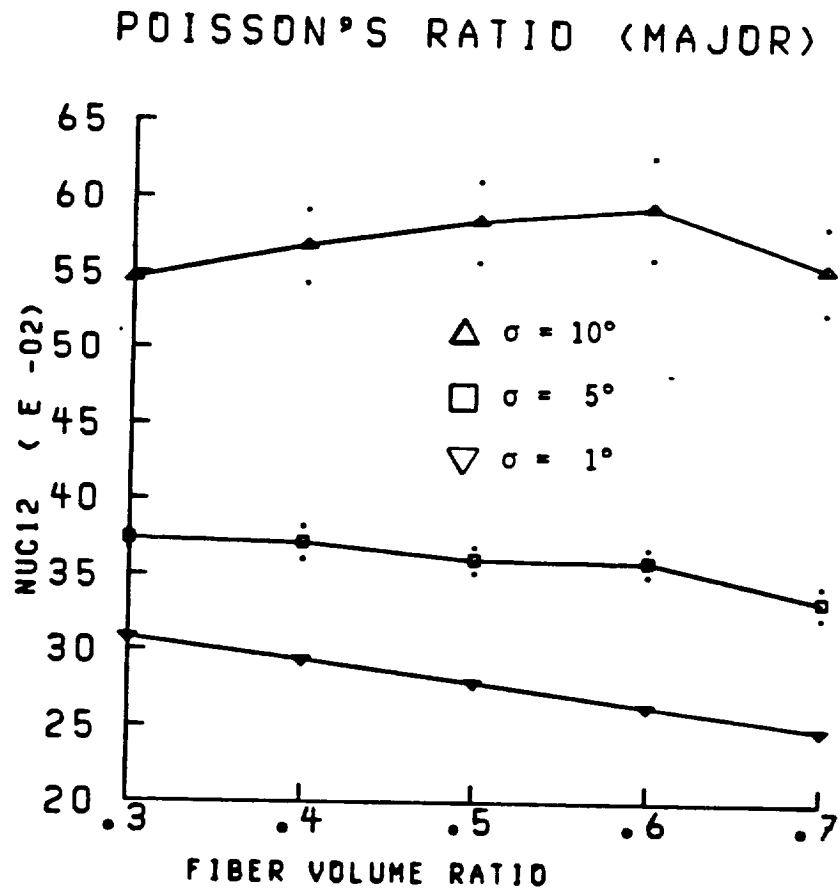


Fig. 56- Poisson's Ratio (major); for various
shape parameters of fiber orientation.
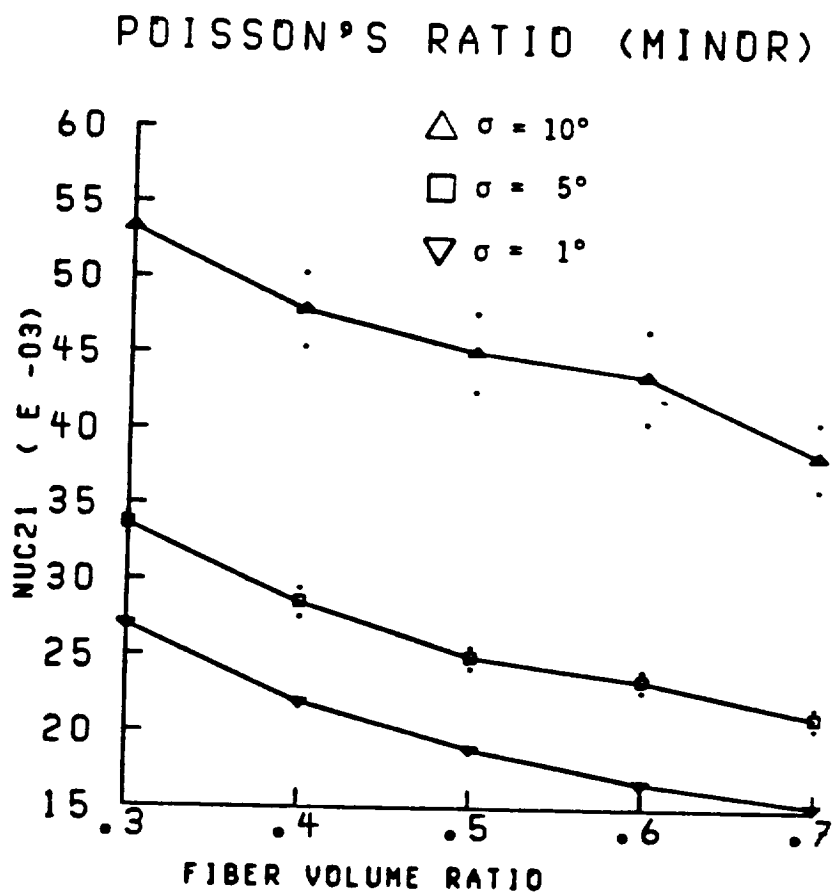
Fig. 57- Poisson's Ratio (minor); for various
shape parameters of fiber orientation.

# LONG. ELASTIC MODULUS
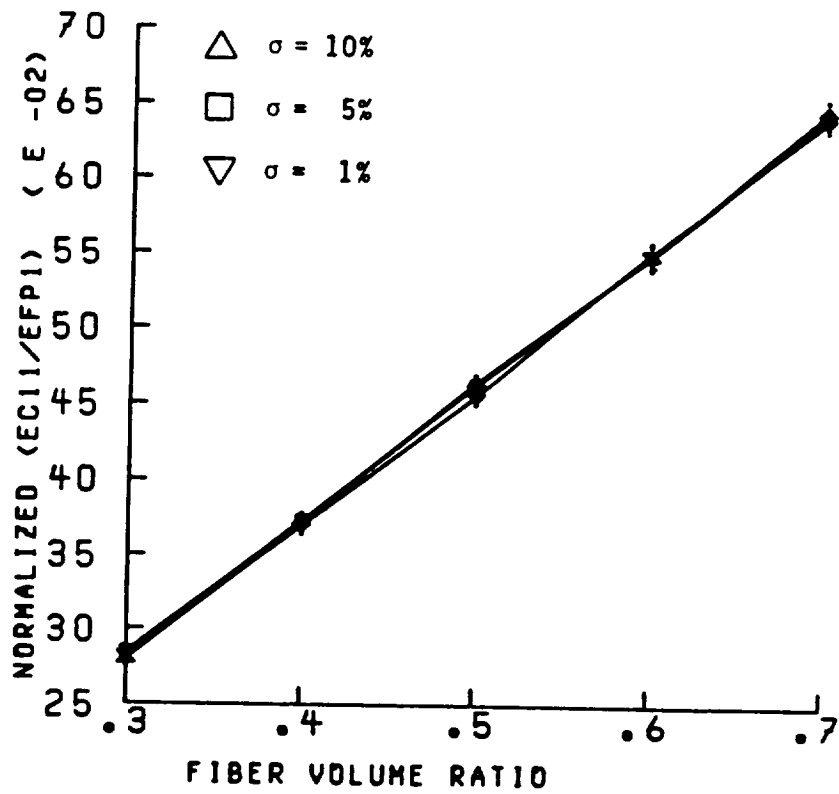


Fig. 58- Longitudinal Elastic Modulus; for various
shape parameters of fiber modulus.

# TRANS. ELASTIC MODULUS
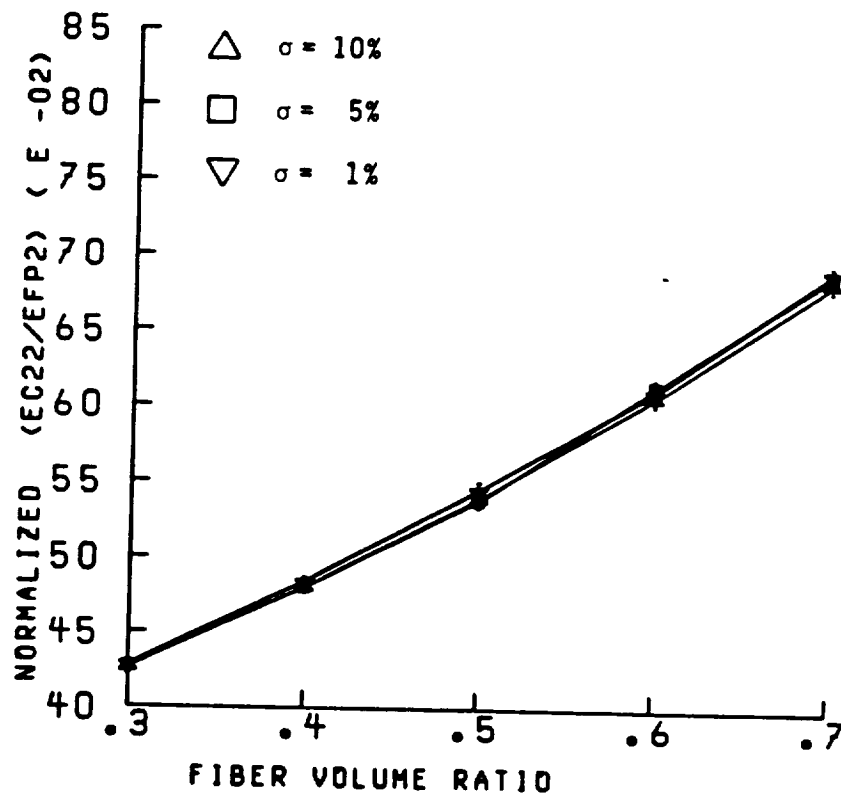


Fig. 59- Transverse Elastic Modulus; for various shape parameters of fiber modulus.

Fig. 60- In Plane Shear Modulus; for various
shape parameters of fiber modulus.

# POISSON'S RATIO (MAJOR)
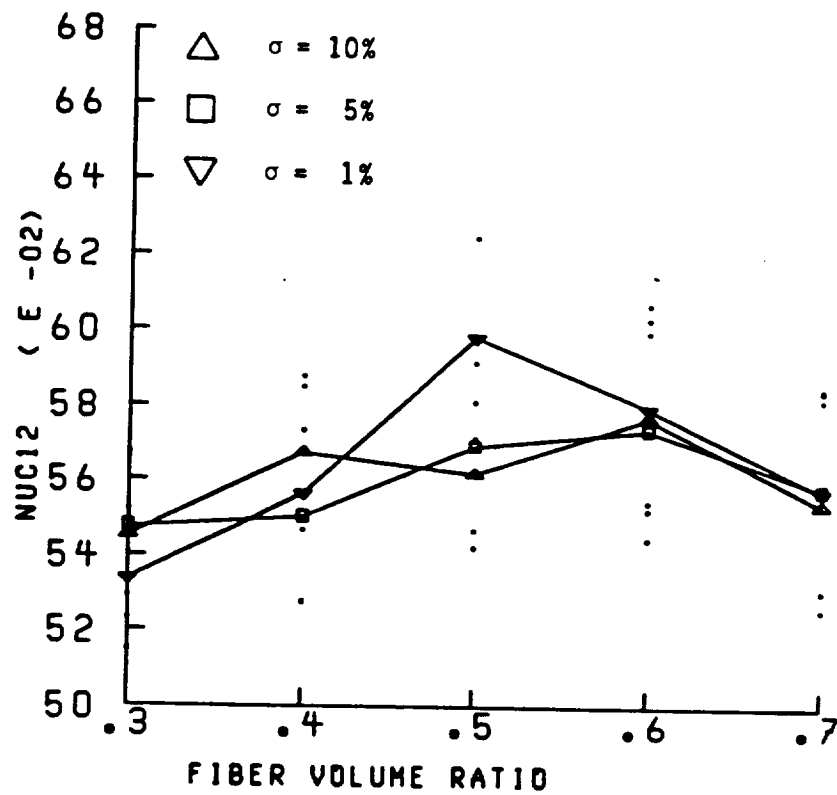


Fig. 61- Poisson's Ratio (major); for various
shape parameters of fiber modulus.

# POISSON'S RATIO (MINOR)
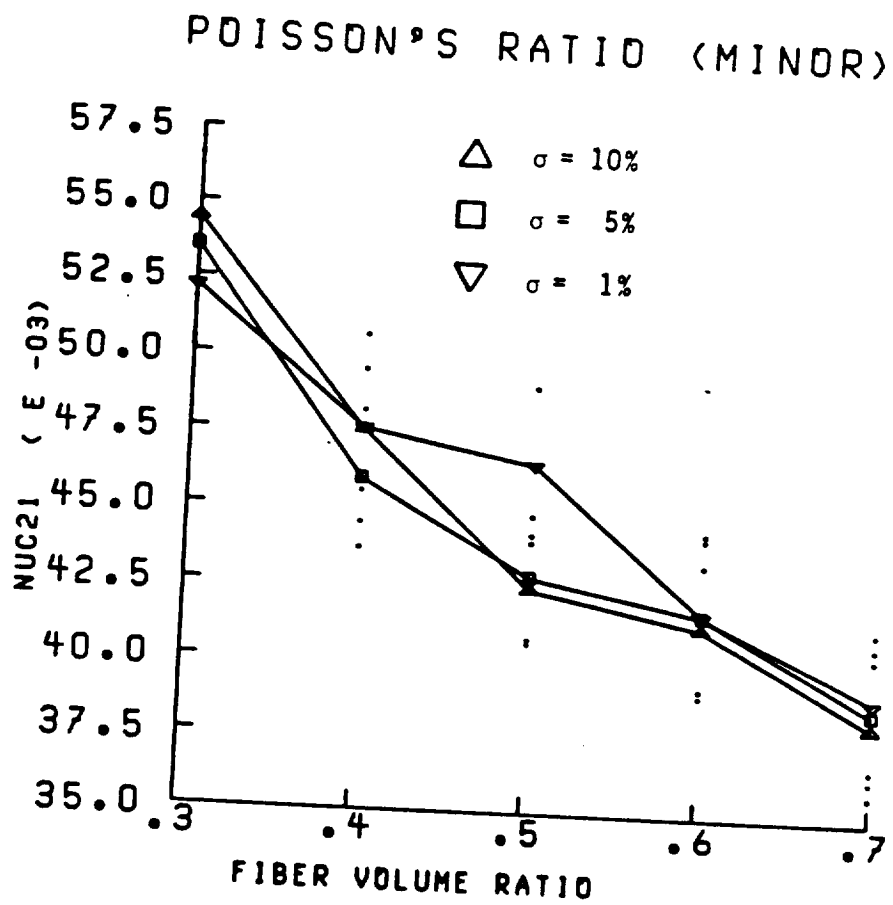


Fig. 62- Poisson's Ratio (minor) for various shape parameters of fiber modulus.

# LONG. TENSILE STRENGTH
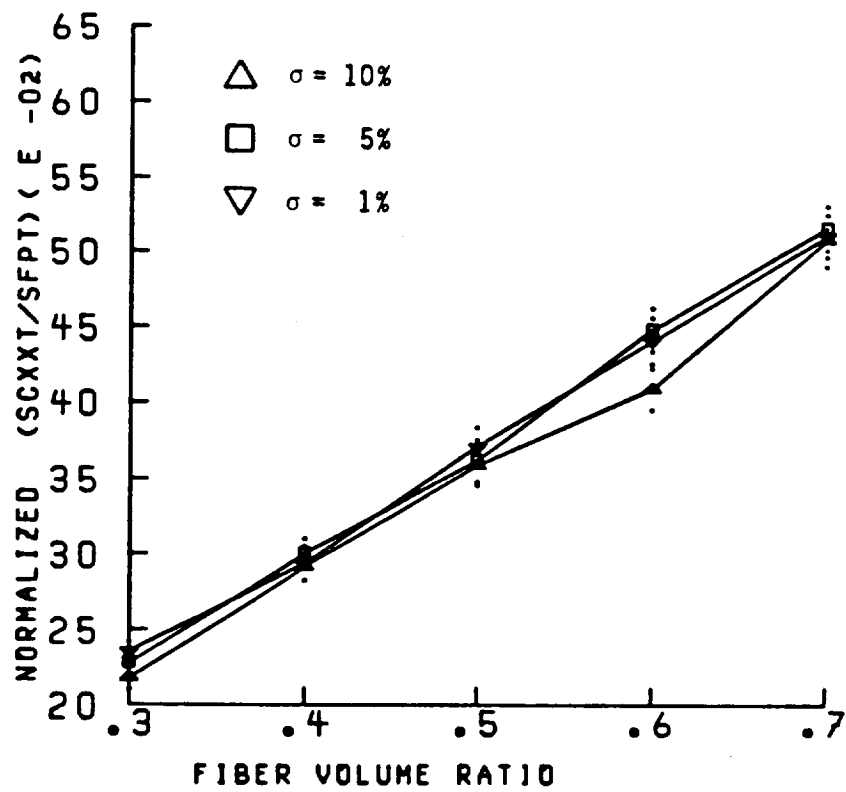


Fig. 63- Longitudinal Tensile Strength; for various shape parameters of fiber modulus.
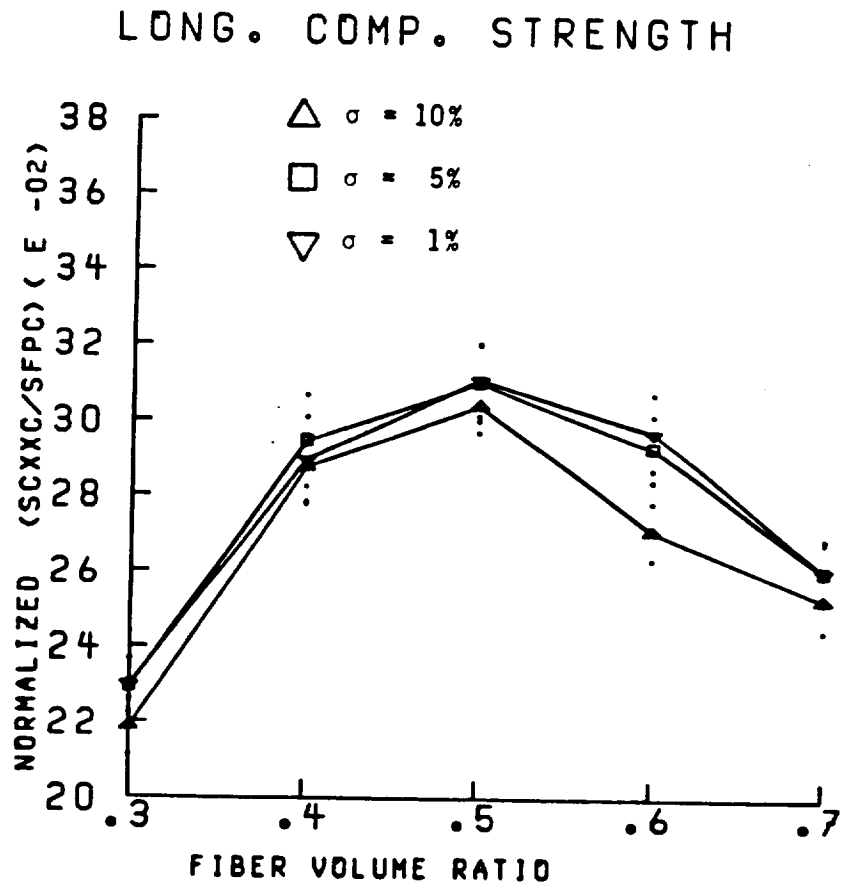
Fig. 64- Longitudinal Compressive Strength; for various shape parameters of fiber modulus.

# TRANS. TENSILE STRENGTH
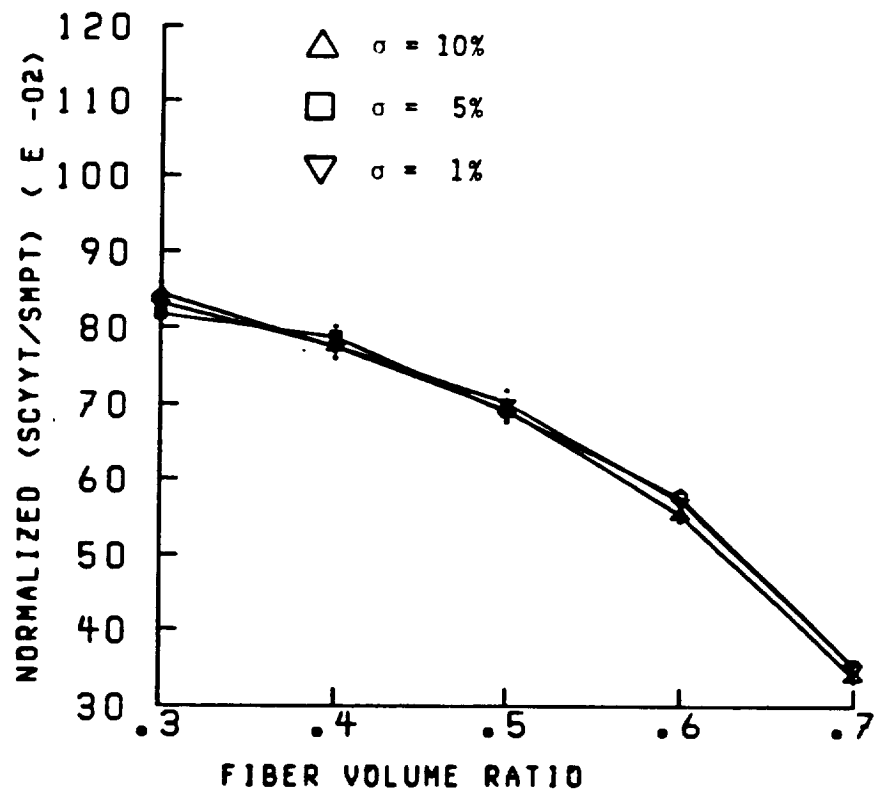


Fig. 65- Transverse Tensile Strength; for various shape parameters of fiber modulus.

# TRANS. COMP. STRENGTH
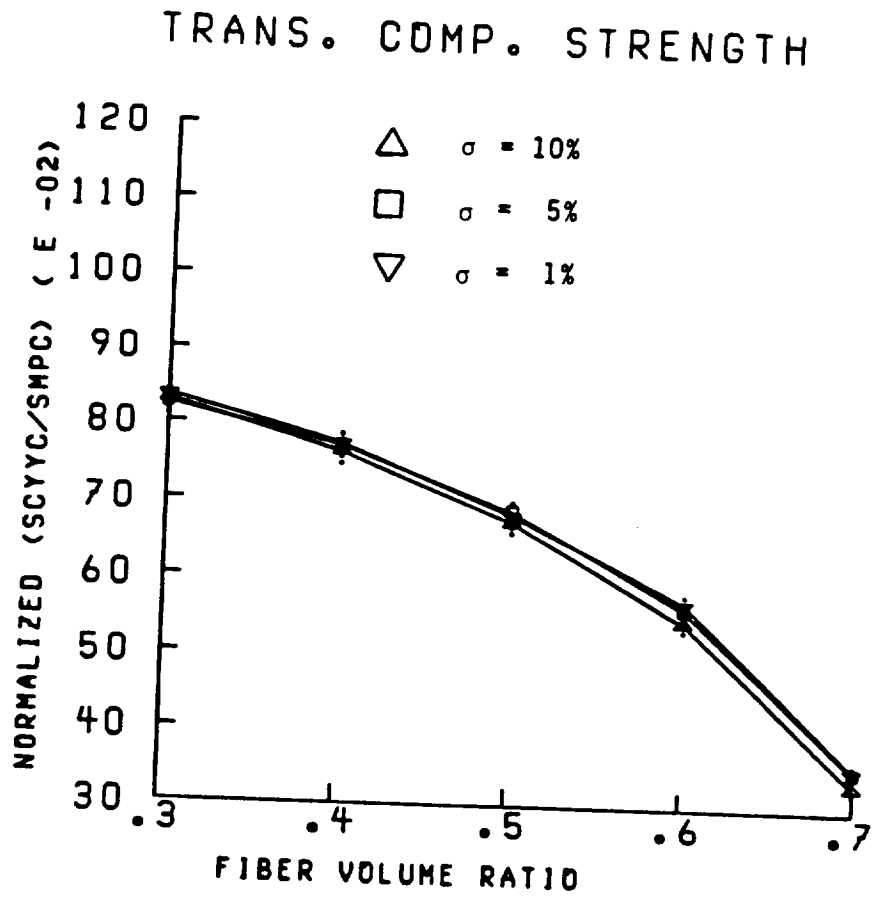


Fig. 66- Transverse Compressive Strength; for various shape parameters of fiber modulus.

# IN PLANE SHEAR STRENGTH
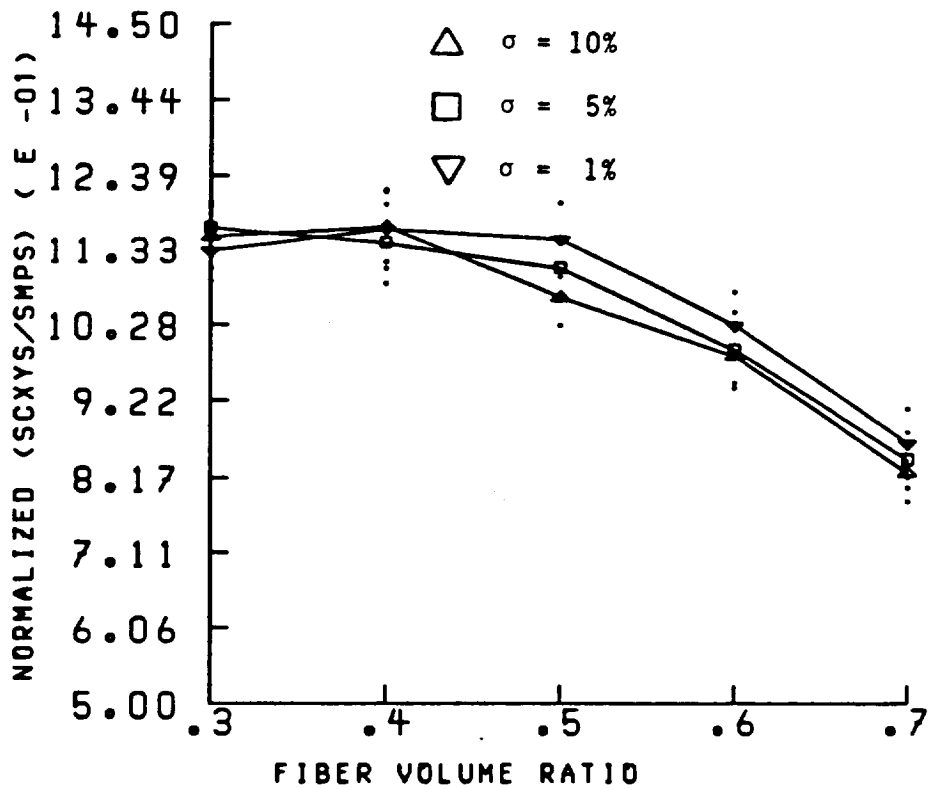


Fig. 67- In Plane Shear Strength; for various
shape parameters of fiber modulus.

## G. Regression Models

The output data of cases 2 through 11 are used as successive inputs to the regression scheme. The goal of stepwise regression, as used here, is to measure the degree of correlation between a dependent and a set of independent variables for a given set of data. The outputs of the regressions conducted show the independent variables accepted into the model (based on F-test criteria) in order of degree of correlation with the dependent variable of interest, along with the final $R^2$ statistic. (The $R^2$ values represent the square of the multiple correlation coefficient, a convenient measure of the fit between data values and values predicted by the regression equation.)

The ordering of predictor variables by stepwise regression has several important uses. In this study, the scheme facilitates easy investigation of the effects of material changes on composite properties. Since the monte carlo scheme permits generation of large amounts of data, the regression is easy, inexpensive, and can provide insight concerning the sensitivity of dependent variables for assumed distributions of predictor variables. A variety of material configurations and constituent distributions are examined, and a model constructed for each dependent (or response) variable. It must be noted that the relative correlations of predictor variables with response variables will be functions of the assumed distributions, the particular data sample considered, and the functional manner in which the predictor variables are incorporated into the model.

A simple regression model was assumed for each response variable.

The first set of "simple" regression models uses as predictor functions only the independent variables as individual terms. To be more precise, the predictor variables used are not simply the independent variable values, for there are 15 of these for each layup. The arithmetic mean of independent variable values is thus used as the predictor variable in the first set of regression models. The only exception to this is the use of the $\sin^2$ of the average of the fiber orientation angles as the angular dependence predictor, denoted by THETA in the tables to follow. The simpler response variables can be adequately described using the linear function forms in the regression models. The simple variables include the elastic constants, (EC11, EC22, EC12, NUC12, NUC21) and coefficients of thermal expansion (CTE11, CTE22). The results of the regressions performed in the "simple" manner are given in Tables III - XIV. In the tables the input labeled with N1 through N5 and W1 through W5 represent narrow and wide distributions of all properties. Input labeled N6 through N10 and W6 through W10 describe the same distributions, except that the composite is assumed unidirectional, i.e. no angular variation. The distinction shows the reduction in predictive capability induced by deviations of the fibers from aligned orientation.

The models assumed for the response (output) variables are of the form

$$Y = B_0 + B_1 X_1 + B_2 X_2 + B_3 X_3 + \ldots + B_n X_n$$

where

$Y$ = response variable (EC11, EC22, EC12, etc.)

$B_n$ = regression parameters to be obtained

$X_n$ = average of independent variable values through the thickness of the ply (THETA, FVR, VVR, etc.)

Each model postulated contains all independent variables that appear in the equations for the related ply property (see Appendix B).

## TABLE III- LONGITUDINAL MODULUS (EC11)

### SIMPLE MODEL

| INPUT | FVR | TERMS ACCEPTED | R² |
|---|---|---|---|
| N1 | 0.3 | FVR,EFP1 | 83.17 |
| N2 | 0.4 | FVR,EFP1,THETA | 92.63 |
| N3 | 0.5 | FVR,EFP1,THETA | 94.02 |
| N4 | 0.6 | FVR,EFP1,THETA | 94.59 |
| N5 | 0.7 | FVR,EFP1 | 84.00 |
| W1 | 0.3 | FVR,THETA,EFP1 | 64.49 |
| W2 | 0.4 | FVR,EFP1,THETA | 89.88 |
| W3 | 0.5 | FVR,THETA,EFP1 | 72.85 |
| W4 | 0.6 | FVR,THETA,EFP1 | 65.37 |
| W5 | 0.7 | FVR,EFP1,THETA | 57.83 |
| N6 | 0.3 | FVR,EFP1,EMP | 99.83 |
| N7 | 0.4 | FVR,EFP1 | 99.81 |
| N8 | 0.5 | FVR,EFP1 | 99.69 |
| N9 | 0.6 | FVR,EFP1,EMP | 99.74 |
| N10 | 0.7 | FVR,EFP1 | 99.77 |
| W6 | 0.3 | FVR,EFP1,VVR | 99.13 |
| W7 | 0.4 | FVR,EFP1 | 98.40 |
| W8 | 0.5 | FVR,EFP1 | 98.90 |
| W9 | 0.6 | FVR,EFP1 | 99.59 |
| W10 | 0.7 | FVR,EFP1 | 99.34 |

## TABLE IV- TRANSVERSE MODULUS (EC22)

### SIMPLE MODEL

| INPUT | FVR | TERMS ACCEPTED | $R^2$ |
|-------|-----|----------------|-------|
| N1 | 0.3 | FVR,EFP2 | 83.50 |
| N2 | 0.4 | FVR | 85.23 |
| N3 | 0.5 | FVR,EFP2 | 91.83 |
| N4 | 0.6 | FVR,EFP2 | 93.26 |
| N5 | 0.7 | FVR,EFP2,THETA | 93.06 |
| W1 | 0.3 | FVR,THETA,EFP2 | 78.36 |
| W2 | 0.4 | FVR,THETA,EFP2 | 90.73 |
| W3 | 0.5 | FVR,THETA,EFP2 | 80.15 |
| W4 | 0.6 | FVR,THETA,EFP2 | 86.05 |
| W5 | 0.7 | FVR,THETA,EFP2 | 87.14 |
| | | | |
| N6 | 0.3 | FVR,EFP2 | 87.13 |
| N7 | 0.4 | FVR,EFP2 | 86.15 |
| N8 | 0.5 | FVR,EFP2 | 90.97 |
| N9 | 0.6 | FVR,EFP2 | 93.47 |
| N10 | 0.7 | FVR,EFP2 | 92.05 |
| W6 | 0.3 | FVR,EFP2 | 79.72 |
| W7 | 0.4 | FVR,EFP2 | 70.71 |
| W8 | 0.5 | FVR,EFP2 | 81.92 |
| W9 | 0.6 | FVR,EFP2 | 88.62 |
| W10 | 0.7 | FVR,EFP2 | 84.05 |

# TABLE V- SHEAR MODULUS (EC12)

| INPUT | FVR | SIMPLE MODEL TERMS ACCEPTED | $R^2$ |
|---|---|---|---|
| N1 | 0.3 | THETA,FVR,GMP | 97.01 |
| N2 | 0.4 | THETA,FVR,GMP,GFP23 | 98.85 |
| N3 | 0.5 | THETA,FVR,GMP,GFP12 | 97.50 |
| N4 | 0.6 | THETA,FVR,GMP | 98.01 |
| N5 | 0.7 | THETA,FVR,GMP,GFP12 | 98.42 |
| W1 | 0.3 | THETA,FVR,GMP | 94.79 |
| W2 | 0.4 | THETA,FVR | 94.27 |
| W3 | 0.5 | THETA,FVR,GFP23 | 93.71 |
| W4 | 0.6 | THETA,FVR | 95.62 |
| W5 | 0.7 | THETA,FVR,GMP,GFP23 | 96.67 |
| | | | |
| N6 | 0.3 | FVR,GMP | 97.66 |
| N7 | 0.4 | FVR,GMP,GFP12 | 98.02 |
| N8 | 0.5 | FVR,GMP,GFP23 | 96.65 |
| N9 | 0.6 | FVR,GMP,GFP12 | 97.11 |
| N10 | 0.7 | FVR,GMP,GFP12 | 98.55 |
| W6 | 0.3 | FVR,GMP,GFP12 | 96.93 |
| W7 | 0.4 | FVR,GMP,GFP12 | 92.45 |
| W8 | 0.5 | FVR,GMP,GFP12 | 95.16 |
| W9 | 0.6 | FVR,GMP | 97.18 |
| W10 | 0.7 | FVR,GMP,GFP12 | 96.90 |

# TABLE VI- POISSON'S RATIO, MAJOR (NUC12)

## SIMPLE MODEL

| INPUT | FVR | TERMS ACCEPTED | R² |
|-------|-----|----------------|-----|
| N1 | 0.3 | THETA,EFP1 | 96.39 |
| N2 | 0.4 | THETA,FVR | 97.88 |
| N3 | 0.5 | THETA,FVR | 96.60 |
| N4 | 0.6 | THETA,FVR,EFP1 | 98.32 |
| N5 | 0.7 | THETA,FVR,EFP2 | 96.62 |
| W1 | 0.3 | THETA,EFP1 | 88.43 |
| W2 | 0.4 | THETA,FVR | 84.62 |
| W3 | 0.5 | THETA | 89.48 |
| W4 | 0.6 | THETA,VVR | 84.05 |
| W5 | 0.7 | THETA,FVR | 92.05 |
| N6 | 0.3 | FVR | 97.83 |
| N7 | 0.4 | FVR | 98.48 |
| N8 | 0.5 | FVR | 97.77 |
| N9 | 0.6 | FVR | 98.40 |
| N10 | 0.7 | FVR | 99.17 |
| W6 | 0.3 | FVR | 97.32 |
| W7 | 0.4 | FVR,VVR | 96.45 |
| W8 | 0.5 | FVR | 96.38 |
| W9 | 0.6 | FVR,GFP12,EFP2 | 98.34 |
| W10 | 0.7 | FVR,EFP2 | 96.96 |

## <u>TABLE VII- POISSON'S RATIO, MINOR (NUC21)</u>

### SIMPLE MODEL

| INPUT | FVR | TERMS ACCEPTED | $R^2$ |
|-------|-----|----------------|-------|
| N1 | 0.3 | THETA,FVR | 91.15 |
| N2 | 0.4 | THETA,FVR,EFP1 | 94.78 |
| N3 | 0.5 | THETA,FVR | 94.31 |
| N4 | 0.6 | THETA,FVR,EFP1,EFP2 | 97.18 |
| N5 | 0.7 | THETA,FVR,EFP1 | 95.87 |
| W1 | 0.3 | THETA,FVR | 90.87 |
| W2 | 0.4 | THETA,FVR,EFP2 | 89.86 |
| W3 | 0.5 | THETA,FVR | 91.93 |
| W4 | 0.6 | THETA | 92.57 |
| W5 | 0.7 | THETA,FVR,EFP1 | 94.78 |
| | | | |
| N6 | 0.3 | FVR,EFP1,EFP2 | 95.64 |
| N7 | 0.4 | FVR,EFP1,EFP2 | 94.90 |
| N8 | 0.5 | FVR,EFP1,EFP2 | 95.40 |
| N9 | 0.6 | FVR,EFP1,EFP2 | 93.12 |
| N10 | 0.7 | FVR,EFP1,EFP2 | 91.83 |
| W6 | 0.3 | FVR,EFP1,GFP12 | 87.73 |
| W7 | 0.4 | FVR,EFP1,EFP2 | 85.06 |
| W8 | 0.5 | FVR,EFP1,EFP2 | 84.29 |
| W9 | 0.6 | FVR,EFP1,EFP2 | 90.37 |
| W10 | 0.7 | EFP1,FVR,EFP2 | 91.42 |

## TABLE VIII- LONG. THERM. EXPANSION (CTE11)

### SIMPLE MODEL

| INPUT | FVR | TERMS ACCEPTED | $R^2$ |
|---|---|---|---|
| N1 | 0.3 | FVR,THETA,EFP1 | 90.29 |
| N2 | 0.4 | THETA,FVR,EFP1,VVR | 94.46 |
| N3 | 0.5 | FVR,THETA,EFP1,VVR | 95.72 |
| N4 | 0.6 | FVR,THETA,EFP1,VVR | 95.23 |
| N5 | 0.7 | THETA,FVR | 87.63 |
| W1 | 0.3 | THETA,FVR,EFP1 | 80.53 |
| W2 | 0.4 | THETA,FVR | 78.91 |
| W3 | 0.5 | THETA,FVR | 84.77 |
| W4 | 0.6 | THETA,FVR,VVR | 74.37 |
| W5 | 0.7 | THETA | 80.50 |
| N6 | 0.3 | FVR,EFP1,VVR | 97.21 |
| N7 | 0.4 | FVR,EFP1,VVR | 96.96 |
| N8 | 0.5 | FVR,EFP1,VVR | 96.53 |
| N9 | 0.6 | FVR,EFP1 | 96.60 |
| N10 | 0.7 | FVR,EFP1 | 96.24 |
| W6 | 0.3 | FVR,EFP1 | 91.60 |
| W7 | 0.4 | FVR,EFP1 | 90.88 |
| W8 | 0.5 | FVR,EFP1 | 91.55 |
| W9 | 0.6 | FVR,EFP1,VVR | 96.03 |
| W10 | 0.7 | FVR,EFP1 | 94.13 |

## TABLE IX- TRANS. THERM. EXPANSION (CTE22)

### SIMPLE MODEL

| INPUT | FVR | TERMS ACCEPTED | $R^2$ |
|-------|-----|----------------|-------|
| N1 | 0.3 | FVR,THETA,VVR | 99.60 |
| N2 | 0.4 | FVR,THETA,VVR | 99.21 |
| N3 | 0.5 | FVR,THETA,VVR | 99.46 |
| N4 | 0.6 | FVR,THETA | 99.69 |
| N5 | 0.7 | FVR,THETA | 99.79 |
| W1 | 0.3 | FVR,THETA | 95.04 |
| W2 | 0.4 | FVR,THETA,EFP1,VVR | 98.60 |
| W3 | 0.5 | FVR,THETA | 95.19 |
| W4 | 0.6 | FVR,THETA | 94.84 |
| W5 | 0.7 | FVR,THETA | 97.98 |
| N6 | 0.3 | FVR,VVR,EFP1 | 99.70 |
| N7 | 0.4 | FVR,VVR | 99.53 |
| N8 | 0.5 | FVR,VVR | 99.65 |
| N9 | 0.6 | FVR | 99.67 |
| N10 | 0.7 | FVR | 99.75 |
| W6 | 0.3 | FVR,EFP1 | 99.15 |
| W7 | 0.4 | FVR | 98.81 |
| W8 | 0.5 | FVR | 98.88 |
| W9 | 0.6 | FVR | 99.47 |
| W10 | 0.7 | FVR | 99.22 |

## TABLE X- LONG. TENSILE STRENGTH (SCXXT)

### SIMPLE MODEL

| INPUT | FVR | TERMS ACCEPTED | $R^2$ |
|-------|-----|----------------|-------|
| N1 | 0.3 | FVR | 12.25 |
| N2 | 0.4 | FVR,SFPT | 43.72 |
| N3 | 0.5 | FVR | 21.68 |
| N4 | 0.6 | FVR,SFPT,THETA | 43.68 |
| N5 | 0.7 | FVR | 40.97 |
| W1 | 0.3 | FVR,SFPT | 33.37 |
| W2 | 0.4 | SFPT,FVR | 39.02 |
| W3 | 0.5 | EFP1,SFPT | 26.13 |
| W4 | 0.6 | FVR,EMP | 42.27 |
| W5 | 0.7 | FVR,SFPT | 33.55 |
| | | | |
| N6 | 0.3 | FVR,SFPT | 52.12 |
| N7 | 0.4 | FVR,SFPT,EFP1 | 68.43 |
| N8 | 0.5 | FVR,SFPT | 34.89 |
| N9 | 0.6 | FVR,SFPT | 49.00 |
| N10 | 0.7 | SFPT,FVR | 24.00 |
| W6 | 0.3 | SFPT,FVR | 46.61 |
| W7 | 0.4 | FVR | 19.33 |
| W8 | 0.5 | FVR,SFPT | 33.13 |
| W9 | 0.6 | FVR,SFPT | 34.40 |
| W10 | 0.7 | SFPT,FVR | 37.65 |

## TABLE XI- LONG. COMPRESSIVE STRENGTH (SCXXC)

### SIMPLE MODEL

| INPUT | FVR | TERMS ACCEPTED | $R^2$ |
|-------|-----|----------------|-------|
| N1 | 0.3 | FVR | 12.25 |
| N2 | 0.4 | FVR | 18.23 |
| N3 | 0.5 | NONE | |
| N4 | 0.6 | SFPC | 8.52 |
| N5 | 0.7 | FVR | 8.08 |
| W1 | 0.3 | VVR | 8.02 |
| W2 | 0.4 | THETA | 9.29 |
| W3 | 0.5 | GMP,SMPC | 20.59 |
| W4 | 0.6 | THETA | 9.18 |
| W5 | 0.7 | NONE | |
| | | | |
| N6 | 0.3 | SFPC | 11.30 |
| N7 | 0.4 | NONE | |
| N8 | 0.5 | NONE | |
| N9 | 0.6 | NONE | |
| N10 | 0.7 | GFP12 | 12.01 |
| W6 | 0.3 | FVR | 9.40 |
| W7 | 0.4 | VVR | 10.76 |
| W8 | 0.5 | VVR | 9.85 |
| W9 | 0.6 | GFP12 | 8.87 |
| W10 | 0.7 | NONE | |

## TABLE XII- TRANSVERSE TENSILE STRENGTH (SCYYT)

### SIMPLE MODEL

| INPUT | FVR | TERMS ACCEPTED | $R^2$ |
|-------|-----|----------------|-------|
| N1 | 0.3 | FVR | 27.03 |
| N2 | 0.4 | FVR | 32.91 |
| N3 | 0.5 | SMPT | 8.10 |
| N4 | 0.6 | FVR | 41.92 |
| N5 | 0.7 | NONE | |
| W1 | 0.3 | FVR,VVR,SMPT | 26.89 |
| W2 | 0.4 | FVR | 41.43 |
| W3 | 0.5 | FVR | 14.74 |
| W4 | 0.6 | NONE | |
| W5 | 0.7 | FVR,SMPT | 31.05 |
| | | | |
| N6 | 0.3 | FVR | 9.43 |
| N7 | 0.4 | FVR | 8.19 |
| N8 | 0.5 | FVR,EFP2 | 15.58 |
| N9 | 0.6 | NONE | |
| N10 | 0.7 | NONE | |
| W6 | 0.3 | FVR | 33.87 |
| W7 | 0.4 | FVR | 13.39 |
| W8 | 0.5 | SMPT | 8.62 |
| W9 | 0.6 | FVR | 27.85 |
| W10 | 0.7 | FVR | 32.77 |

## TABLE XIII- TRANSVERSE COMPRESSIVE STRENGTH (SCYYC)

### SIMPLE MODEL

| INPUT | FVR | TERMS ACCEPTED | $R^2$ |
|-------|-----|----------------|-------|
| N1 | 0.3 | FVR,SMPC | 33.17 |
| N2 | 0.4 | FVR | 30.10 |
| N3 | 0.5 | NONE | |
| N4 | 0.6 | FVR | 38.93 |
| N5 | 0.7 | NONE | |
| W1 | 0.3 | FVR,VVR | 28.19 |
| W2 | 0.4 | FVR | 43.26 |
| W3 | 0.5 | FVR,SMPC | 19.57 |
| W4 | 0.6 | NONE | |
| W5 | 0.7 | FVR | 15.85 |
| | | | |
| N6 | 0.3 | NONE | |
| N7 | 0.4 | NONE | |
| N8 | 0.5 | NONE | |
| N9 | 0.6 | NONE | |
| N10 | 0.7 | NONE | |
| W6 | 0.3 | FVR | 28.68 |
| W7 | 0.4 | FVR | 11.64 |
| W8 | 0.5 | NONE | |
| W9 | 0.6 | FVR | 31.97 |
| W10 | 0.7 | FVR | 33.05 |

## TABLE XIV- IN PLANE SHEAR STRENGTH (SCXYS)

### SIMPLE MODEL

| INPUT | FVR | TERMS ACCEPTED | $R^2$ |
|---|---|---|---|
| N1 | 0.3 | FVR,THETA,GFP12 | 28.51 |
| N2 | 0.4 | FVR | 8.74 |
| N3 | 0.5 | THETA | 14.96 |
| N4 | 0.6 | THETA,GFP12,FVR,SMPS | 31.84 |
| N5 | 0.7 | NONE | |
| W1 | 0.3 | THETA,VVR,SMPS,FVR | 48.16 |
| W2 | 0.4 | FVR | 43.26 |
| W3 | 0.5 | THETA | 8.40 |
| W4 | 0.6 | THETA | 14.75 |
| W5 | 0.7 | NONE | |
| N6 | 0.3 | NONE | |
| N7 | 0.4 | NONE | |
| N8 | 0.5 | NONE | |
| N9 | 0.6 | SMPS | 8.25 |
| N10 | 0.7 | VVR | 8.53 |
| W6 | 0.3 | FVR,SMPS,GMP | 29.06 |
| W7 | 0.4 | NONE | |
| W8 | 0.5 | NONE | |
| W9 | 0.6 | GFP12,FVR | 22.20 |
| W10 | 0.7 | SMPS | 17.73 |

Further regression models were studied, in an attempt to improve the predictive capability of the models, especially for the strengths. These models, incorporating higher order functions and combinations of predictor variables used in the simple models, show some improvement over the simple models, proving the value of including the "interaction" effects of predictor variables in the regression models. In addition, the higher order interaction models can fit response functions over a wider range of fiber volume ratio, with associated improvements in the $R^2$ statistics. The data cases CON1 and CON2 contain selected points from the entire range of fiber volume ratios, to supply the samples for these runs. Furthermore, since higher order models are postulated, THETA is taken to be the cosine of the average of fiber orientation angles. The variable MVR is a "dummy" variable, that is a function of other variables in the model. It is defined as

$$MVR = 1 - FVR - VVR$$

and is intended to represent an "average" matrix volume ratio over the thickness of the ply. The interaction models are shown in Tables XV - XXVI.

The general form of the postulated models now includes higher order terms, so the predictor variables are tested up to the fourth power. Symbolically,

$$
\begin{aligned}
Y = \ & B_0 + B_1(\text{THETA}) + B_2(\text{FVR}) + B_3(\text{VVR}) + B_4(\text{EFP1}) + B_5(\text{EMP}) + \\
& B_6(\text{MVR}) + B_7(\text{THETA})^2 + B_8(\text{THETA})(\text{FVR}) + B_9(\text{THETA})(\text{VVR}) + \\
& B_{10}(\text{THETA})(\text{EFP1}) + \ldots + B_{11}(\text{THETA})^2(\text{FVR})(\text{EFP1}) + \ldots \\
& B_{12}(\text{THETA})^4 + B_{13}(\text{FVR})^2 + \ldots \quad \text{etc.}
\end{aligned}
$$

The number of terms possible in a complete fourth power polynomial expansion becomes unwieldy for the cases studied. Considering the limitation of the size of the predictor matrix in the regression package used (100 x 100), the terms are intuitively grouped in the hope of eliminating large groups at one time. The regressions are conducted using "unlikely" candidates for admission into a particular model, and if no terms are entered, subsequent regressions are conducted without those terms. The justification for this approach is not a statistical argument, rather an interpretation of the physical principles active in any chosen model. The regressions to eliminate terms are merely used as a check on what seems intuitively reasonable.

## TABLE XV- LONGITUDINAL MODULUS (EC11)

### INTERACTION MODEL

| INPUT | FVR | TERMS ACCEPTED | $R^2$ |
|-------|-----|----------------|-------|
| N1 | 0.3 | $THETA^4*FVR*EFP1$ | 84.50 |
| N2 | 0.4 | $THETA^4*FVR*EFP1$ | 92.66 |
| N3 | 0.5 | $THETA^4*FVR*EFP1$ | 93.76 |
| N4 | 0.6 | $THETA^4*FVR*EFP1$ | 94.24 |
| N5 | 0.7 | $THETA^4*FVR*EFP1$ | 85.08 |
| W1 | 0.3 | $THETA^4*FVR*EFP1$ | 63.84 |
| W2 | 0.4 | $THETA^4*FVR*EFP1$ | 89.86 |
| W3 | 0.5 | $THETA^4*FVR*EFP1$ | 71.79 |
| W4 | 0.6 | $THETA^4*FVR*EFP1$ | 64.37 |
| W5 | 0.7 | $THETA^4*FVR*EFP1$ | 55.68 |
| N6 | 0.3 | $FVR*EFP1, EMP^2*MVR$ | 99.82 |
| N7 | 0.4 | $FVR*EFP1, FVR^4$ | 99.83 |
| N8 | 0.5 | $FVR*EFP1$ | 99.72 |
| N9 | 0.6 | $FVR*EFP1, EMP^2*VVR, VVR^4$ | 99.79 |
| N10 | 0.7 | $FVR*EFP1, EMP*MVR$ | 99.79 |
| W6 | 0.3 | $FVR*EFP1, VVR$ | 99.17 |
| W7 | 0.4 | $FVR*EFP1, MVR^2*FVR$ | 98.53 |
| W8 | 0.5 | $FVR*EFP1, MVR^2*EMP$ | 98.99 |
| W9 | 0.6 | $FVR*EFP1$ | 99.58 |
| W10 | 0.7 | $FVR*EFP1, EMP*MVR$ | 99.38 |
| CON1 | VARIES | $THETA^4*FVR*EFP1$ | 96.48 |
| CON2 | VARIES | $FVR*EFP1, VVR^4$ | 99.92 |

## TABLE XVI- TRANSVERSE MODULUS (EC22)

| INPUT | FVR | INTERACTION MODEL TERMS ACCEPTED | $R^2$ |
|---|---|---|---|
| N1 | 0.3 | FVR*EFP2*EMP,EFP2$^2$*FVR,THETA*FVR*MVR | |
| N2 | 0.4 | FVR*EFP2*EMP,EFP2$^2$*FVR,THETA | 99.19 |
| N3 | 0.5 | FVR*EFP2*EMP,THETA$^2$*EFP2,MVR$^4$ | 99.55 |
| N4 | 0.6 | FVR*EFP2*EMP,THETA$^2$*EFP2,EFP2$^2$*FVR | 98.92 |
| N5 | 0.7 | *** NEARLY SINGULAR | 99.22 |
| W1 | 0.3 | THETA$^2$*MVR,EMP$^2$*EFP2,MVR$^2$ | |
| W2 | 0.4 | FVR*EMP,THETA,EFP2$^2$*FVR | 93.26 |
| W3 | 0.5 | FVR*EFP2*EMP,THETA,FVR*EFP2*MVR | 96.79 |
| W4 | 0.6 | THETA$^2$*MVR,MVR$^2$*EFP2,EMP*MVR | 93.49 |
| W5 | 0.7 | *** NEARLY SINGULAR | 88.35 |
| | | | |
| N6 | 0.3 | FVR*EFP2*EMP,EFP2$^2$*FVR,EMP*MVR | |
| N7 | 0.4 | FVR*EFP2*EMP,EMP$^2$FVR | 99.22 |
| N8 | 0.5 | FVR*EFP2*EMP,FVR*EFP2*MVR | 99.07 |
| N9 | 0.6 | FVR*EFP2*EMP,FVR$^2$*EMP | 98.89 |
| N10 | 0.7 | FVR$^4$,EFP2*EMP | 99.14 |
| W6 | 0.3 | FVR*EFP2*EMP,EFP2,EFP2$^2$*EMP,FVR*EFP2 | 99.23 |
| W7 | 0.4 | FVR*EFP2*EMP,FVR*EFP2*MVR,FVR*VVR | 98.62 |
| W8 | 0.5 | FVR*EFP2*EMP,FVR*EFP2*MVR | 98.28 |
| W9 | 0.6 | FVR*EFP2*EMP,EFP2$^2$*MVR | 97.93 |
| W10 | 0.7 | FVR*EFP2*EMP,MVR$^2$*FVR | 98.44 |
| | | | 97.86 |
| | | | |
| CON1 | VARIES | *** NEARLY SINGULAR | |
| CON2 | VARIES | FVR*EFP2*EMP,FVR*EFP2*MVR | 99.79 |

## TABLE XVII- IN PLANE SHEAR MODULUS (EC12)

### INTERACTION MODEL

| INPUT | FVR | TERMS ACCEPTED | $R^2$ |
|-------|-----|----------------|-------|
| N1 | 0.3 | THETA, FVR*GMP, THETA$^4$*FVR*GMP | 97.86 |
| N2 | 0.4 | *** NEARLY SINGULAR | |
| N3 | 0.5 | THETA$^2$, FVR$^2$*GMP, GFP12*GMP | 97.75 |
| N4 | 0.6 | THETA, FVR$^2$*MVR | 98.01 |
| N5 | 0.7 | THETA, FVR$^2$*GMP, GFP12 | 98.46 |
| W1 | 0.3 | THETA$^4$, FVR$^4$*GMP, FVR$^2$ | 95.49 |
| W2 | 0.4 | *** NEARLY SINGULAR | |
| W3 | 0.5 | THETA$^4$*FVR*MVR, THETA$^4$*VVR, VVR*GMP | 91.04 |
| W4 | 0.6 | THETA$^4$, FVR$^3$*GMP, THETA | 96.70 |
| W5 | 0.7 | *** NEARLY SINGULAR | |
| N6 | 0.3 | FVR*GMP, MVR$^2$*GFP12 | 97.73 |
| N7 | 0.4 | FVR*GMP, GFP12 | 97.97 |
| N8 | 0.5 | FVR*GMP, FVR*GFP12 | 96.52 |
| N9 | 0.6 | FVR*GMP, FVR$^2$*GFP12 | 97.10 |
| N10 | 0.7 | FVR$^4$*GMP, FVR*GFP12*GMP, MVR$^2$*GMP | 98.90 |
| W6 | 0.3 | FVR*GMP, FVR*GFP12 | 96.91 |
| W7 | 0.4 | FVR*GMP, FVR*GFP12 | 92.37 |
| W8 | 0.5 | FVR*GMP, FVR*GFP12 | 95.08 |
| W9 | 0.6 | FVR*GMP, FVR$^2$*GFP12 | 97.42 |
| W10 | 0.7 | FVR$^4$*GMP, FVR*GFP12*GMP, MVR$^2$*GMP | 96.85 |
| CON1 | VARIES | FVR$^2$*VVR, VVR*MVR, FVR*GMP, THETA$^4$*FVR*GMP | 99.09 |
| CON2 | VARIES | FVR$^2$*GMP, VVR*GMP, GFP12*GMP | 99.54 |

## TABLE XVIII- LONG. THERMAL EXPANSION (CTE11)

### INTERACTION MODEL

| INPUT | FVR | TERMS ACCEPTED | $R^2$ |
|-------|-----|----------------|-------|
| N1 | 0.3 | $THETA^2*MVR, MVR^2, FVR*EFP1*MVR, EMP^2*EFP1$ | 92.51 |
| N2 | 0.4 | $THETA^2*MVR, THETA^4, EFP1^4, EMP^2*FVR, MVR^2*EFP1$ | 96.38 |
| N3 | 0.5 | $THETA^2*MVR, MVR, EMP^2*MVR, EMP^2*EFP1$ | 97.26 |
| N4 | 0.6 | $FVR*EFP1, THETA*FVR*EFP1, EMP^2*MVR$ | 96.32 |
| N5 | 0.7 | $THETA, EMP*MVR$ | 90.66 |
| W1 | 0.3 | *** NEARLY SINGULAR | |
| W2 | 0.4 | $THETA^4, MVR^2*EMP$ | 80.81 |
| W3 | 0.5 | $THETA^4, EMP^2*MVR,$ | 87.98 |
| W4 | 0.6 | $THETA^4, MVR^2*VVR$ | 75.20 |
| W5 | 0.7 | $THETA^4, FVR^2*MVR$ | 82.97 |
| | | | |
| N6 | 0.3 | $MVR^2*EMP, EFP1^2*EMP, FVR^4$ | 99.29 |
| N7 | 0.4 | $MVR^2*EMP, FVR*EFP1*MVR, MVR^2*VVR$ | 99.17 |
| N8 | 0.5 | $MVR^2*EMP, EFP1, FVR^4$ | 98.94 |
| N9 | 0.6 | $MVR^2*EMP, EFP1^2*MVR$ | 98.94 |
| N10 | 0.7 | $MVR^2*EMP, EFP1*MVR.$ | 99.33 |
| W6 | 0.3 | $MVR^2*EMP, FVR*EFP1*MVR$ | 98.35 |
| W7 | 0.4 | $MVR^2*EMP, FVR*EFP1*MVR$ | 98.55 |
| W8 | 0.5 | $MVR^2*EMP, EFP1^2*MVR$ | 98.56 |
| W9 | 0.6 | $MVR^2*EMP, EFP1^2*MVR$ | 99.00 |
| W10 | 0.7 | $MVR^2*EFP1, EMP^2*MVR$ | 98.20 |
| | | | |
| CON1 | VARIES | $THETA, MVR^3, EFP1^2*VVR, FVR*VVR*EFP1$ | 96.82 |
| CON2 | VARIES | $MVR^2*EMP, FVR*EFP1*MVR, FVR^4, FVR^2*VVR...$ | 99.84 |

## TABLE XIX- TRANS. THERMAL EXPANSION (CTE22)

### INTERACTION MODEL

| INPUT | FVR | TERMS ACCEPTED | $R^2$ |
|---|---|---|---|
| N1 | 0.3 | $THETA^2*MVR, VVR$ | 99.60 |
| N2 | 0.4 | $THETA^2*MVR, MVR^2*FVR, FVR*EFP1*EMP$ | 99.38 |
| N3 | 0.5 | $THETA^2*MVR, MVR^2*FVR, FVR^4$ | 99.48 |
| N4 | 0.6 | $THETA^2*MVR, MVR^2*FVR, EMP^2*VVR, MVR^2*VVR$ | 99.73 |
| N5 | 0.7 | $FVR^2, THETA, THETA^2*FVR$ | 99.81 |
| W1 | 0.3 | $THETA^2*MVR, MVR, EFP1^2*VVR$ | 95.16 |
| W2 | 0.4 | $THETA^2*MVR, MVR, FVR*EFP1*MVR$ | 98.71 |
| W3 | 0.5 | $THETA^2*MVR, MVR^2*FVR, EFP1^2*VVR$ | 95.91 |
| W4 | 0.6 | $THETA^2*MVR, THETA, THETA^4$ | 95.69 |
| W5 | 0.7 | *** NEARLY SINGULAR | |
| N6 | 0.3 | $FVR, MVR^3$ | 99.70 |
| N7 | 0.4 | $FVR, MVR^4$ | 99.59 |
| N8 | 0.5 | $FVR, MVR^2$ | 99.67 |
| N9 | 0.6 | $FVR, EMP^2*EFP1$ | 99.70 |
| N10 | 0.7 | $FVR, MVR^4$ | 99.82 |
| W6 | 0.3 | $FVR, FVR*EFP1*EMP$ | 99.26 |
| W7 | 0.4 | $FVR, MVR^4$ | 98.97 |
| W8 | 0.5 | $FVR$ | 98.88 |
| W9 | 0.6 | $FVR, MVR^4$ | 99.57 |
| W10 | 0.7 | $FVR, EMP^2*FVR$ | 99.29 |
| CON1 | VARIES | $THETA^2*MVR$ | 99.32 |
| CON2 | VARIES | $FVR, FVR^3, MVR^2*EMP$ | 99.95 |

## TABLE XX- POISSON RATIO; MAJOR (NUC12)

### INTERACTION MODEL

| INPUT | FVR | TERMS ACCEPTED | $R^2$ |
|-------|-----|----------------|-------|
| N1 | 0.3 | *** NEARLY SINGULAR | |
| N2 | 0.4 | THETA,EFP2*MVR | 97.96 |
| N3 | 0.5 | THETA,GFP112*MVR | 96.71 |
| N4 | 0.6 | THETA,EFP1*MVR | 98.17 |
| N5 | 0.7 | THETA,FVR*EFP2 | 96.48 |
| W1 | 0.3 | *** NEARLY SINGULAR | |
| W2 | 0.4 | THETA,THETA$^4$*FVR*GFP12 | 84.73 |
| W3 | 0.5 | THETA | 89.43 |
| W4 | 0.6 | THETA,VVR*GFP12 | 84.27 |
| W5 | 0.7 | THETA,FVR*MVR | 92.10 |
| N6 | 0.3 | FVR | 97.83 |
| N7 | 0.4 | FVR | 98.48 |
| N8 | 0.5 | FVR | 97.77 |
| N9 | 0.6 | FVR,FVR*MVR | 98.52 |
| N10 | 0.7 | FVR | 99.17 |
| W6 | 0.3 | FVR | 97.32 |
| W7 | 0.4 | FVR,VVR*EFP2 | 96.50 |
| W8 | 0.5 | FVR | 96.38 |
| W9 | 0.6 | FVR,EFP1*EFP2,GFP12*MVR | 98.41 |
| W10 | 0.7 | FVR,FVR*EFP2 | 96.97 |
| CON1 | VARIES | *** SINGULAR | |
| CON2 | VARIES | MVR,FVR*MVR,EFP1*MVR | 99.77 |

## TABLE XXI- POISSON RATIO; MINOR (NUC21)

### INTERACTION MODEL

| INPUT | FVR | TERMS ACCEPTED | $R^2$ |
|-------|-----|----------------|-------|
| N1 | 0.3 | THETA,THETA$^4$*FVR*EFP1 | 91.69 |
| N2 | 0.4 | THETA,FVR*EFP1 | 94.66 |
| N3 | 0.5 | THETA,FVR*EFP1,EFP2*GFP12 | 95.10 |
| N4 | 0.6 | THETA,THETA$^4$*FVR*EFP1,EFP2 | 97.15 |
| N5 | 0.7 | THETA,THETA$^4$*FVR*EFP1 | 95.82 |
| W1 | 0.3 | THETA,FVR*GFP12 | 91.16 |
| W2 | 0.4 | THETA,EFP2*MVR | 89.52 |
| W3 | 0.5 | THETA,FVR*EFP1 | 92.06 |
| W4 | 0.6 | THETA | 92.53 |
| W5 | 0.7 | THETA,FVR*EFP1,THETA$^4$*FVR*MVR,EFP2*MVR | 95.60 |
| | | | |
| N6 | 0.3 | FVR*EFP1,FVR*EFP2 | 95.48 |
| N7 | 0.4 | FVR*EFP1,FVR*EFP2 | 94.69 |
| N8 | 0.5 | FVR*EFP1,FVR*EFP2,FVR*GFP12 | 95.52 |
| N9 | 0.6 | FVR*EFP1,FVR*EFP2 | 92.85 |
| N10 | 0.7 | FVR*EFP1,FVR*EFP2 | 91.77 |
| W6 | 0.3 | FVR*EFP1,GFP12*MVR | 87.83 |
| W7 | 0.4 | FVR*EFP1,FVR*EFP2,FVR*MVR | 86.48 |
| W8 | 0.5 | FVR*EFP1,EFP2 | 84.36 |
| W9 | 0.6 | FVR*EFP1,FVR*EFP2 | 89.84 |
| W10 | 0.7 | FVR*EFP1,FVR*EFP2 | 91.55 |
| | | | |
| CON1 | VARIES | THETA,FRV*GFP12,EFP2,THETA$^4$*FVR*MVR,... | 98.70 |
| CON2 | VARIES | FVR*EFP1,FVR*MVR,EFP2,VVR*GFP12 | 98.35 |

## TABLE XXII- LONGITUDINAL TENSILE STRENGTH (SCXXT)

### INTERACTION MODEL

| INPUT | FVR | TERMS ACCEPTED | $R^2$ |
|-------|-----|----------------|-------|
| N1 | 0.3 | $THETA^4$*FVR*SFPT | 17.72 |
| N2 | 0.4 | $THETA^4$*FVR*SFPT,$MVR^4$ | 47.65 |
| N3 | 0.5 | $THETA^4$*FVR*SFPT | 27.65 |
| N4 | 0.6 | $THETA^4$*FVR*SFPT,$FVR^2$*EMP | 44.67 |
| N5 | 0.7 | $THETA^4$*FVR*SFPT | 45.35 |
| W1 | 0.3 | FVR*SFPT,FVR*EFP1*MVR | 39.18 |
| W2 | 0.4 | FVR*SFPT,$FVR^2$*MVR | 42.87 |
| W3 | 0.5 | EFP1*SFPT,EMP*MVR | 33.97 |
| W4 | 0.6 | $EMP^2$*MVR,$THETA^2$*SFPT*MVR | 45.09 |
| W5 | 0.7 | $THETA^2$*FVR*SFPT | 32.56 |
| N6 | 0.3 | FVR*SFPT,$FVR^2$*EMP | 52.95 |
| N7 | 0.4 | FVR*SFPT,FVR*EFP1 | 64.41 |
| N8 | 0.5 | FVR*SFPT,$MVR^2$*FVR | 39.12 |
| N9 | 0.6 | FVR*SFPT | 47.13 |
| N10 | 0.7 | FVR*SFPT,FVR*EMP | 27.43 |
| W6 | 0.3 | FVR*SFPT,$MVR^2$*EFP1 | 49.71 |
| W7 | 0.4 | FVR*SFPT | 25.19 |
| W8 | 0.5 | FVR*SFPT | 32.16 |
| W9 | 0.6 | FVR*SFPT | 34.06 |
| W10 | 0.7 | FVR*SFPT | 35.09 |
| CON1 | VARIES | $THETA^4$*FVR*SFPT,FVR*VVR*MVR,FVR*EFP1*MVR | 81.20 |
| CON2 | VARIES | FVR*SFPT,FVR*VVR,$MVR^2$*SFPT | 84.79 |

# TABLE XXIII- LONGITUDINAL COMPRESSIVE STRENGTH (SCXXC)

### INTERACTION MODEL

| INPUT | FVR | TERMS ACCEPTED | $R^2$ |
|-------|-----|----------------|-------|
| N1 | 0.3 | SFPC*SMPC | |
| N2 | 0.4 | FVR*MVR | 12.53 |
| N3 | 0.5 | NONE | 19.45 |
| N4 | 0.6 | SFPC*GMP | |
| N5 | 0.7 | FVR*GFP12 | 9.81 |
| W1 | 0.3 | $VVR^4$ | 10.20 |
| W2 | 0.4 | $THETA^4$ | 10.40 |
| W3 | 0.5 | EMP*SMPC, $THETA^2$*EMP | 9.32 |
| W4 | 0.6 | $THETA^4$ | 23.32 |
| W5 | 0.7 | NONE | 9.20 |
| | | | |
| N6 | 0.3 | SFPC, GFP12*SMPC | |
| N7 | 0.4 | NONE | 20.04 |
| N8 | 0.5 | NONE | |
| N9 | 0.6 | NONE | |
| N10 | 0.7 | GFP12*EMP | |
| W6 | 0.3 | FVR*MVR | 14.96 |
| W7 | 0.4 | VVR | 11.91 |
| W8 | 0.5 | VVR | 10.76 |
| W9 | 0.6 | $GFP12^4$ | 9.85 |
| W10 | 0.7 | NONE | 9.10 |
| | | | |
| CON1 | VARIES | FVR*VVR | |
| CON2 | VARIES | FVR*VVR, SFPC | 46.48 |
| | | | 44.44 |

## TABLE XXIV- TRANSVERSE TENSILE STRENGTH (SCYYT)

### INTERACTION MODEL

| INPUT | FVR | TERMS ACCEPTED | $R^2$ |
|---|---|---|---|
| N1 | 0.3 | $MVR^2*SMPT$ | 31.60 |
| N2 | 0.4 | $MVR^2*SMPT$ | 37.23 |
| N3 | 0.5 | $EMP*SMPT$ | 9.61 |
| N4 | 0.6 | $FVR^2*MVR$ | 47.59 |
| N5 | 0.7 | NONE | |
| W1 | 0.3 | $FVR^2*VVR,SMPT$ | 25.39 |
| W2 | 0.4 | $SMPT*MVR$ | 43.94 |
| W3 | 0.5 | $MVR^2*FVR$ | 16.32 |
| W4 | 0.6 | $FVR*VVR*EFP2,EMP$ | 24.10 |
| W5 | 0.7 | $FVR*SMPT$ | 30.29 |
| | | | |
| N6 | 0.3 | $FVR*MVR$ | 10.47 |
| N7 | 0.4 | $MVR^2*FVR$ | 8.94 |
| N8 | 0.5 | $FVR*EFP2*SMPT$ | 13.54 |
| N9 | 0.6 | $SMPT^2*MVR$ | 9.40 |
| N10 | 0.7 | $FVR*EMP$ | 9.13 |
| W6 | 0.3 | $MFR^2*EMP$ | 35.13 |
| W7 | 0.4 | $MVR^2*VVR$ | 19.34 |
| W8 | 0.5 | $SMPT^2*MVR$ | 12.89 |
| W9 | 0.6 | $FVR^2*EFP2$ | 29.27 |
| W10 | 0.7 | $MVR^2*SMPT$ | 36.77 |
| | | | |
| CON1 | VARIES | $THETA^4*SMPT*MVR,FVR*EFP2*MVR,*SMPT^2*MVR$ | 73.42 |
| CON2 | VARIES | $SMPT^2*MVR,FVR*VVR*MVR$ | 76.40 |

## TABLE XXV- TRANSVERSE COMPRESSIVE STRENGTH (SCYYC)

### INTERACTION MODEL

| INPUT | FVR | TERMS ACCEPTED | $R^2$ |
|-------|-----|----------------|-------|
| N1 | 0.3 | SMPC*MVR | 33.39 |
| N2 | 0.4 | $FVR^2$*EMP | 32.99 |
| N3 | 0.5 | NONE | |
| N4 | 0.6 | $FVR^2$*MVR | 42.31 |
| N5 | 0.7 | NONE | |
| W1 | 0.3 | $FVR^2$*VVR | 26.24 |
| W2 | 0.4 | $FVR^2$*EMP | 43.86 |
| W3 | 0.5 | $SMPC^2$*MVR | 21.13 |
| W4 | 0.6 | FVR*VVR*EFP2,EMP | 25.75 |
| W5 | 0.7 | SMPC*MVR | 18.63 |
| | | | |
| N6 | 0.3 | $SMPC^2$*MVR | 11.57 |
| N7 | 0.4 | EFP2*MVR | 9.03 |
| N8 | 0.5 | FVR*EFP2 | 9.87 |
| N9 | 0.6 | NONE | |
| N10 | 0.7 | $SMPC^2$*MVR,$FVR^2$*MVR | 19.07 |
| W6 | 0.3 | $MVR^2$*EMP | 32.50 |
| W7 | 0.4 | EFP2*MVR | 14.58 |
| W8 | 0.5 | NONE | |
| W9 | 0.6 | $MVR^2$*SMPC | 32.85 |
| W10 | 0.7 | $MVR^4$ | 35.79 |
| | | | |
| CON1 | VARIES | $THETA^4$*SMPC*MVR,$FVR^4$ | 76.43 |
| CON2 | VARIES | $MVR^4$,$FVR^2$*MVR,$MVR^2$*SMPC | 75.59 |

## TABLE XXVI- IN PLANE SHEAR STENGTH (SCXYS)

### INTERACTION MODEL

| INPUT | FVR | TERMS ACCEPTED | $R^2$ |
|-------|-----|----------------|-------|
| N1 | 0.3 | FVR*GFP12*GMP,THETA$^4$ | |
| N2 | 0.4 | FVR*GFP12*EMP | 27.64 |
| N3 | 0.5 | THETA | 13.51 |
| N4 | 0.6 | THETA$^4$*GFP12,SMPS*MVR | 14.97 |
| N5 | 0.7 | NONE | 30.84 |
| W1 | 0.3 | THETA,FVR*VVR*EMP,THETA$^4$*SMPS,FVR*MVR | 52.20 |
| W2 | 0.4 | THETA$^4$*FVR,THETA$^4$*GFP12 | 26.58 |
| W3 | 0.5 | THETA$^4$ | 12.89 |
| W4 | 0.6 | THETA,FVR*VVR | 22.33 |
| W5 | 0.7 | THETA$^4$*FVR | 10.72 |
| N6 | 0.3 | NONE | |
| N7 | 0.4 | SMPS*MVR | 11.24 |
| N8 | 0.5 | NONE | |
| N9 | 0.6 | SMPS,SMPS$^4$ | 16.14 |
| N10 | 0.7 | FVR$^2$*MVR | 11.40 |
| W6 | 0.3 | SMPS*MVR,GMP$^4$ | 28.58 |
| W7 | 0.4 | FVR*GFP12*MVR | 8.28 |
| W8 | 0.5 | NONE | |
| W9 | 0.6 | FVR*GFP12*MVR | 19.20 |
| W10 | 0.7 | SMPS | 17.73 |
| CON1 | VARIES | THETA$^4$*FVR,FVR$^2$*SMPS | 36.74 |
| CON2 | VARIES | FVR*VVR,MVR$^4$,FVR$^2$*VVR | 61.46 |

# CHAPTER IV

## DISCUSSION

### A. Overview

The numerical simulations conducted show that certain assumptions about the statistical distribution of local nonuniformities in fiber composites lead directly to quantifiable variations in material properties. The advantages inherent in the stochastic characterization are numerous. The development of quality control and reliabilty measures for composites is crucial to their acceptance in aircraft designs. The reduction in needed experimental data achievable through judicious simulation of the wide variety of available composite material systems could significantly lower the costs of material selection and acceptance testing. In the results of this study, the confidence intervals calculated can be interpreted as the product of an experimental program, specifically designed as an analog of the physical processes which occur in real materials.

## B. Histograms and Distributions

Data cases 1, 2, and 3 demonstrate the differences between a deterministic base case and random cases with narrow and wide dispersion of input data about the base case.

In Fig. 30, it is apparent that the deterministic case 1 value of 15750 ksi. for longitudinal modulus falls near the mean of the case 2 data. However, the case 3 sample appears to have a mean slightly lower (approximately 15000 ksi.). It should be noted that the size of the interval over which the sample occurs is noticeably larger in the widely distributed case 3 run.

Transverse modulus, (Fig. 31) demonstrates a higher mean value for the wide distribution than for the narrow, which is greater than the deterministic value of 1065 ksi. reported in Table II. The increased transverse modulus is related to the added stiffness available in fibers with high misalignment relative to longitudinal direction.

Shear modulus, (Fig. 32) is measurably changed by nonuniformities. The deterministic value of 516 ksi is exceeded by the case 2 value of approximately 620 ksi, which is further exceeded by the case 3 value near 900 ksi. Fiber misalignment has a significant effect in shear modulus variation.

Poisson's ratios (Fig. 33, 34) show similar trends in location of sample means and relative dispersion of the sample for the data studied. Poisson's ratios generally increase with fiber misalignment and volume fraction changes.

The coefficients of thermal expansion (Figs. 35, 36) for the sample studied reflect the longitudinal contraction of graphite fibers when heated. The longitudinal coefficient of thermal expansion for AS-graphite fiber is $-0.550 \times 10^{-6}/$ F, while the transverse coefficient is $0.560 \times 10^{-5}/$ F. The offset orientation of crystal lattice planes in graphite fibers can explain this behavior. These values, the fiber misalignment, and fiber volume ratio near 0.5 all contribute to the occurrence of a negative longitudinal coefficient of thermal expansion for the composite. At higher fiber volume ratios, the values calculated would be less than in the present case, because of the contolling fiber behavior for high fiber volume ratio.

The longitudinal strengths (Fig. 38, 39) are significantly reduced when nonuniformities are present. The deterministic case 1 value of 203 ksi. for tensile strength is compared to a mean near 160 ksi for case 2 and a mean near 130 for case 3. In compression, the deterministic value of 165 ksi. compares to means near 100 ksi. and 80 ksi. for the narrow and wide distributions, respectively. The failure mode in compression varies in the random samples.

Transverse strengths (Fig. 40, 41) show sensitivity to the variations assumed. Misalignments, volume fraction nonuniformities, and constituent strength variations all contibute to reduction in the strength values. Sub-ply shear failures occur, which undermine the already low transverse composite strengths.

In plane shear strength (Fig. 42) values decline from 10.01 ksi. for case 1 to a mean near 8.0 ksi. for case 2. However, case 3 shows a

value of a mean near 8.0 also. It appears that the added shear strength due to fiber misalignment is balanced by the reduced strength due to variable fiber volume fraction.


## C. Confidence Curves

The effects of various shape parameters of fiber strength are shown in Figs. 43 and 44. The higher weibull distribution shape parameter of 20 produces a narrow distribution of fiber strength values. The composite that has few weaker fibers is expected to be stronger, and Fig. 43 demonstrates this for lonitudinal tensile strength. However, compressive failure (Fig. 44) is a more complex phenomenon. In the region of low fiber volume ratio, the 'rule of mixtures' failure criteria for a subply can control the failure mode. At higher fiber volume ratio, however, compressive failure can be initiated by delamination, or by a shear failure in a sub-ply. The mixture of failure modes in compressive failure is not well understood, but can explain the seeming inconsistency of the intersection of the curves in Fig. 44. At a fiber volume of 0.7, the weakest fibers ($\alpha = 10$) are in the strongest composite, when strength is normalized with respect to fiber compressive strength.

The effects of various shape parameters for matrix strengths are studied in Figs. 45, 46, and 47. Transverse tensile and compressive strengths show expected reductions for lower matrix strengths. In-plane shear strength shows lower dispersion at a large fiber volume of 0.7, and also declines in general for higher fiber volume.

The fiber misalignment effects are studied in Figs. 48-57. Longitudinal modulus (Fig. 48) shows narrow intervals and slight reductions for greater misalignment. Transverse modulus (Fig. 49) and in plane shear modulus (Fig. 50) are enhanced by fiber misalignment. Longitudinal tensile and compressive strengths are degraded by misalignment (Figs. 51, 52). Transverse tensile and compressive strengths are enhanced (Figs. 53, 54). In-plane shear strength shows total separation of confidence intervals between curves with different degrees of misalignment. Poisson's ratios (Figs. 56, 57) increase for high fiber misalignment values.

The fiber stiffness effects (Figs. 58-67) are very small for the distribution parameters studied.


D. Examination of Regression Models

The regression models for thermoelastic properties demonstrate resonably high predictive capability in the simple models assumed. Marginal improvements are achieved in expanding the models to include higher order interaction terms. Further improvement is gained by using sample data from the wide range of volume percent values. The higher multiple correlation coefficients of these models may be due to the additional information available in the sample size of 100 that was used. The nearly singular predictor matrices which occur in the higher order models indicate that terms must by selectively removed to eliminate linearity between assumed predictor terms. The regression results support the use of the simple models for thermoelastic

properties, because improvements in predictive capability in the higher order models for the same data are small.

Strengths are not modeled well by the simple or the interaction models. The predictors chosen are average properties, whereas the strengths are based on the weakest points in the material. Even the unidirectional cases (N6-N10, W6-W10) present data that the interaction models have considerable difficulty in accomodating. Somewhat greater predictive value is gained by using the expanded data for strength model prediction. Using fourth order algebraic functions, values of the multiple correlation coefficient square approach 85% for longitudinal tensile strength. The other strengths generally have poorer results.

# CHAPTER V

## CONCLUSIONS

A tractable, constituent based, probabilistic analysis procedure for fiber composites has been developed using the ICAN program as a basis. Within the limitations of the mechanics of material model, properties and strengths of a variety of composite material configurations can be simulated.

This study quantifies the thermoelastic and strength properties of a graphite/epoxy ply subject to assumed uncertainties for fiber misalignment, constituent volume fractions, and constituent properties. The results show several advantages of probabilistic characterization of this material. These include the identification of unforseen variations in composite material properties, and the mechanical effects of local nonuniformities. The relative importance of the various fabrication and material variables on composite properties is identified, and the resulting behavior quantified.

The advantages of a probabilistic formulation of composite material

properties over a deterministic one are numerous. Comparison of the results of this study with test data could reveal some sources of previously unaccounted scatter in the data. Expected value ranges could be predicted for experimental results. Since the simulations provide data that is analagous to experimental data at lower cost, laboratory classification, material selection, and acceptance testing of composites can be guided by the information made available by these methods.

Although the method presented provides results for only the basic ply, extension of the simulation to include lamination angle variations in a general layup is feasible. Since finite element material property cards are generated, structural analysis of components with randomly varied properties defined at a number of points in the body can supply a more realistic description of the random nature of structural response due to material inhomogeneity.

The stochastic formulation of material properties is generally recognized as one requirement of failure theories for materials. Although the failure criteria in the models used in this study are conservative, progressive failure of fiber composites could be modeled by incorporating load redistribution and material property recalculation in the vicinity of failed material.

# REFERENCES

1. Harter, H. Leon: A Survey on the Literature on the Size Effect on Material Strength. AFFDL-TR-77-11, Wright Patterson AFB, April, 1977.

2. Griffith, A. A.: The Phenomena of Rupture and Flow in Solids. Philosophical Transactions of the Royal Society of London A, Vol. 221, pp. 163-198.

3. Murthy, P. L. N. and Chamis, C. C.: Integrated Composites Analyzer (ICAN) User's and Programmer's Maunual. NASA TP 2515, March 1986.

4. Flaggs, D. L.: ADVLAM- An Advanced Composite Laminate Analysis Code. Lockheed Missles and Space Company, Inc., 1983.

5. Chamis, C. C. and Sinclair, J. H.: Micromechanics of Intraply Hybrid Composites: Elastic and Thermal Properties. NASA TM 79253.

6. Kural, M. H. and Min, B. K.: The Effects of Matrix Plasticity on the Thermal Deformation of Continuous Fiber Graphite/Metal Composites. J. Comp. Mater., v.18, Nov. 1984, pp.519-535.

7. Bolotin, V. V.: Statistical Methods in Structural Mechanics (trans. S. Aroni). San Francisco, Holden Day, Inc. 1969

8. Sobol, I. M. (USSR Academy of Sciences): The Monte Carlo Method. Chicago, The University of Chicago, 1974.

9. Nance, R. E. and Overstreet, C.: A Bibliography of Random Number Generation. Computing Reviews, Oct. 1972, pp. 495-508.

10. Lehmer, D. H.: Mathematical Methods in Large-Scale Computing Units, Proceedings of the 2nd Symposium on Large-Scale Digital Computing Machinery, Cambridge, Harvard University Press, 1951 pp. 141-146.

11. Hammersly, J. M. and Handscomb, D. C.: Monte Carlo Methods. London, Menthuen & Co. Ltd., 1964, pp. 28-31.

12. Oh, Kong P.: A Monte Carlo Study of the Strength of Unidirectional Fiber-Reinforced Composite Materials. Journal of Composite Materials, Vol. 13, p. 311.

13. Box, G. E. P., and Mueller, M. E.: A Note on the Generation of Random Normal Deviates. Annals of Mathematical Statistics, Vol. 29(2), 1958, pp. 610-611.

14. Howell, L. W. and Rheinfurth, M. H.: Generation of Pseudo-Random Numbers. NASA TP 2105, 1982, pp. 7-8.

15. Weibull, W.: Statistical Theory of Strength of Materials. (In English) Ingenoirs Vetenskaps Akademien Handlinger, Vol. 151, p. 45.

16. Chamis, C. C.: Simplified Composite Micromechanics Equations for Strength, Fracture Toughness, Impact Resistance, and Environmental Effects. NASA TM 83696, 1984.

17. Ryan, Thomas A., Jr.: MINITAB. The Pennsylvania State University Computation Center, Jan 15, 1981.

18. Draper, N.R. and Smith, H.: Applied Regression Analysis. New York, John Wiley & Sons, Inc., 1981.

19. Ginty, C. A.: unpublished data.

APPENDIX A

```
C ************************************************************
C ************************************************************
C **                                                      **
C **    PROBABILISTIC INTEGRATED COMPOSITES ANALYZER ( P I C A N )  **
C **    ---------------------------------------------------  **
C **  A COMPUTER CODE FOR ANALYSIS OF PROBABILISTIC VARIATIONS IN  **
C **  COMPOSITE PROPERTIES USING THE INTEGRATED COMPOSITES ANALYZER **
C **  (ICAN).  THE ANALYSIS SAMPLES FROM INPUT DISTRIBUTIONS TO OBTAIN **
C **  COMPOSITE PROPERTIES AND GEOMETRY.  WHICH ARE THEN INPUT TO ICAN. **
C **  AS MANY TIMES AS THE USER REQUESTS.                   **
C **  FINAL OUTPUT INCLUDES OUTPUT DATASETS OF ICAN WHICH ARE NAMED **
C **  "ICAMOUT", AND CAN BE REPEATEDLY USED BY ANALYSIS ROUTINE.  **
C ************************************************************
C ************************************************************
C
C---   THIS IS A MASTER PROGRAM FOR "ICAN" WHICH ALLOCATES   ---
C---   DYNAMICALLY SUFFICIENT STORAGE FOR THE ARRAY VARIABLES  ---
C---   IN "ICAN" AND "PICAN" CODES.
C
      COMMON A(9000)
      COMMON /PSIZE/ MAXLEN,M(100)
      MAXLEN = 9000
      CALL SPINIT
      STOP
      END
```

```
      SUBROUTINE SPINIT
C READ INPUT DATASET TO DETERMINE IF PROBABILISTIC ANALYSIS IS DESIRED
      COMMON A(1)
      COMMON /ILAB1&/ IMHYDI,OUTF,INF,IMPF,INDS,IDBK
      DIMENSION L(8)
      LOGICAL BSTAT,ANGLEV,VORATV,FIRATV
      CHARACTER*4 CDUM
      INTEGER PIN,RUNS,RUNNO,OUTF
      DATA PIN/51/
      READ (PIN,1003) CDUM
      READ (PIN,1002) NL,NUMS,BSTAT
      IF (.NOT. BSTAT) GO TO 500
C
      READ (PIN,1001) RUNS
C SET UP POINTERS FOR MASTER ARRAY
      L(1) = 1
      L(2) = L(1) + NUMS
      L(3) = L(2) + NUMS
      L(4) = L(3) + NUMS
      L(5) = L(4) + NUMS
      L(6) = L(5) + NUMS
      L(7) = L(6) + NL
      L(8) = L(7) + NL
      L1 = L(1)
      L2 = L(2)
      L3 = L(3)
      L4 = L(4)
      L5 = L(5)
      L6 = L(6)
      L7 = L(7)
      L8 = L(8)
C LOOP 'RUNS' TIMES THROUGH DATA CREATION AND ICAM ROUTINE
      DO 100 RUNNO = 1,RUNS
      CALL UPDAT(A,A(L2),A(L3),A(L4),A(L5),A(L6),A(L7),A(L8),NL,NUMS)
      REWIND IDBK
      CALL ICAMNN
      ENDFILE OUTF
100   CONTINUE
      REWIND OUTF
      GO TO 6000
500   CONTINUE
      CALL COPY
      CALL ICAMNN
1001  FORMAT (6X,I6)
1002  FORMAT (8X,I8,8X,I8,2X,L6)
1003  FORMAT(A4)
6000  CONTINUE
      RETURN
      END
```

```
      SUBROUTINE UPDAT(VFS,VSC,VVS,VFP,VVP,THETA,THMU,TMSIG,NL,NUMS)
C ================================================================
C ROUTINE UPDAT READS INPUT AND GENERATES STATISTICALLY VARYING INPUT =
C FILE TO ICAM USING VARIOUS RANDOM NUMBER GENERATION SCHEMES         =
C ================================================================
      DIMENSION DECK(20),PL(75,1),CODES(2,2,1),VFS(1),VSC(1),VVS(1),
     1THETA(1),MBS(3,1),DBS(4,1),MBS(3,1),MBS(3,1),VFP(1),VVP(1),IDENT(5),
      LOGICAL CSAMB,COMSAT,BIDE,RINDV,MONUDF,ANGLEV,VORATV,FIRATV,CONV
      INTEGER NL,NLC,NMS,INT,IR,IMPF
      INTEGER PIN,ISEEDF,ISEED
      CHARACTER*8 PLY,IDENT
      COMMON /SEED/ ISEED
      COMMON /CONST/ CONV
      DATA PIN,IMPF,ISEEDF,ISEEDF/31,5,55/
      REAL TU,TCU,NBS,MBS
      DATA PLY/          PLY'/
C
C READ IN UNIFORM RANDOM NUMBER GENERATOR SEED
      REWIND ISEEDF
      READ(ISEEDF,6) ISEED
C
C
      REWIND IMPF
      REWIND PIN
      READ(PIN,7) (DECK(I),I=1,20)
      WRITE (IMPF,7) (DECK(I),I=1,20)
C
      READ(PIN,9) IDENT(1),NL,NLC,NMS
      IF(NL.EQ.NMS) GO TO 30
      WRITE (IMPF,24)
      STOP
C
C  30 WRITE (IMPF,10) IDENT(1),NL,NLC,NMS
C
      READ(PIN,12) COMSAT,ANGLEV,FIRATV,VORATV,CONV
      WRITE (IMPF,11) COMSAT
      READ(PIN,13) CSAMB,THMU,TMSIG,VFPMU,VFPSIG,VVPLAM,KVVP
      WRITE (IMPF,11) CSAMB
      READ (PIN,11) BIDE
      WRITE (IMPF,11) BIDE
      READ (PIN,11) RINDV
      WRITE(IMPF,11) RINDV
      READ(PIN,11) MONUDF
      WRITE (IMPF,11) MONUDF
C READ LAYER DATA
      READ (PIN,14) IDENT(2),TU,TCU,PL(72,1),PL(7,1)
      IF (IDENT(2).EQ.PLY) GO TO 88
      WRITE (IMPF,8) IDENT(2)
      WRITE (IMPF,2) IDENT(2)
      STOP
C
C  80 IF (ANGLEV) GO TO 84
      DO 82 IR = 1,NL
      THETA(IR) = THMU
   82 CONTINUE
```

```
84    GO TO 101
      DO 100 IR = 1,NL
      CALL URAND(X1)
      CALL URAND(X2)
      CALL NORM(X1,X2,THMU,THSIG,Y)
      THETA(IR) = Y
100   CONTINUE
101   DO 105 IR = 1,NL
      WRITE(INPF,15) IDENT(2),IR,IR,TU,TCU,PL(72,1),THETA(IR),PL(7,1)
105   CONTINUE
C
C     READ MATERIAL DATA
      READ(PIN,16) IDENT(4),(CODES(1,J,1),J=1,2),
     1(CODES(2,J,1),J=1,2),VSC(1),VFS(1),VVS(1)
C
      IF (FIXATV) GO TO 114
      DO 110 IR = 1,NMS
      VFP(IR) = VFPMU
110   CONTINUE
      GO TO 128
114   DO 125 IR = 1,NMS
      CALL URAND(X1)
      CALL URAND(X2)
      CALL NORM(X1,X2,VFPMU,VFPSIG,Y)
      IF (Y .GT. 0.78) GO TO 115
      IF (Y .LT. 0.30) GO TO 115
      VFP(IR) = Y
125   CONTINUE
C
128   IF (VORATV) GO TO 140
      DO 130 IR = 1,NMS
      VVP(IR) = VVPLAM
130   CONTINUE
      GO TO 200
C
140   DO 190 IR = 1,NMS
      CALL GAM(VVPLAM,KVVP,VVP(IR))
      VVP(IR) = VVP(IR)/100.
190   CONTINUE
C
200   DO 203 IR = 1,NMS
      WRITE (INPF,17) IDENT(4),(CODES(1,J,1),J=1,2),VFP(IR),VVP(IR).
     1(CODES(2,J,1),J=1,2),VSC(1),VFS(1),VVS(1)
203   CONTINUE
C
C     READ LOADING CONDITIONS
C
      DO 300 IR = 1,NLC
      READ (PIN,18) IDENT(3),MBS(1,IR),MBS(2,IR),MBS(3,IR),THCS
      WRITE(INPF,19) IDENT(3),MBS(1,IR),MBS(2,IR),MBS(3,IR),THCS
      READ (PIN,18) IDENT(3),MBS(1,IR),MBS(2,IR),MBS(3,IR)
      WRITE (INPF,19) IDENT(3),MBS(1,IR),MBS(2,IR),MBS(3,IR)
      READ(PIN,18) IDENT(3),(DBS(I,IR),I=1,4)
      WRITE (INPF,19) IDENT(3),(DBS(1,IR),I=1,4)
```

```
      300 CONTINUE
C
C     READ OUTPUT OPTIONS
C
         READ(PIN,20) IDENT(5),IOUT
         WRITE (INPF,21) IDENT(5),IOUT
C
C     INCREMENT AND REFILE SEED FOR FUTURE RUNS
         ISEED = ISEED + 100
         REWIND ISEEDF
         WRITE (ISEEDF,6) ISEED
C
    2    FORMAT (1X,10HIDENT(2) =,A8)
    6    FORMAT (I6)
    7    FORMAT (20A4)
    8    FORMAT (' THERE IS A MIX UP IN THE LAYER PROPERTIES CARD')
    9    FORMAT (A8,3I8)
   10    FORMAT (A8,3I8)
   11    FORMAT (L6)
   12    FORMAT (L6,6X,4L6)
   13    FORMAT (L6,6X,2(2X,F5.1),2(2X,F5.3),2X,F5.2,2X,F5.2,2X,I4)
   14    FORMAT (A8,16X,3F8.3,8X,F8.3)
   15    FORMAT (A8,2I8,5F8.3)
   16    FORMAT (A8,2A4,16X,2A4,3F8.2)
   17    FORMAT (A8,2A4,2F8.2,2A4,3F8.2)
   18    FORMAT (A8,7F8.4)
   19    FORMAT (A8,7F8.4)
   20    FORMAT (A8,I8)
   21    FORMAT (A8,I8)
   22    FORMAT (I5)
   23    FORMAT (5F10.3)
   24    FORMAT (' INPUT ERROR...  NMS MUST BE SET EQUAL TO NL.')
         RETURN
         END
```

```fortran
      SUBROUTINE URAND(Z)
C ********************************************************
C     SUBROUTINE FOR GENERATING RANDOM NUMBERS HAVING A UNIFORM
C     DISTRIBUTION, BY THE MIXED MULTIPLICATIVE CONGRUENTIAL METHOD.
C ********************************************************
      DATA I/1/
      INTEGER A, X
      COMMON /SEED/ ISEED
      IF (I .EQ. 0) GO TO 1
      I = 0
      M = 2**20
      FM = M
      X = ISEED
      A = 2**10 + 3
C
    1 X = MOD(A*X, M)
      FX = X
      Z = FX/FM
      RETURN
      END
```

```fortran
      SUBROUTINE NORM(X1,X2,MU,SIGMA,Y)
C ***************************************************
C     SUBROUTINE FOR GENERATING RANDOM VARIABLE Y ACCORDING
C     TO THE NORMAL DISTRIBUTION N(MU,SIGMA), USING THE
C     UNIFORM RANDOM VARIABLES X1 AND X2.
C ***************************************************
      REAL PI,MU,SIGMA,X1,X2,Y
      PI = ATAN(1.)*4
      Y = (SIGMA*((-2*ALOG(X1))**0.5)*(COS(2*PI*X2)))+MU
      RETURN
      END
```

```fortran
      SUBROUTINE GAM(RLAMDA,K,X)
C ************************************************************
C     SUBROUTINE FOR GENERATING GAMMA VARIATES WITH PARAMETERS
C     RLAMDA AND K.
C ************************************************************
      DIMENSION U(100)
      DIMENSION P(100)
      COMMON /SEED/ ISEED
      DO 50 I = 1,K
      CALL URAND(U(I))
   50 P(I) = U(I)
      DO 100 I = 2,K
  100 P(I) = U(I) * P(I-1)
      X = (-1.0/RLAMDA) * ALOG(P(K))
      RETURN
      END
```

```
      SUBROUTINE WEIB(X1,ALPHA,BETA,Y)
C***************************************************
C     THIS ROUTINE GENERATES THE DESIRED WEIBULL DISTRIBUTED RANDOM
C     VARIABLES PRESCRIBED BY INPUT OF SHAPE AND SCALE PARAMETERS.
C***************************************************
C     VARIABLE DISCRIPTIONS
C     ALPHA = SHAPE PARAMETER
C     BETA  = SCALE PARAMETER
C     X1    = UNIFORMLY DISTRIBUTED RANDOM VARIABLE ON (0,1)
C     Y     = WEIBULL DISTRIBUTED RANDOM VARIABLE
C
C     USE IS MADE OF THE WEIBULL DISTRIBUTION FUNCTION
C
C     F(X) = 1 - EXP( - (X/BETA) ** ALPHA)       FOR X .GE. ZERO
C
      OMX1 = 1 - X1
      Y = BETA * ( -ALOG(OMX1)) ** (1/ALPHA)
      RETURN
      END
```

```fortran
      SUBROUTINE COPY
C **********************************************************************
C     THIS ROUTINE SIMPLY COPIES THE INPUT DATA INTO THE FILE TO BE READ
C     BY ICAN.
C **********************************************************************
      DIMENSION DECK(20),PL(75,20),IP(20),INP(20),CODES(2,2,20),VFS(8),
     1VSC(8),VVS(8),THETA(15),MBS(35,1),DBS(4,1),MBS(4,1),VFP(8),VVP(8)
      DIMENSION IDENT(5)
      CHARACTER*8 IDENT,PLY
      LOGICAL CSAMB,COMSAT,BIDE,RINDV,NONUDF
      INTEGER NL,NLC,NMS,INT,IR
      INTEGER PIM,POUT
      DATA PIM/51/,POUT/5/
      REAL TU,TCU,MBS,MBS
      DATA PLY/'        PLY'/
C
      READ(PIM,6) (DECK(I),I=1,20)
      WRITE (POUT,7) (DECK(I),I=1,20)
C
      READ(PIM,9) IDENT(1),NL,NLC,NMS
      WRITE (POUT,10) IDENT(1),NL,NLC,NMS
C
      READ(PIM,12) COMSAT
      WRITE (POUT,11) COMSAT
      READ(PIM,12) CSAMB
      WRITE (POUT,13) CSAMB
      READ (PIM,12) BIDE
      WRITE (POUT,13) BIDE
      READ (PIM,12) RINDV
      WRITE(POUT,13)RINDV
      READ(PIM,12) NONUDF
      WRITE (POUT,13) NONUDF
C
C     READ LAYER DATA
      IR=1
  100 READ (PIM,14) IDENT(2),INP(IR),IP(IR),TU,TCU,PL(72,IR),THETA(IR),
     1PL(7,IR)
      IF (IDENT(2).NE.PLY) GO TO 105
      GO TO 106
  105 WRITE (POUT,8)
      WRITE (POUT,2) IDENT(2)
      STOP
  106 WRITE (POUT,15) IDENT(2),INP(IR),IP(IR),TU,TCU,PL(72,IR),
     1THETA(IR),PL(7,IR)
      IF (IR.EQ.NL) GO TO 109
      IR=IR+1
      GO TO 100
C
C     READ MATERIAL DATA
  109 IR=0
  110 IR=IR+1
      READ(PIM,16) IDENT(4),(CODES(1,J,IR),J=1,2),VFP(IR),VVP(IR),
     1(CODES(2,J,IR),J=1,2),VSC(IR),VFS(IR),VVS(IR)
```

```
      WRITE (POUT,17) IDENT(4),(CODES(1,J,IR),J=1,2),VFP(IR),VVP(IR),
     1(CODES(2,J,IR),J=1,2),VSC(IR),VFS(IR),VVS(IR)
      IF (IR.EQ.NMS) GO TO 120
      GO TO 110
C
C     READ LOADING CONDITIONS
C
  120 IR=0
  130 IR=IR+1
      READ (PIN,18) IDENT(3),MBS(1,IR),MBS(2,IR),MBS(3,IR),THCS
      WRITE(POUT,19) IDENT(3),MBS(1,IR),MBS(2,IR),MBS(3,IR),THCS
      READ (PIN,18) IDENT(3),MBS(1,IR),MBS(2,IR),MBS(3,IR)
      WRITE (POUT,19) IDENT(3),MBS(1,IR),MBS(2,IR),MBS(3,IR)
      READ(PIN,18) IDENT(3),(DBS(I,IR),I=1,4)
      WRITE (POUT,19) IDENT(3),(DBS(I,IR),I=1,4)
      IF (IR.EQ.NLC) GO TO 140
      GO TO 130
C
  140 CONTINUE
C
C     READ OUTPUT OPTIONS
C
      READ(PIN,19) IDENT(5),IOUT
      WRITE (POUT,20) IDENT(5),IOUT
    2 FORMAT (1X,18H(IDENT(2) =,A8)
    6 FORMAT (20A4)
    7 FORMAT (20A4)
    8 FORMAT (' THERE IS A MIX UP IN THE LAYER PROPERTIES CARD')
   10 FORMAT (A8,5I8)
   12 FORMAT (A8,5I8)
   13 FORMAT (L4)
   14 FORMAT (A8,2I8,5F8.3)
   15 FORMAT (A8,2I8,5F8.3)
   16 FORMAT (A8,2A4,2F8.2,2A4,3F8.2)
   17 FORMAT (A8,2A4,2F8.2,2A4,3F8.2)
   18 FORMAT (A8,7F8.4)
   19 FORMAT (A8,7F8.4)
   20 FORMAT (A8,I8)
   21 FORMAT (A8,I8)
   22 FORMAT (I5)
   23 FORMAT (4E10.3)
      RETURN
      END
```

```
      SUBROUTINE VARCON(PFP,PFS,PMP,PMS,CODES,NMS)
C =========================================================
C     SUBROUTINE TO SUPPLY VARIATIONS IN CONSTITUENT PROPERTIES
C     AS DESIRED BY THE USER ON INPUT PROMPT BOOLEANS.
C =========================================================
      INTEGER PIN
      DATA PIN/52/
      LOGICAL BOOL
      DIMENSION DUM1(19),PFP(21,1),PFS(21,1),PMP(16,1),PMS(16,1),
     1 CODES(2,2,1)
C VARY EACH PROPERTY WHICH CORRESPONDS TO A BOOLEAN WITH VALUE 'TRUE'
C
      DO 90 J = 1,NMS
C
C GENERATE FIBER PROPERTIES
C
      READ(PIN,1001) BOOL,SMEAN,STDEV
      IF(.NOT.BOOL) GO TO 5
         CALL URAND(X1)
         CALL URAND(X2)
         CALL NORM(X1,X2,SMEAN,STDEV,EFP11)
         PFP(5,J) = EFP11
C
    5 READ(PIN,1001) BOOL,SMEAN,STDEV
      IF(.NOT.BOOL) GO TO 6
         CALL URAND(X1)
         CALL URAND(X2)
         CALL NORM(X1,X2,SMEAN,STDEV,EFP22)
         PFP(6,J) = EFP22
C
    6 READ(PIN,1001) BOOL,SMEAN,STDEV
      IF(.NOT.BOOL) GO TO 7
         CALL URAND(X1)
         CALL URAND(X2)
         CALL NORM(X1,X2,SMEAN,STDEV,GFP12)
         PFP(7,J) = GFP12
C
    7 READ(PIN,1001) BOOL,SMEAN,STDEV
      IF(.NOT.BOOL) GO TO 8
         CALL URAND(X1)
         CALL URAND(X2)
         CALL NORM(X1,X2,SMEAN,STDEV,GFP23)
         PFP(8,J) = GFP23
C
    8 READ(PIN,1001) BOOL,BETA,ALPHA
      IF(.NOT.BOOL) GO TO 9
         CALL URAND(X1)
         CALL WEIB(X1,ALPHA,BETA,SFPT)
         PFP(14,J) = SFPT
C
    9 READ(PIN,1001) BOOL,BETA,ALPHA
      IF(.NOT.BOOL ) GO TO 10
         CALL URAND(X1)
         CALL WEIB(X1,ALPHA,BETA,SFPC)
```

```
      PFP(15,J) = SFPC
C
   10 CONTINUE
C
C  GENERATE MATRIX PROPERTIES
C
   20 READ(PIM,1001) BOOL,SMEAN,STDEV
      IF(.NOT. BOOL) GO TO 21
         CALL URAND(X1)
         CALL URAND(X2)
         CALL NORM(X1,X2,SMEAN,STDEV,EMMP)
         PMP(3,J) = EMMP
C
   21 READ(PIM,1001) BOOL,BETA,ALPHA
      IF(.NOT. BOOL) GO TO 22
         CALL URAND(X1)
         CALL WEIB(X1,ALPHA,BETA,SMTP)
         PMP(9,J) = SMTP
C
   22 READ(PIM,1001) BOOL,BETA,ALPHA
      IF(.NOT. BOOL) GO TO 23
         CALL URAND(X1)
         CALL WEIB(X1,ALPHA,BETA,SMCP)
         PMP(10,J) = SMCP
C
   23 READ(PIM,1001) BOOL,BETA,ALPHA
      IF(.NOT. BOOL) GO TO 24
         CALL URAND(X1)
         CALL WEIB(X1,ALPHA,BETA,SMSP)
         PMP(11,J) = SMSP
C
   24 CONTINUE
C
      REWIND PIM
   50 CONTINUE
 1001 FORMAT(14X,L6,2E20.10)
      RETURN
      END
```

APPENDIX B

This appendix outlines the theories and equations in the ICAN program that are used in this project. In the first section on composite micromechanics, the elastic and thermal properties of a composite ply are defined with respect to its principal material axes. The next section, devoted to laminate theory, contains the transformations and summations of ply properties used to arrive at laminate properties. The last section contains a brief discussion of the failure criteria.

## 1. Composite micromechanics

The theory for calculation of the properties of a unidirectional fiber composite ply based on the properties, volume fractions, and orientation of its constituents is known as composite micromechanics. In this section, the subscripts $f$, $m$, $v$, and $l$ represent fiber, matrix, void, and laminate, respectively. The symbolic notation and the equations used are summarized below:

Volume fractions:

$$k_f + k_m + k_v = 1$$

Longitudinal Modulus:

$$E_{l11} = k_f E_{f11} + k_m E_m$$

Transverse Modulus:

$$E_{I22} = E_{I33} = \frac{E_m}{1 - \sqrt{k_f}\,(1 - E_m/E_{f22})}$$

Shear Moduli:

$$G_{I12} = \frac{G_m}{1 - \sqrt{k_f}\,(1 - G_m/G_{f12})}$$

$$G_{I23} = \frac{G_m}{1 - \sqrt{k_f}\,(1 - G_m/G_{f23})}$$

Poisson's Ratios:

$$\nu_{I12} = \nu_{I13} = \nu_m + k_f(\nu_{f12} - \nu_m)$$

$$\nu_{I23} = k_f\,\nu_{f23} + k_m \left[ 2\nu_m - \frac{\nu_{I12}}{E_{I11}}\,E_{I22} \right]$$

Coefficients of thermal expansion

$$\alpha_{I11} = \frac{\alpha_{f11} + k_m[(\alpha_m E_m/E_{f11}) - \alpha_{f11}]}{1 + k_m(E_m/E_{f11} - 1)}$$

$$\alpha_{I22} = \alpha_m(1 - \sqrt{k_f})\left[ \frac{1 + k_f \nu_m E_{f11}}{E_{f11} + k_m(E_m - E_{f11})} \right] + \alpha_{f22}k_f$$

$$\alpha_{33} = \alpha_{I22}$$

## 2. Laminate Theory

This section describes the methods which are used to calculate the elastic properties of laminates from the properties, orientation, and distribution of individual laminae. The elastic properties are then used to predict the response of the laminate to external loads. The methods used to predict stresses in the laminae under application of external loads are also described. Failure loads can be predicted by using these methods; as described in a following section.

### a. Generalized Hooke's Law

The stresses acting at a point in a solid can be represented by the stresses acting on the planes normal to the coordinate directions, or equivalently, on the surfaces of an infinitesimal cube as shown in Fig. B-1. The stresses $(\sigma_{ij})$ on each face are resolved into three components: one normal stress and two shearing stresses. The first subscript refers to the direction normal to the plane in which the stress acts and the second subscript to the direction in which the stress acts. The stress components shown on the faces of the cube are taken as positive and can be taken as the forces (per unit area) exerted by the material outside the cube upon the material inside. A stress component is positive if it acts in the positive direction on a positive face of the cube. Thus normal tensile stresses are positive, and normal compressive stresses are negative. Nine stress components must be used to define the state of stress at a point, namely $\sigma_{11}$, $\sigma_{22}$, $\sigma_{33}$, $\sigma_{23}$, $\sigma_{31}$, $\sigma_{12}$, $\sigma_{32}$, $\sigma_{13}$, and $\sigma_{21}$. There are nine corresponding strain

components, following the same subscript convention.

For bodies in which each strain component is a linear function of all six stress components, the generalized Hooke's Law can be expressed

$$\sigma_{ij} = E_{ijkl}\,\varepsilon_{kl}$$

where $E_{ijkl}$ is a fourth order tensor of elastic constants. For nine stress components and nine strain components, there must be 81 elastic constants defining $E_{ijkl}$. Certain reductions in the number of independent constants for an anisotropic body are due to symmetry properties of the tensor $E_{ijkl}$. By considering moment equilibrium about the center of the cube, it can be shown that at any point $\sigma_{23} = \sigma_{32}$, $\sigma_{31} = \sigma_{13}$, and $\sigma_{12} = \sigma_{21}$. Thus, $E_{ijkl}$ is symmetric with respect to the first two indices. Second, because the strains are symmetric (that is, $\varepsilon_{ij} = \varepsilon_{ji}$), $E_{ijkl}$ must be symmetric with respect to the second two indices. This reduces the number of elastic constants to 36. Further reduction to the final 21 elastic constants for a general anisotropic material is accomplished by assuming the existence of a strain energy density function, such that

$$U = U\!\left(\varepsilon_{ij}\right)$$

with the property

$$\frac{\partial U}{\partial \varepsilon_{ij}} = \sigma_{ij}$$

From the generalized Hooke's Law,

$$\frac{\partial U}{\partial \varepsilon_{ij}} = E_{ijkl}\varepsilon_{kl}$$

Partial differentiation with respect to $\varepsilon_{kl}$ yields

$$\frac{\partial}{\partial \varepsilon_{kl}} \left[ \frac{\partial U}{\partial \varepsilon_{ij}} \right] = E_{ijkl}$$

Since the order of partial differentiation is immaterial,

$$\frac{\partial}{\partial \varepsilon_{kl}} \left[ \frac{\partial U}{\partial \varepsilon_{ij}} \right] = \frac{\partial}{\partial \varepsilon_{ij}} \left[ \frac{\partial U}{\partial \varepsilon_{kl}} \right]$$

and the subscripts can be interchanged to yield

$$\frac{\partial}{\partial \varepsilon_{kl}} \left[ \frac{\partial U}{\partial \varepsilon_{ij}} \right] = E_{klij}$$

so that

$$E_{ijkl} = E_{klij}$$

Thus the first pair of subscripts in $E_{ijkl}$ can be interchanged with the second pair without any change in the values. The number of elastic constants is thus reduced to 21.

b. Lamina Constitutive Relation

Several simplifications to the generalized Hooke's Law can be made for the special case of a thin orthotropic material, which approximates a unidirectional fiber composite lamina. By considering the invariance of elastic properties under coordinate transformation for planes of symmetry, the tensor $E_{ijkl}$ can be reduced to the following nine constants:

$$E_{ijkl} = \begin{bmatrix} E_{1111} & E_{1122} & E_{1133} & & & \\ E_{1122} & E_{2222} & E_{2233} & & & \\ E_{1133} & E_{2233} & E_{3333} & & & \\ & & & \varnothing & & \\ & & & & \varnothing & \\ & & & & & \varnothing \end{bmatrix}$$

It is now convenient to make the following notation changes:

$$\sigma_{11} = \sigma_1 \qquad\qquad e_{11} = \varepsilon_1$$

$$\sigma_{22} = \sigma_2 \qquad\qquad e_{22} = \varepsilon_2$$

$$\sigma_{33} = \sigma_3 \qquad\qquad e_{33} = \varepsilon_3$$

$$\sigma_{23} = \tau_{23} = \sigma_4 \qquad 2e_{23} = \gamma_{23} = \varepsilon_4$$

$$\sigma_{13} = \tau_{13} = \sigma_5 \qquad 2e_{13} = \gamma_{13} = \varepsilon_5$$

$$\sigma_{12} = \tau_{12} = \sigma_6 \qquad 2e_{12} = \gamma_{12} = \varepsilon_6$$

The generalized form of Hooke's Law can now be written

$$\sigma_i = \sum_{j=1}^{6} C_{ij}\varepsilon_j \quad \text{for} \quad i,j = 1,\ldots,6$$

The matrix $C_{ij}$ is known as the stiffness matrix, and $\varepsilon_j$ are the engineering strain components. In matrix form Hooke's Law is written

$$
\begin{Bmatrix} \sigma_1 \\ \sigma_2 \\ \sigma_3 \\ \tau_{23} \\ \tau_{31} \\ \tau_{12} \end{Bmatrix}
=
\begin{bmatrix}
C_{11} & C_{12} & C_{13} & 0 & 0 & 0 \\
C_{12} & C_{22} & C_{23} & 0 & 0 & 0 \\
C_{13} & C_{23} & C_{33} & 0 & 0 & 0 \\
0 & 0 & 0 & C_{44} & 0 & 0 \\
0 & 0 & 0 & 0 & C_{55} & 0 \\
0 & 0 & 0 & 0 & 0 & C_{66}
\end{bmatrix}
\begin{Bmatrix} \varepsilon_1 \\ \varepsilon_2 \\ \varepsilon_3 \\ \gamma_{23} \\ \gamma_{31} \\ \gamma_{12} \end{Bmatrix}
$$

where the coordinate axes coincide with the symmetry axis of the material. For laminae that are assumed sufficiently thin, the through the thickness stresses are zero. Thus $\sigma_3 = \sigma_4 = \sigma_5 = 0$, for plane stress. It is apparent that $\varepsilon_4 = \varepsilon_5 = 0$

The stress strain relations for a thin unidirectional lamina are written

$$
\begin{bmatrix} \sigma_1 \\ \sigma_2 \\ \tau_{12} \end{bmatrix} = \begin{bmatrix} Q_{11} & Q_{12} & 0 \\ Q_{12} & Q_{22} & 0 \\ 0 & 0 & 2Q_{66} \end{bmatrix} \begin{bmatrix} \epsilon_1 \\ \epsilon_2 \\ \frac{1}{2}\gamma_{12} \end{bmatrix}
$$

using the tensorial strain $\frac{1}{2}\gamma_{12}$ instead of the engineering strain $\gamma_{12}$.

The Q terms are known as reduced stiffnesses, i.e.

$$
Q_{11} = C_{11} = \frac{E_1}{1 - \nu_{12}\nu_{21}}
$$

$$
Q_{12} = C_{12} = \frac{\nu_{12}E_2}{1 - \nu_{12}\nu_{21}} = \frac{\nu_{21}E_1}{1 - \nu_{12}\nu_{21}}
$$

$$
Q_{22} = C_{22} = \frac{E_2}{1 - \nu_{12}\nu_{21}}
$$

$$
Q_{66} = \frac{1}{2} (C_{11} - C_{12}) = G_{12}
$$

where $E_1$, $E_2$, $\nu_{12}$, $\nu_{21}$, and $G_{12}$ are the ply elastic constants, measured with respect to the natural material system. It may be noted that only four of these constants are independent.

The stress- strain relation above shows that there is no coupling between tensile and shear strains, as long as the applied stresses are coincident with the principal material directions. However, coupling appears when a lamina is tested at arbitrary angles with respect to the principal material directions. The general form of the stress-strain relation for any angular orientation of a lamina is considered next.

c. Stiffness matrix transformations

A lamina is loaded along a coordinate system x-y oriented at some

angle $\theta$ with respect to the principal material directions as shown in Fig. B-2. Since stress and strain are second order tensors, they are transformed by

$$\begin{Bmatrix} \sigma_1 \\ \sigma_2 \\ \tau_{12} \end{Bmatrix} = [T] \begin{Bmatrix} \sigma_x \\ \sigma_y \\ \tau_{xy} \end{Bmatrix}$$

and

$$\begin{Bmatrix} \varepsilon_1 \\ \varepsilon_2 \\ \frac{1}{2}\gamma_{12} \end{Bmatrix} = [T] \begin{Bmatrix} \varepsilon_x \\ \varepsilon_y \\ \frac{1}{2}\gamma_{xy} \end{Bmatrix}$$

where $[T]$ is the transformation matrix for plane stress and plane strain transformed by clockwise rotation about the $(3,z)$ axes, given by

$$[T] = \begin{bmatrix} \cos^2\theta & \sin^2\theta & 2\sin\theta\cos\theta \\ \sin^2\theta & \cos^2\theta & -2\sin\theta\cos\theta \\ -\sin\theta\cos\theta & \sin\theta\cos\theta & \cos^2\theta - \sin^2\theta \end{bmatrix}$$

Inversion and substitution yields

$$\begin{Bmatrix} \sigma_x \\ \sigma_y \\ \tau_{xy} \end{Bmatrix} = [T]^{-1}[Q][T] \begin{Bmatrix} \varepsilon_x \\ \varepsilon_y \\ \frac{1}{2}\gamma_{xy} \end{Bmatrix}$$

which is the stress strain relation for a lamina referred to arbitrary axes. For simplicity, the notation $[\bar{Q}]$ is introduced

$$[\bar{Q}] = [T]^{-1}[Q][T]$$

where $[\bar{Q}]$ is called the transformed reduced stiffness matrix.

Using the approach outlined above, it is possible to obtain

expressions for the elastic properties referred to the x-y coordinate system.

d. Elastic properties of laminates

A number of assumptions are made in laminate theory to obtain theoretical predictions. These are:

1. the lamina are perfectly bonded and do not slip relative to each other
2. the bond between the laminae is infinitesimally thin
3. the laminate has the properties of a thin sheet

These assumptions allow the laminate to be treated as a thin elastic plate. The classical hypothesis of Kirchhoff is applied to derive the strain distribution throughout the plate under external forces. Because the laminate is composed of laminae oriented in different directions with respect to each other, the stress-strain equation for each layer (k) is defined as

$$
\begin{Bmatrix} \sigma_x \\ \sigma_y \\ \tau_{xy} \end{Bmatrix}_k =
\begin{bmatrix} \bar{Q}_{11} & \bar{Q}_{12} & \bar{Q}_{16} \\ \bar{Q}_{12} & \bar{Q}_{22} & \bar{Q}_{26} \\ \bar{Q}_{16} & \bar{Q}_{26} & \bar{Q}_{66} \end{bmatrix}_k
\begin{Bmatrix} \varepsilon_x \\ \varepsilon_y \\ \frac{1}{2}\gamma_{xy} \end{Bmatrix}
$$

Thus for a given strain distribution, the stress in each layer can be determined. The strain at any point in a laminate undergoing deformation must be related to the displacements and curvatures of its midplane. The discussion which follows assumes that the laminate is thin. Kirchhoff plate theory is used in this formulation.

The deformation of an arbitrary section of a laminate is shown in Fig. B-3. It is assumed that lines straight and perpendicular to the

midplane before deformation remain so after deformation. This is equivalent to neglecting transverse shearing deformations. Comparing Fig. B-4(b) with Fig. B-4(a), in which the normals to the midplane remain perpendicular after deformation, it is seen that the upper and lower surfaces of the plate must not shift their relative positions. It is obvious that the resistance of a thin plate to such deformation is large, much larger than its resistance to deformations perpendicular to the midplane.

It is assumed that the point B at the midplane undergoes displacements $u_0$, $v_0$, and $w_0$ along the x, y, and z axes, respectively. The displacement u in the x direction of a point C located on the normal ABCD at a distance z from the midplane is given by

$$u = u_0 - z\alpha$$

where $\alpha$ is the slope of the midplane in the x direction,

$$\alpha = \frac{\partial w_0}{\partial x}$$

The last two equations can be used to obtain the displacement u of an arbitrary point at a distance z from the midplane as

$$u = u_0 - z \frac{\partial w_0}{\partial x}$$

Similarly,

$$v = v_0 - z \frac{\partial w_0}{\partial y}$$

Since the strains normal to the midplane are neglected (plane strain), the displacement w at any point is taken equal to the displacement $w_0$ at the midplane. The strains in terms of displacement u and v are

$$\varepsilon_x = \frac{\partial u}{\partial x} = \frac{\partial u_0}{\partial x} - z \frac{\partial^2 w_0}{\partial x^2}$$

$$\varepsilon_y = \frac{\partial v}{\partial y} = \frac{\partial v_0}{\partial y} - z \frac{\partial^2 w_0}{\partial y^2}$$

$$\gamma_{xy} = \frac{\partial u}{\partial y} + \frac{\partial v}{\partial x} = \frac{\partial u_0}{\partial y} + \frac{\partial v_0}{\partial x} - 2z \frac{\partial^2 w_0}{\partial x \partial y}$$

In terms of midplane strains and plate curvatures, the strains in a laminate vary linearly through the thickness,

$$\begin{Bmatrix} \varepsilon_x \\ \varepsilon_y \\ \gamma_{xy} \end{Bmatrix} = \begin{Bmatrix} \varepsilon_x^0 \\ \varepsilon_y^0 \\ \gamma_{xy}^0 \end{Bmatrix} + z \begin{Bmatrix} k_x \\ k_y \\ k_{xy} \end{Bmatrix}$$

where midplane strains are given by

$$\begin{Bmatrix} \varepsilon_x^0 \\ \varepsilon_y^0 \\ \gamma_{xy}^0 \end{Bmatrix} = \begin{Bmatrix} \frac{\partial u_0}{\partial x} \\ \frac{\partial v_0}{\partial y} \\ \frac{\partial u_0}{\partial y} + \frac{\partial v_0}{\partial x} \end{Bmatrix}$$

and the plate curvatures by

$$\begin{Bmatrix} k_x \\ k_y \\ k_{xy} \end{Bmatrix} = - \begin{Bmatrix} \frac{\partial^2 u_0}{\partial x^2} \\ \frac{\partial^2 w_0}{\partial y^2} \\ \frac{\partial^2 w_0}{\partial x \partial y} \end{Bmatrix}$$

The stresses in any (k) lamina can be obtained by substituting the previous equation into the stress strain equation

$$\begin{Bmatrix} \sigma_x \\ \sigma_y \\ \tau_{xy} \end{Bmatrix}_k = \begin{bmatrix} \bar{Q}_{11} & \bar{Q}_{12} & \bar{Q}_{16} \\ \bar{Q}_{12} & \bar{Q}_{22} & \bar{Q}_{26} \\ \bar{Q}_{16} & \bar{Q}_{26} & \bar{Q}_{66} \end{bmatrix}_k \left[ \begin{Bmatrix} \varepsilon_x^0 \\ \varepsilon_y^0 \\ \gamma_{xy}^0 \end{Bmatrix} + z \begin{Bmatrix} k_x \\ k_y \\ k_{xy} \end{Bmatrix} \right]$$

### e. Laminate Stiffness Matrix

Classical laminate theory provides a method of calculating the resultant forces and moments per unit length acting on the laminate by integrating the stresses acting in each lamina through the thickness (h) of the laminate. Resultant forces are obtained by

$$N_x = \int_{-h/2}^{h/2} \sigma_x \, dz$$

$$N_y = \int_{-h/2}^{h/2} \sigma_y \, dz$$

$$N_{xy} = \int_{-h/2}^{h/2} \tau_{xy} \, dz$$

The moment resultants are obtained by integration through the thickness of the corresponding moments of stresses about the midplane:

$$M_x = \int_{-h/2}^{h/2} \sigma_x \, z \, dz$$

$$M_y = \int_{-h/2}^{h/2} \sigma_y \, z \, dz$$

$$M_{xy} = \int_{-h/2}^{h/2} \tau_{xy} \, z \, dz$$

The units of $N_x$, $N_y$, $N_{xy}$ are force per unit length and $M_x$, $M_y$, $M_{xy}$ are moment per unit length. The sign conventions are shown in Fig. B-5.

Using the resultant force and moment relations, a system is defined that is statically equivalent to the laminate stress system, but applied

at the midplane. Thus, the external loading has been reduced to a system that does not contain the laminate thickness or z coordinate explicitly.

For a laminate consisting of n laminae (Fig. B-6), the resultant force-moment system acting at the midplane can be obtained by adding integrals representing the contribution of each layer by

$$
\begin{Bmatrix} N_x \\ N_y \\ N_{xy} \end{Bmatrix} = \int_{-h/2}^{h/2} \begin{Bmatrix} \sigma_x \\ \sigma_y \\ \tau_{xy} \end{Bmatrix} dz = \sum_{k=1}^{n} \int_{h_{k-1}}^{h_k} \begin{Bmatrix} \sigma_x \\ \sigma_y \\ \tau_{xy} \end{Bmatrix}_k dz
$$

$$
\begin{Bmatrix} M_x \\ M_y \\ M_{xy} \end{Bmatrix} = \int_{-h/2}^{h/2} \begin{Bmatrix} \sigma_x \\ \sigma_y \\ \tau_{xy} \end{Bmatrix} z \, dz = \sum_{k=1}^{n} \int_{h_{k-1}}^{h_k} \begin{Bmatrix} \sigma_x \\ \sigma_y \\ \tau_{xy} \end{Bmatrix}_k z \, dz
$$

Using the expressions for the stresses in the k-th lamina derived earlier, and noting that the midplane strains and plate curvatures are constant not only within the lamina, but for all laminae, it is apparent that they can be taken outside the integral sign. The stiffness matrix [Q̄] is constant within a lamina so it also can be taken outside the integration to give

$$
\begin{Bmatrix} N_x \\ N_y \\ N_{xy} \end{Bmatrix} = \left[ \sum_{k=1}^{n} \begin{bmatrix} \bar{Q}_{11} & \bar{Q}_{12} & \bar{Q}_{16} \\ \bar{Q}_{12} & \bar{Q}_{22} & \bar{Q}_{26} \\ \bar{Q}_{16} & \bar{Q}_{26} & \bar{Q}_{66} \end{bmatrix}_k \int_{h_{k-1}}^{h_k} dz \right] \begin{Bmatrix} \varepsilon_x^0 \\ \varepsilon_y^0 \\ \gamma_{xy}^0 \end{Bmatrix}
$$

$$
+ \left[ \sum_{k=1}^{n} \begin{bmatrix} \bar{Q}_{11} & \bar{Q}_{12} & \bar{Q}_{16} \\ \bar{Q}_{12} & \bar{Q}_{22} & \bar{Q}_{26} \\ \bar{Q}_{16} & \bar{Q}_{26} & \bar{Q}_{66} \end{bmatrix}_k \int_{h_{k-1}}^{h_k} z \, dz \right] \begin{Bmatrix} k_x \\ k_y \\ k_{xy} \end{Bmatrix}
$$

$$\left\{ \begin{array}{c} M_x \\ M_y \\ M_{xy} \end{array} \right\} = \left[ \sum_{k=1}^{n} \begin{bmatrix} \bar{Q}_{11} & \bar{Q}_{12} & \bar{Q}_{16} \\ \bar{Q}_{12} & \bar{Q}_{22} & \bar{Q}_{26} \\ \bar{Q}_{16} & \bar{Q}_{26} & \bar{Q}_{66} \end{bmatrix}_k \int_{h_{k-1}}^{h_k} z \, dz \right] \left\{ \begin{array}{c} \varepsilon_x^0 \\ \varepsilon_y^0 \\ \gamma_{xy}^0 \end{array} \right\}$$

$$+ \left[ \sum_{k=1}^{n} \begin{bmatrix} \bar{Q}_{11} & \bar{Q}_{12} & \bar{Q}_{16} \\ \bar{Q}_{12} & \bar{Q}_{22} & \bar{Q}_{26} \\ \bar{Q}_{16} & \bar{Q}_{26} & \bar{Q}_{66} \end{bmatrix}_k \int_{h_{k-1}}^{h_k} z^2 \, dz \right] \left\{ \begin{array}{c} k_x \\ k_y \\ k_{xy} \end{array} \right\}$$

Three new matrices, $A_{ij}$, $B_{ij}$, and $D_{ij}$, are defined, where

$$A_{ij} = \sum_{k=1}^{n} (\bar{Q}_{ij})_k (h_k - h_{k-1})$$

$$B_{ij} = \frac{1}{2} \sum_{k=1}^{n} (\bar{Q}_{ij})_k (h_k^2 - h_{k-1}^2)$$

$$D_{ij} = \frac{1}{3} \sum_{k=1}^{n} (\bar{Q}_{ij})_k (h_k^3 - h_{k-1}^3)$$

These new matrices, A, B, and D, simplify the resultant force and moment relations, and are known as the extensional, coupling, and bending stiffness matrices, respectively. The total plate constitutive equation is then

$$\left\{ \begin{array}{c} N \\ M \end{array} \right\} = \left[ \begin{array}{cc} A & B \\ B & D \end{array} \right] \left\{ \begin{array}{c} \varepsilon^0 \\ k \end{array} \right\}$$

It may be recalled that in an orthotropic lamina with arbitrary orientation the shear stress is coupled with the normal strain and the normal stresses are coupled with the shear strain. In general, a resultant shearing force on a laminated plate produces midplane normal strains in addition to the expected shearing strain. Similarly, a

resultant normal force will induce shear strains in addition to midplane normal strains.

The nonzero coupling matrix B in the plate constitutive equation explains the coupling between bending and extension of the laminated plate. Thus, normal and shear forces at the midplane induce not only midplane deformations, (and hence, midplane strains) but also twisting and bending, producing plate curvatures. Similarly, resultant bending and twisting moments induce midplane strains.

f. Lamina stresses and strains

The aim of the analysis of a laminated composite is to determine the stresses and strains in each of the laminae forming the laminate. These stresses and strains are used with failure criteria to predict the loads for failure initiation for a laminate. The failure criteria are discussed in the section devoted specifically to that purpose.

The strains in a lamina caused by external loading are a function of laminate midplane strains and plate curvatures, as previously discussed. Once the lamina strains are known, lamina stresses can be found using the lamina stress-strain law. Thus, the starting point for calculating lamina stresses is the determination of laminate midplane strains and plate curvatures in terms of the applied loading. The plate constitutive equation given previously can be inverted to give the midplane strains and plate curvatures explicitly in terms of the resultant external forces and moments. The result of the inversion process is

$$\begin{bmatrix} \varepsilon^0 \\ k \end{bmatrix} = \begin{bmatrix} A' & B' \\ C' & D' \end{bmatrix} \begin{bmatrix} N \\ M \end{bmatrix} = \begin{bmatrix} A' & B' \\ B' & D' \end{bmatrix} \begin{bmatrix} N \\ M \end{bmatrix}$$

where $A'$, $B'$, and $D'$ are simplified forms of the inversion process results, and are functions of the $A$, $B$, and $D$ matrices of the original form of the plate constitutive equation.

It is now apparent that with these equations, an analysis of a laminate subjected to external forces and moments can be conducted:

1. calculate midplane strains and plate curvatures

$$\begin{bmatrix} \varepsilon^0 \\ k \end{bmatrix} = \begin{bmatrix} A' & B' \\ B' & D' \end{bmatrix} \begin{bmatrix} N \\ M \end{bmatrix} \quad .$$

2. calculate lamina stresses in global (x-y) system

$$\begin{bmatrix} \sigma_x \\ \sigma_y \\ \tau_{xy} \end{bmatrix}_k = \begin{bmatrix} \bar{Q}_{11} & \bar{Q}_{12} & \bar{Q}_{16} \\ \bar{Q}_{12} & \bar{Q}_{22} & \bar{Q}_{26} \\ \bar{Q}_{16} & \bar{Q}_{26} & \bar{Q}_{66} \end{bmatrix}_k \left( \begin{bmatrix} \varepsilon_x^0 \\ \varepsilon_y^0 \\ \gamma_{xy}^0 \end{bmatrix} + z \begin{bmatrix} k_x \\ k_y \\ k_{xy} \end{bmatrix} \right)$$

3. calculate lamina stresses in natural (longitudinal and transverse to fiber) system.

$$\begin{bmatrix} \sigma_1 \\ \sigma_2 \\ \tau_{12} \end{bmatrix} = [T] \begin{bmatrix} \sigma_x \\ \sigma_y \\ \tau_{xy} \end{bmatrix}$$

The strain variations in a lamina are calculated in an analagous manner. The stress-strain variation is compared with the allowable stresses and strains in each lamina. Thus the load at which failure is initiated in one of the lamina can be calculated, as long as a strength criteria exists in terms of the lamina natural axis system. The formulation of lamina failure criteria is discussed in the next section.

## 3. Strength Theories

It is assumed that the strength of a laminate must be related to the strengths of the individual laminae. A simple failure criteria consists of evaluating the lamina strengths in their principal material directions subject to induced stresses or strains at the boundaries of the lamina. In this context, it is assumed that the lamina and its constituents behave in a linear elastic manner to failure. The strength analysis described here assumes that the behavior of each lamina in an arbitrary laminate is the same as the behavior observed in the natural axis system when the lamina is part of any other laminate under the same stresses or strains. In other words, it is assumed that the strength criteria for a lamina in plane stress is valid for any orientation of the lamina in a laminate. In the ICAN program, the lamina strengths are calculated using the expressions given below.

Longitudinal tension

$$S_{l11T} = S_{fT} \ (k_f + k_m E_m / E_{f11})$$

Longitudinal compression:

The longitudinal compressive strength must be computed on the basis of three different criteria:

a. rule of mixtures

$$S_{l11C} = S_{fC} \ (k_f + k_m E_m / E_{f11})$$

b. delamination

$$S_{l11C} = (13 \ S_{l12} + S_{mC})$$

c. fiber microbuckling

$$S_{l11C} = \frac{F_2 G_m}{1 - k_f(1 - G_m/G_{f12})}$$

Transverse tension

$$S_{l22T} = S_{mT}(FACT/DENOM)$$

Transverse compression

$$S_{l22C} = S_{mC} / DENOM$$

Transverse shear

$$S_{l12} = \frac{[(F_1 - 1 + G_m/G_{f12})F_2 \, G_{l12} \, S_{mS}]}{G_m F_1} FACT$$

where $F_1$ and $F_2$ are given by

$$F_1 = \sqrt{\frac{\pi}{4k_f}}$$

$$F_2 = 1 - \sqrt{\frac{4k_v}{\pi k_m}}$$

The variable DENOM is introduced for convenience:

$$DENOM = [1 - \sqrt{k_f}(1 - E_m/E_{f22})] \sqrt{1 + \varphi(\varphi - 1) + \frac{1}{3}(\varphi - 1)^2}$$

where $\varphi$ is given by

$$\varphi = \frac{F_1 - \frac{E_m}{E_{f22}[1 - \sqrt{k_f}(1 - E_m/E_{f22})]}}{F_1 - 1}$$

The variable FACT is used to correlate the strengths of HMS and Kevlar fiber composites with the experimentally observed values. Since neither of these fibers is used in this work, FACT takes the value unity.
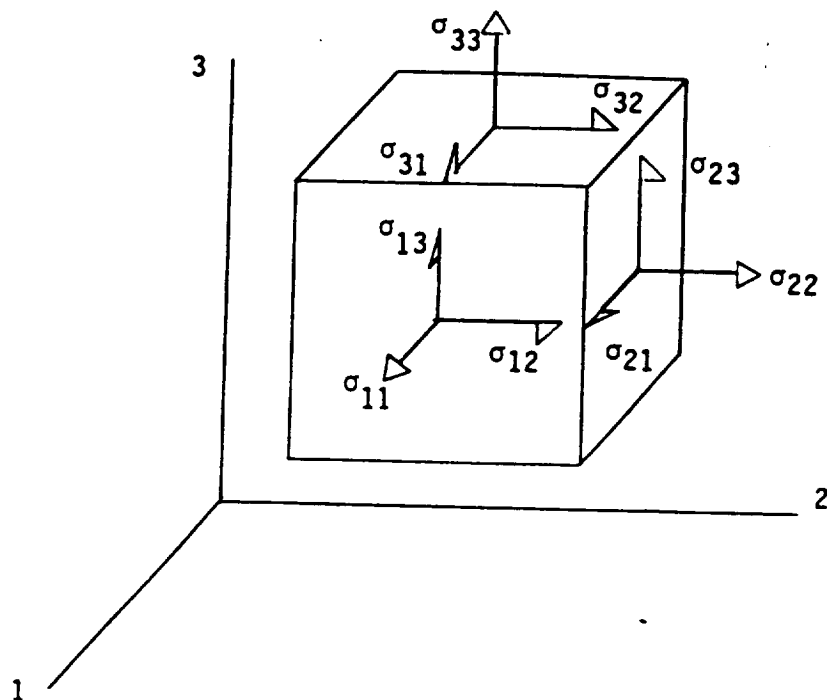
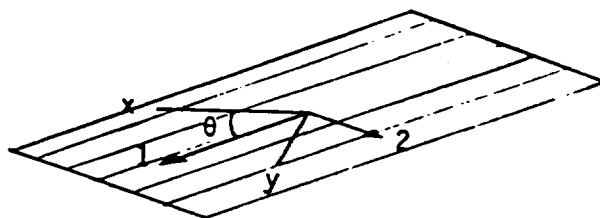Fig. B.1- Components of Stress acting on elemental unit cube.



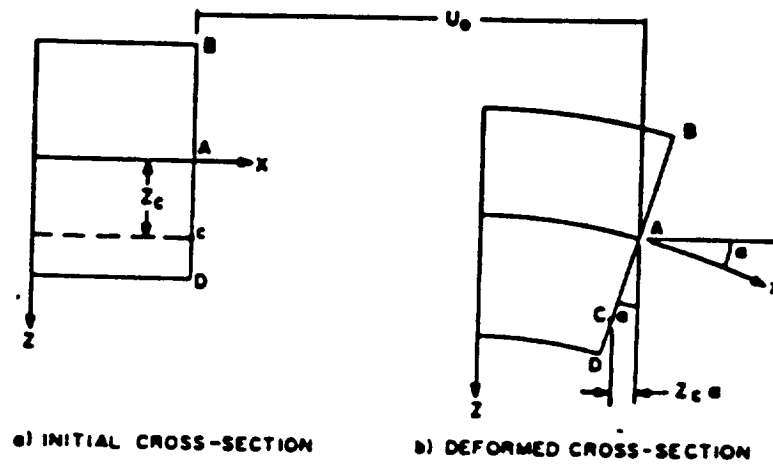Fig. B.2- Rotation of coordinates from 1-2 to x-y.

Fig. B.3- Bending geometry in the x-z plane.



a. *Deflected bar without shear deformations*
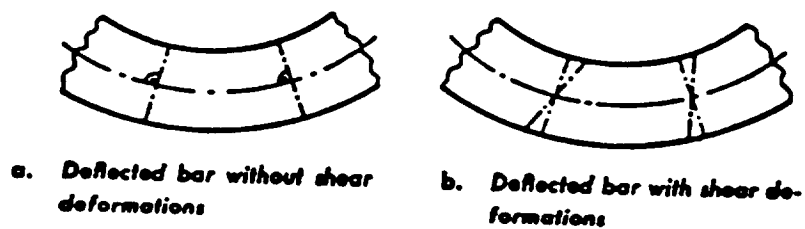
b. *Deflected bar with shear deformations*

Fig. B.4-Shearing force deformations on straight cross section.
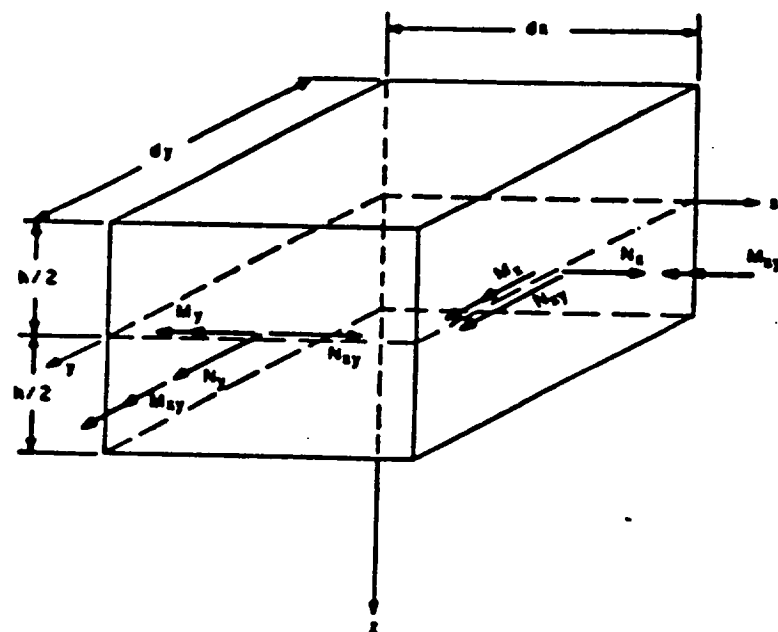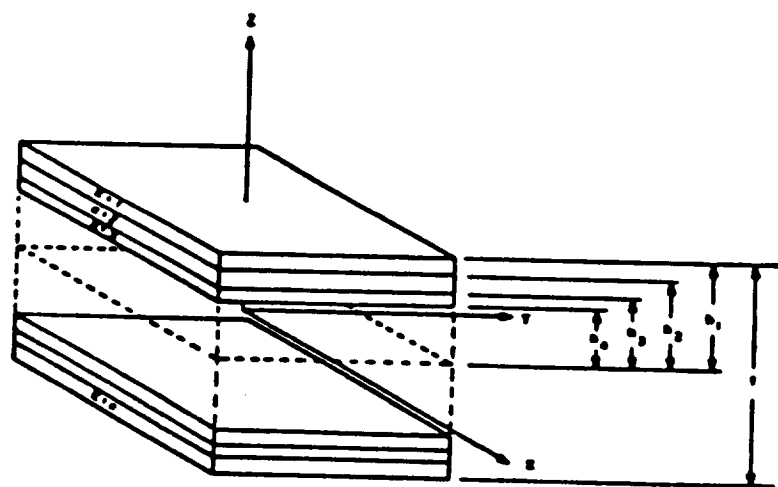
Fig. B.5- Plate stress and moment resultants

Fig. B.6- Laminate index notation convention.